The Impact of Persistent Organic Pollutants on Neural Development Using an *In Vitro* Approach

A study on how complex mixtures of persistent organic pollutants affect neural development using human neuronal stem cells

Nichlas Davidsen

Thesis Submitted for the Degree of
Master's in Molecular Biology
60 credits

Department of Biosciences
Faculty for Mathematics and Natural Sciences

UNIVERSITY OF OSLO

June 2018

2018

The Impact of Persistent Organic Pollutants on Neural Development using an *In Vitro* approach

Nichlas Davidsen

http://www.duo.uio.no/

Trykk: Reprosentralen, Universitetet i Oslo

Acknowledgements

This master´s thesis is the result of a collaboration between The Norwegian Institute of Public Health, The European Union Reference Laboratory for Alternatives to Animal Testing (EURL-ECVAM), The Norwegian University of Life Sciences (NMBU), and the University of Oslo (UIO). Experiments on PC12 cells has been carried out in the lab of Professor Ragnhild Paulsen at UIO, experiments on human induced pluripotent stem cells have been performed in the labs of EURL-ECVAM under the supervision of Dr. Anna Price and Dr. Francesca Pistollato at the Joint Research Center (JRC) in Ispra, Italy. The mixtures of persistent organic pollutants used in these experiments were supplied to us from the lab of Professor Erik Ropstad at NMBU.

Firstly, I would like to thank my supervisor Dr. Oddvar Myhre for his guidance throughout this entire process, for everything I have learned and for the opportunity to work on this project. I really appreciate all the time you have invested and help you have provided writing this thesis. Additionally, I want to thank my co-supervisor Professor Erik Ropstad and my internal supervisor Professor Ketil Hylland, for all your help in making this project possible and all the feedback you have provided during the writing process.

I want to thank Professor Ragnhild Paulsen for all your contributions to the project and the guidance in the writing of my thesis. Also, I am grateful to Mona and Mussie for all your guidance in the lab.

I want to extend my gratitude to Dr. Anna Price and Dr. Francesca Pistollato at the JRC for all your guidance and enthusiasm, and to Dr. Emilio Mendoza for all those hours in the lab. Thank you all for making me feel so welcome in Ispra, and for everything you have taught me.

I want to thank all my friends and fellow students, and especially Ane and May-Britt for five great years. Lastly, I want to extend a big thank you to my family, for your love, for always believing in me and for supporting me throughout all my endeavours.

Nichlas Davidsen, June 2018

Abstract

Persistent Organic Pollutants (POPs) are highly stable chemicals that are widespread in nature with potential hazardous effects in humans and wildlife. POPs have been used in a multitude of industrial applications and household products over several decades. Due to persistent, bioaccumulative and toxic (PBT) properties, regulations have been imposed for compounds like perfluorinated alkylated substances (PFASs), brominated flame retardants (BFRs) and polychlorinated biphenyls (PCBs). Because of high resistance against degradation, they are still present at considerable amounts in the environment, even after widespread bans.

The deleterious effects of some POPs upon human health are well documented. They are known to cause cancer, immunotoxicity, neurotoxicity and interfere with reproduction and development. Concerns have been raised about the impact of POPs upon neuronal development and possibly neurodevelopmental disorders. Children are thought to be especially at risk due to the immature blood-brain barrier (BBB) and the highly dynamic, complex events of neuronal development occurring early in life. However, very few studies have previously been reported on the effects of POPs in mixture, and on neurodevelopmental mechanisms using *in vitro* test models at human relevant exposures. Aiming to close this knowledge gap, our studies were conducted on PC12 cells and Neuronal Stem Cells (NSCs) derived from human induced pluripotent stem cells (HiPSC) using concentrations of POPs comparable to human blood levels. Four different mixtures of 29 perfluorinated, brominated, and chlorinated substances were used. Cells were examined using cell viability methods, immunological techniques with high-content imaging (HCI), and qPCR, probing for changes in neurodevelopmental endpoints connected to molecular initiating events (MIE) and key events (KEs) of the adverse outcome pathway (AOP) framework.

The present study showed that exposure to mixtures of POPs induced decreased cell viability in PC12 cells. In contrast to this, relevant concentrations of the POPs induced a concentration-dependent increase in cell viability in the NSCs. Mechanistic studies revealed increases in key neurodevelopmental proteins (SYP, PSD95, MAP2, and BDNF) at exposures below human blood level average. This was, however not reflected in gene expression. Our results indicate that exposure to POPs during early neurodevelopment may lead to detrimental perturbation of essential MIE or KEs important for learning and memory and the developing brain of children.

Abbreviations

ACh	Acetylcholine
AChE	Acetylcholine Esterase
AMPA	α-amino-5-hydroxy-3-methyl-4-isoxazole propionic acid
AOP	Adverse Outcome Pathway
BBB	Blood Brain Barrier
BDE	Brominated Diphenyl Ether
BFR	Brominated Flame Retardants
CNS	Central Nervous System
DA	Dopamine
DAT	Dopamine Transporter
DIV	Days In Vitro
DIV	Days In Vitro
EB	Embryoid Bodies
EDI	Estimated Daily Intake
GABA	Gamma-Aminobutyric Acid
HCI	High Content Imaging
hESCs	Human Induced Embryonic Stem Cell
HiPSC	Human Induced Pluripotent Stem Cell
KE	Key Event
KER	Key Event Relationship
LTP	Long Term Potentiation
MIE	Molecular Initiating Event

NA	Noradrenaline
ND	Neural Differentiation
NGF	Nerve Growth Factor
NI	Neural Induction
NPC	Neuronal Progenitor Cell
NSC	Neural Stem Cell
PBDE	Polybrominated Diphenyl Ether
PBT	Persistent, Bioaccumulative, Toxic
PCB	Polychlorinated Bipheyls
PFAS	Perfluorinated Alkylated Substances
POP	Persistent Organic Pollutant
PTP	Post-Tetaninc Potentiation
TH	Tyrosine Hydroxylase
TSH	Thyroid Stimulating Hormone
VMAT	Vesicular Monoamine Transporter

Table of Contents

1. Introduction

1.1 Background

1.1.1 Regulatory Toxicology

Under the Stockholm Convention of 2004 the use and production of a wide range of chemicals known as persistent organic pollutants (POPs) were restricted and banned based on the known and unknown harmful effects that they pose to human health and the environment. POPs is a collective term used to describe compounds that share a set of characteristics in relation to their physical and chemical properties. They are highly stable substances that are able to remain in the ecosystem for long periods of time, spanning years to decades. They encompass the ability to be distributed over large distances with varied means of transport, such as natural cycles involving soil and water, and especially by air, moving distances surpassing national borders and even continents. POPs being hydrophobic in nature (with the exception of PFASs), they will readily pass biological membranes and accumulate in the fat and other biological tissues of humans and animals. Combined with their persistence, this results in higher concentrations in organisms high in the food chain. Multiple POPs have been identified as eliciting harmful effects to humans, wildlife and the environment, maybe most notably is the ability of certain POPs to act as endocrine disruptors. This in turn raises the question on how and whether all these compounds may act in unison to produce additive, or synergistic effects when occurring in a mixture [1, 2].

The goal of the Stockholm convention was to limit and regulate the widespread use of POPs around the world, by establishing guidelines for the production and use of POPs worldwide. The guidelines focus on eliminating the production, use, import, and export of the recognized POPs, as well as limiting their release through safe management [2]. Following the Stockholm convention, the European Union implemented the Registration, Evaluation, Authorisation and Restriction of Chemicals (REACH) which requires companies producing and using chemicals to document the associated risk factors with the

chemicals and be able to communicate how to safely manage them before being allowed to release them to the European market [3].

The possible toxicity of POPs first started to gain notice in the late 1960s when the effects of some compounds started to become apparent. Maybe most notable is the case of bird populations located in Britain. It was found that since the late 1940s the eggs of peregrine falcons, sparrowhawks and golden eagles had decreased significantly in shell thickness and weight [4]. At the time, this was attributed to the introduction and subsequent widespread use of dichlorodiphenyltrichloroethane (DDT), of which the affected birds were found to be significantly contaminated. DDT was thought to possibly interfere with the calcium metabolism of the birds through endocrine disruption with the estrogen and parathyroid receptors, leading to perturbation of the Ca-ATPase [4].

1.1.2 Health impact

Studies has been conducted finding that POPs may play a significant impact in human health by inducing harmful carcinogenic, immunological, reproductive and neurological effects, either through endocrine disruption or other mechanisms [5]. Early life exposure to chemicals can be especially deleterious as the immune system and detoxification system of the body is not yet fully developed, this in turn may be the background for the development of diseases and deficiencies in adult life [6]. The developing nervous system is particularly vulnerable to chemical insults due to its complex nature of glia and neuronal cell proliferation, migration, and differentiation [7-9]. The nervous system of the foetus is thought to be especially prone to toxic insults as it does not yet exhibit a fully formed blood brain barrier, offering little protection of the neonatal brain [10].

Concerns about the neurological effects of POPs is an increasing concern as studies has found a relationship between exposure to POPs and the onset of neurodevelopmental and behavioural effects in children. As POPs have been found capable of crossing the human placenta [11], and studies suggest that exposure to POPs may affect areas of cognition related to intelligence, attention, mental and motor development in children, concerns has been raised [12]. Among endpoints typically found to be affected is abilities related to intelligence quotient (IQ), attention span and fine motor function [12].

1.1.3 Experimental

Studies conducted on zebrafish larvae using a mixture of POPs with concentrations relevant to humans found that swimming capabilities was severely affected at levels approximately 20 times higher than that found normally in humans, though the same effects could be replicated by exposing the zebrafish to the most predominant compound in the mixture, perfluorooctanesulfonic acid (PFOS). Genes related to the central nervous system (CNS) was also found to be affected, though expression was differently affected when comparing the mixture and the single compound [13]. *In utero* studies performed with rats found that mixtures of POPs with human relevant concentrations induced transcriptional changes related to neurodevelopmental processes of the rat brain, which in turn affected the rat in adult life [14]. Another study investigating the effects of a complex mixture of 29 different POPs upon female mice and their offspring found that the POPs induced perturbation of the function of corticosterone (analogue to cortisol in humans) [15], a glucocorticoid important for the proper function and orchestration of the stress response in mice, as well as playing key roles in foetal and brain development [16, 17]. Generally, the levels observed in the offspring were lower than that found in the mothers. Though, the glucocorticoid system was shown to be perturbed, there were no observable changes in behaviour. The study concluded that further studies were needed to evaluate the effects of POP on neural development, as dysregulation of the glucocorticoid system is linked with neurological disease in humans [15].

1.2 Persistent Organic Pollutants (POPs)

1.2.1 Exposure

Affinity for nonpolar organic matter and hydrophobicity are among the general characteristics applicable to most POPs and which make them capable of accumulating in the fatty tissue and plasma of animals in food chains, ultimately leading to humans. Due these characteristics they are less likely to be metabolized as they will accumulate in the fat, or bind to proteins in the plasma, effectively contributing to a long biological half-life [1, 18].

Environmental sources of contamination stem from widespread use of POPs for a large range of applications spanning over multiple decades, starting before the second world war until present time [19]. They have been used as pesticides in agriculture, capacitors and transformers in electrical equipment, as flame retardants in various settings, and as additives in paints, and inks. They have also been widely used in the plastic and metal industry and is also frequently released through waste incineration [20, 21]. Many of the perfluorinated POPs, have also commonly been used in water and oil repellant coatings in textiles, leather, and the paper industry, as well as components in materials used in food wrapping [22].

Human exposure relies on a number of different routes like inhalation of contaminated air, dermal exposure to soil or other substances containing POPs, as well as ingestion of food and water. It has been estimated that approximately 90% of overall ambient exposure to POPs that humans are subjected to comes from food, with fish being the main contributor [21]. Other food sources of POP exposure range from all sorts of meat to eggs, cereals, and dairy products [21]. Consumption habits may affect amount of exposure and ratios of different POPs, as fat rich food is likely to contain more POPs than other less fatty food. This is likely to contribute to different exposure levels between countries, as diet often is related to culture [21, 23]. Other routes of exposure are also thought to contribute to overall exposure, contamination of POPs have been detected in outside air in both rural and urban areas around the world. Similarly, contamination has been found in indoor air from various households, generally with higher concentrations than that found outside. Also, household dust is found to contain POPs. Though concentrations in drinking water

has been established to be very low, trace amounts has been found in some locations [22]. Another concern is the ability of POPs to cross the placenta and affect children prenatally, although the distribution between child and mother varies as the placenta will demonstrate a certain selectivity [11].

1.2.2 POP Mixtures

Most studies conducted to this date has been mostly concerned with the toxicity that single compounds elicit on health and wildlife. Few studies have looked into the effects that multiple POPs may exhibit when appearing in a mixture. Therefore, efforts were made to design a mixture of POPs with concentrations relevant to what human would be exposed to in their natural environment. Using studies that looked into the estimated daily intake (EDI) of POPs in Scandinavian populations, as well as blood and breast milk concentrations, a mixture encompassing 29 compounds was designed based on the most prevalent POPs for use in *in vitro* experiments. The compounds were chosen based on their prominence in food, blood and breast milk, encompassing chemicals of different groups, such as chlorinated, brominated, and perfluorinated compounds. Concentrations were set to mimic the concentrations found in human blood following normal environmental exposure, maintaining the ratios of the different compounds [19].

The different groups of POPs were sorted based on their chemical composition into different subgroups. One mixture was made based on each subgroup giving three different sub-mixtures, all diluted in dimethyl sulfoxide (DMSO), which also was combined to create one total mixture. All sub-mixtures and possible combinations were made, in the current study, the different groups were mixed with the chlorinated compounds. A perfluorinated mixture, containing 6 perfluorinated compounds was combined with 16 chlorinated compounds, one brominated mixture containing 7 brominated compounds was combined with 16 chlorinated compounds, and one mixture contained 16 chlorinated compounds [19].

Table 1.1: The table shows the mixture of all the 29 POPs that was constructed based on human blood levels of the Scandinavian population [19]. The table is adapted from Berntsen et al. (2017) [19].

Compound	Average human blood levels[a] ng/g lipid	Average human blood levels[b] ng/ml	Total mixture stock nominal concentration[c] mg/ml	Total mixture stock measured concentration[d] mg/ml	Total mixture stock measured concentration[e] µM	Measured % of nominal
PCB						
PCB 28	2.13	0.013	0.013	0.008	31.1	62
PCB 52	1.60	0.010	0.010	0.006	20.5	60
PCB 101	1.30	0.008	0.008	0.008	24.5	100
PCB 118	10.67	0.064	0.064	0.045	137.9	70
PCB 138	37.00	0.222	0.222	0.155	429.5	70
PCB 153	60.33	0.362	0.362	0.252	698.3	70
PCB 180	32.33	0.194	0.194	0.134	339.0	69
Σ PCBs	145.36	0.873	0.873	0.608	1680.8	70
OCP						
p,p′-DDE	83.67	0.502	0.502	0.339	1065.9	68
HCB	19.50	0.117	0.117	0.065	228.2	56
α-Chlordane[f]	1.80	0.011	0.011	0.010	23.7	91
Oxychlordane	3.70	0.022	0.022	0.014	33.0	64
trans-Nonachlor	6.80	0.041	0.041	0.044	99.1	107
α-HCH	1.00	0.006	0.006	0.005	16.8	83
β-HCH	8.77	0.053	0.053	0.022	75.6	42
γ-HCH (Lindane)	1.00	0.006	0.006	0.005	16.8	83
Dieldrin[f]	4.00	0.024	0.024	0.021	56.2	88
Σ OCP	130.24	0.782	0.782	0.525	1615.3	67
Σ PCB + OCP	275.60	1.655	1.655	1.133	3296.1	68
BFR						
PBDE 47	1.43	0.009	0.009	0.009	17.8	100
PBDE 99	0.59	0.004	0.004	0.004	7.5	100
PBDE 100	0.36	0.002	0.002	0.002	3.8	100
PBDE 153	1.64	0.010	0.001*	0.001	2.1	100
PBDE 154	0.29	0.002	0.002	0.002	3.0	100
PBDE 209	1.81	0.011	0.011	0.009	9.4	82
HBCD	4.10	0.025	0.025	0.035	54.5	140
Σ BFR	10.22	0.063	0.053	0.062	98.1	117
PFAA						
PFHxS	N/A	3.450	3.450	3.422	7809.2	99
PFOS	N/A	29.425	29.425	22.348	41,522.1	76
PFOA	N/A	4.523	4.523	1.743	4209.4	39
PFNA	N/A	0.800	0.800	0.507	1092.5	63
PFDA	N/A	0.495	0.495	0.193	375.4	39
PFUnDA	N/A	0.560	0.560	0.190	336.8	34
Σ PFAAs	N/A	39.253	39.253	28.403	55,345.4	72

[a]Average human blood levels of POP based on a literature review of Scandinavian values, providing the basis for the *in vitro* mixture.
[b]Average human blood levels of POP converted to ng/ml. A fat percentage of 0.6% was used. 1 ml blood was considered to have a weight of 1 g.
[c]Nominal concentration of the various compounds in the total mixture stock—100,0000 × the average concentration in blood.
*The nominal concentration of PBDE 153 included in the total mixture stock was ten times lower than originally intended.
[d]Measured concentrations of the various compounds in the total mixture stock in mg/ml.
[e]Measured concentrations of the various compounds in the total mixture stock converted to µM.
[f]Calculated as % of *p,p′*-DDE (84 ng/g lipid)—based on the relationship between alpha—chlordane and *p,p′*-DDE (0.022) and between dieldrin and *p,p′*-DDE (0.048) in breast milk.
Abbreviations: PCB (polychlorinated biphenyls); OCP (organochlorine pesticides); BFR (brominated flame retardants); PFAA (perfluoroalkyl acids).

The concentrations used in the mixtures were based on studies conducted on the blood levels of POPs in human populations living in Scandinavia [19]. The details surrounding the design of the mixtures can be found in Berntsen et al. (2017) [19].

1.2.3 Toxicity of Chlorinated Compounds

The chlorinated POPs encompass a major group of substances widely used for a large range of applications dating back to the 1920s. They all have in common that they exhibit a chlorine carbon bond which is the basis of the deleterious effects they have been found to exhibit [1].

Polychlorinated Biphenyls (PCBs)

The neurotoxic effects of PCBs were first observed in Japan in 1968 when over 1000 people fell ill after eating rice that had been contaminated with PCB containing oils used as heat transfer fluids. Initially, the people affected got acne-like lesions and brown pigmentation of the skin, as well as ocular swelling, neurological complaints was also noted, such as headache, memory loss and numbness, the affliction was named “Yusho”. Later it was found that pregnant women suffering from “Yusho” gave birth to children with various developmental abnormalities, among these slowness, jerkiness, apathy, and lower than average IQ [24, 25].

One cohort study looking into the neurodevelopmental effects of prenatal exposure to a large mixture of PCBs found that exposure caused lower performance in tests related to cognitive and motor activity in the children of mothers living in especially contaminated areas, but stated that this relationship may be causal [26]. In another study looking at pregnant women living in areas within normal levels of contamination found an negative association between PCB-138, PCB-153, PCB-180 and mental development, but not in motor development in infants of 7 months of age, development of memory was also seemingly unaffected [27]. Additionally, PCB-153 has been found to induce cell death and cause upregulation of ROS in cerebellar granule cells from rat [28]. One review established that early life exposure to PCBs are associated with decreased cognitive function and behavioral impairment in adult animals [29]. The same study argued that despite decades of research, outcomes of human studies are often inconsistent, while epidemiological data shows a slight perturbation of neuromotor development, cognition, and behavior [29].

In a study using rat cerebellar granule neurons in culture treated with different PCBs found that the non-coplanar PCB-8, PCB-28, PCB-47, and PCB-52 induced disturbances to the membrane integrity (which is considered a marker of cell viability), accompanied with increase in the intracellular concentration of Ca^{2+} [30]. They also found that some PCBs induced interference with mitochondrial activity and attributed decline in cell viability to this [30]. Some PCBs has been found to reduce synaptosomal dopamine (DA) in striatal synaptosomes in rat, while at the same time increasing concentrations of dopamine in media and of total DOPAC (a metabolite of dopamine). The decrease of synaptosomal dopamine and increase of dopamine in media appeared not to be linked, while the increase in total DOPAC was found to highly correlate with reduction of synaptosomal dopamine. This was attributed to elevated transport of dopamine away from the cell body to nerve the terminals due to vesicular monoamine transporter (VMAT) inhibition [31]. Moreover, has PCBs been found to inhibit the uptake of dopamine, serotonin, glutamate, and GABA into the synaptosomes [32].

Dichlorodiphenyldichloroethylene (DDE)

The possible toxicological effects of DDE, a metabolite of DDT, was noted relatively early but its use as a pesticide has spanned decades. One study conducted on the children of Mexican farm workers found delayed neural development of the children who had been exposed to DDE [33]. Another study conducted in Spain found that DDE caused significant delays in mental and psychomotor development in 13-month-old children who had been prenatally exposed through the cord serum of mother living in a high contaminated area [34]. Others report early DDE exposure to cause long-term detrimental neurodevelopmental effects in children, where negative effects were seen in cognitive, verbal and memory ability at 42 months of age [35]. DDE has been found to activate pro-apoptotic pathways by activating caspase-3, accompanied by genome wide DNA hypomethylation in embryonic neurons from mice [36]. It has been found that DDT and its metabolites cause release of preloaded dopamine from synaptosomes, and further that they hinder or contribute to decreased reuptake of dopamine through inhibition of the dopamine transporter. At the same time, it was found that DDT and its metabolites also are capable of inhibiting the vesicular function of VMAT2, both of which would cause an increase in cytosolic dopamine [37].

Hexachlorobenzene (HCB)

Hexachlorobenzene is a fungicide that was widely used in agriculture and industry in the past until it was banned by the Stockholm convention, and is known to enter humans through diet and readily cross the placenta and breast milk [38]. It has been found to be positively linked with hyperactivity and inattention in Spanish children at 4 years of age with mothers who come from areas with higher than average levels of contamination with HCB [39]. The same study found that these children tended to fare worse in teacher conducted social competence tests designed to assess the behavioral, emotional and academic skills of children [39]. In another study conducted on a Turkish population who were exposed to HCB through bread made out of contaminated grain, found that acute exposure led to the death of multiple 1-2 year old children whose mothers had eaten the bread [40]. Others affected suffered from multiple neurological aberrations, causing symptoms like loss of appetite, tremors, seizures, and muscle weakness [40]. In a study looking at the impact of HCB on neuronal differentiation of embryonic stem cells from mice found that HCB induces cell death at low concentrations, as well as a decrease in the expression of the GABAergic marker GAD1, halting the neuronal differentiation and favouring mesodermal gene expression. Additionally, low dose treatment with HCB caused a decrease in the average neurite outgrowth length in GABAergic neurons accompanied with an increase in ROS production [41].

Chlordane

Chlordane was a commonly use pesticide especially against termites until its ban in the late 1980s, studies has documented its deleterious effects on human health. One study looking at people residing in an apartment complex who had been heavily treated with chlordane shortly before its ban found a significant decrease in reaction time, balance, and cognitive function accompanied with reduced perceptual motor speed, and delayed verbal recollection ability [42]. In an experiment looking at the effects of acute exposure to α-chlordane the authors report that the rate of uptake and release of GABA was perturbed in multiple areas in the brain, leading to overall decreased turnover of GABA in the brain of rats [43]. Another study looking at acute exposure in rats found that α-chlordane caused decrease in the concentration of acetylcholine (ACh) accompanied by increased activity of the acetylcholinesterase (AChE). The same study found that α-chlordane decreased

noradrenaline (NA) in the brain stem, additionally 5-hydroxyindoleacetic acid (5-HIAA, the metabolite of serotonin) was seen to increase drastically in brain stem without significant changes in the amount of 5-hydroxytryptamine (5-HT) [44].

Hexachlorocyclohexane (HCH)

Hexachlorocyclohexane appears in different forms α-, β-, γ-, of varying degrees of toxicity, with γ-HCH (Lindane) being the most toxic. In a study looking at a cohort from the Spanish island Menorca infants were evaluated for physical aberrations following the presence of β-HCH in blood. The study found a positive correlation between the presence of β-HCH and higher levels thyroid-stimulating hormone (TSH) and suggested that brain development could be affected following perturbation of the thyroid function [45]. Another study also conducted in Spain found that infants exposed to β-HCH through cord blood also exhibited higher concentrations of TSH [46]. The presence of β-HCH in serum has additionally been linked to elevated risk of Parkinson's disease [47]. One study found that both β-HCH and γ-HCH induced neurotoxic decrease in motor conduction velocity in rats [48]. Another study looking at the effects of γ-HCH (Lindane) on neurite development in rat cultured hippocampal neurons found that upon acute exposure the neurite initiation was significantly reduced, as well as the number of dendrites per cell, and dendrite branching [49]. Rats treated with γ-HCH (Lindane) exhibited tremors and decreased locomotor activity, coupled with increased expression of the GABA receptor complex and increased concentrations of GABA in the cerebellum [50].

Dieldrin

A study looking at the effects of dieldrin on the gene expression related to neuropeptides and their receptors in PC12 cells report that a wide number of genes related to neuropeptides were up regulated, as well as the genes for a wide range of neuropeptide receptors [51]. I another study looking at the effects of perinatal dieldrin exposure of mice found that the expression of the genes NURR1 and Pitx3, both nuclear transcription factors involved in the regulation of dopamine transporter (DAT) and VMAT2 was upregulated in 12-week-old pups. Consequently, higher protein levels of DAT and VMAT2 was observed, no changes were seen in the GABA transporters or in norepinephrine and serotonin levels, the dopaminergic system were therefore determined

to be the main target of toxicity. In this study the neurotoxic effects were attributed to lactational exposure to dieldrin, and in general the strongest response was observed in the male individuals. Heightened levels of DOPAC was observed in the male individuals, but not in the female [52]. One study which was done on PC12 cells found that acute exposure to dieldrin induced dose-dependent release of dopamine, reaching near depletion of dopamine at the highest tested concentration, this was coupled with an increase in the release of DOPAC at higher concentrations. Additionally, it was shown that dieldrin contributed to apoptotic cell death, and that dopaminergic cells are more vulnerable to the toxicity of dieldrin than non-dopaminergic cells [53].

1.2.4 Toxicity of Brominated Compounds

Brominated flame retardants (BFRs), generally encompass brominated diphenyl ethers (BDEs) and hexabromocyclododecane (HBCD) which are substances exhibiting a bromine carbon bond. These compounds have been widely used to make various products resistant to fire. They have been used in furniture, electronic equipment, construction materials, and even textiles [54].

Brominated Diphenyl Ethers (BDEs)

In a cohort study investigating the effects on 4-year-old children exposed pre- and postnatally to different BDEs (predominantly BDE-47, BDE-99, and BDE-100) found that the children were more at risk of suffering from symptoms of attention deficit disorders, accompanied by poorer performance in tests related to social competence [55]. One longitudinal cohort study looking at the neurodevelopmental effects of prenatal exposure to BDE-47, BDE-99, and BDE-100 found that neurotoxicity was affected at multiple time points after birth. BDE-47 caused significant decrease in mental and physical development at 12-48 and 72 months of age. Children exhibiting the highest concentrations of BDEs were found to score significantly lower in tests related to development, and intelligence [56]. Another follow up study looking at children from the same cohort in the ages 3-7 found positive associations between BDE-47, BDE-99, BDE-100, BDE-153 and attention deficits in all probed ages, except 5 and 6 years old [57].

A study investigating mice that was perinatally exposed to BDE-47 report spatial learning and memory deficits in the Barnes maze. The mice spent significantly longer time and

walked significantly longer distances before escaping the maze at the first day of testing. After multiple trials in the same maze, the treated and the control were the same [58] indicating no long-term effects. Neonatal exposure to BDE-47 in the hippocampus of mice has been shown to affect post-tetanic potentiation (PTP) and long-term potentiation (LTP) through down regulation [59]. Additionally, it was found that proteins related to post-synaptic glutamate receptor signaling was downregulated, the significantly affected proteins being NR2B of the NMDA receptor, and GluR1 subunit of the AMPA receptor, and no effects were observed upon PSD-95 and SAP97 [59]. Another study looking at low level exposure to BDE-47 and BDE-99 in zebrafish embryos, reported induced short- and long-term changes in the behavior. BDE-47 was found to induce decreased locomotion, and slightly increased overall mortality [60], while BDE-99 found to increase locomotion without any effect on overall mortality. Both BDE-47 and BDE-99 induced a reduction in anxiety and stress related responses [60]. Low level exposure studies have reported that BDE-99 induced irreversible disturbances in the spontaneous behavior of rat pups exposed shortly after birth, which indicates disturbances in the rat´s ability to process sensory information and acting upon it in regard to its environment, this over time caused both hypoactivity and hyperactivity [61]. The effects of BDE-99 upon the differentiation of neural progenitor cells (NPC) from humans and mouse was evaluated in another study [62], where BDE-99 was found to disrupt the differentiation towards oligodendrocytes in both human and mouse NPCs and further disrupted the maturation of oligodendrocytes [62]. Exposure of rat pups to BDE-153 through lactation caused impairments of spatial learning and short-term memory, as well as disruption of the normal activity level of the animal [63]. This was accompanied by increased disorder, decreased size and decreased number of cells in the hippocampal region of the rat brain [63]. One study investigating the effects of BDE-209 found that exposure caused the rats to have significant higher latency in maze tests coupled with increased apoptotic death and autophagy of hippocampal neurons [64], indicating that the increased autophagy may lead to decline in learning and memory.

Hexabromocyclododecane (HBCD)

Hexabromocyclododecane is a commonly used flame retardant which has been used in a large range of products. One study investigating the effects of HBCD exposure to newborn mice found a dose-response relationship between exposure to the substance and

a decrease in overall locomotor activity, which over time led to an overall increase in locomotor activity in comparison to the control. Additionally, perturbation of learning and memory was seen in adult individuals [65]. Another study looking at the effects of prenatal exposure to HBCD in rats found that the treatments induced disturbances in the attention, as well affecting other neurodevelopmental endpoints, and increasing over all age-related decline in health [66]. One study looking at the effects of HBCD on the dopamine circuit in the hippocampus found that HBCD disturbed the function of the tyrosine hydroxylase involved in the synthesis of dopamine, additionally it was found that exposure to HBCD induced reduced expression of DAT and VMAT2. Their findings suggested that HBCD interfered with the presynaptic machinery and remarked that this may contribute to causing deficits in memory through interference with the synthesis, and release of neurotransmitters [67]. Another study using mesencephalic neurons from postnatal mice found that HBCD induced decreased cell viability, decrease in the expression of tyrosine hydrolases and reduced neurite branching and length [68].

1.2.5 Toxicity of Perfluorinated Compounds

Perfluorinated POPs has been widely used for industrial and household purposes. One major use is waterproofing of textiles and leather. Additionally, they have been used as surfactants in paints and sprays, and the metal industry. One thing setting them apart from POPs is their apparent lack of hydrophobicity: rather than accumulating in fat, they will bind to proteins in the plasma [69], potentially leading to long half-lives in humans.

Perfluororhexane sulfonate (PFHxS)

PFHxS is commonly used in various surfactants and protective coatings. Neonatal exposure to PFHxS has in one study been found to increase the protein levels of CaMKII, Synaptophysin (SYP), and Tau in the hippocampus, which subsided with age [70]. In another study conducted on adult mice there was seen a dose dependent neurotoxic effect following a single neonatal exposure to PFHxS, where low doses decreased locomotor activity, and high doses acutely decreased locomotion which over time lead to significant increase in locomotion [71]. The study concluded that PFHxS neonatal exposure induced developmental neurotoxic effects which affected spontaneous behavior later in life [71]. Another study conducted on PC12 cells found that PFHxS decreased the viability of the

cells at high concentrations by increased apoptosis following NMDA receptor-mediated Erk activation, this was linked with increased caspase-3 activity and increased number of cells exhibiting DNA fragmentation [72].

Perfluorooctanesulfonic acid (PFOS)

Perfluorooctanesulfonic acid has been a widely used surfactant and is commonly found in various fabrics, textiles, paper coatings, and food packaging. PFOS has been shown to interfere with neurodevelopmental processes upon acute exposure, leading to increased excitability of the neurons in Sprague Dawley rats, heightened sensitivity mainly being attributed to modulation of the presynaptic machinery [73]. Additionally, neurite length and branching has been shown to decrease following chronic exposure to PFOS, this was observed together with an increased concentration of Ca^{2+} and decreased density of the expression of the protein PSD95 [73]. In another study, PFOS was found to weaken the ability of the astrocytes to protect the neuronal cells of rat, making them more prone to deteriorate following disturbance [74]. Additionally, PFOS induced reduced neurite outgrowth following decreased expression of the neuronal dendrite marker MAP2 [74]. One study looking at the effects of neonatal exposure to PFOS in mice found that the levels of CaMKII and GAP-43 was significantly increased in the hippocampus, and the level of synaptophysin (SYP) was significantly upregulated in both the hippocampus and the cerebral cortex, and Tau only upregulated in the cerebral cortex. This indicate disturbance of key developmental processes in the maturing brain [75]. In another related study the effects of PFOS was evaluated in regard to effects on neurobehavior [76]. In adult mice following neonatal exposure, long lasting perturbation of the spontaneous behavior and the cholinergic system in mice was found [76]. This indicated disturbances in the ability of the mice to process the sensory information from its surroundings and functionally acting on that through motoric actions. These kinds of disturbances could hinder cognitive function leading to the mice exhibiting symptoms of hypoactivity and hyperactivity in a time-dependent manner, which with age were believed to worsen. The study also found that exposure to PFOS induced perturbations of the cholinergic system, inducing an upregulated response upon stimulus [76]. PFOS has been shown to cause downregulation of brain-derived neurotrophic factor (BDNF) mRNA and protein [77]. Downregulation of BDNF is believed to play a central role in hypothyroidism and associated neurological impairments [78].

Perfluorooctanoic acid (PFOA)

Perfluorooctanoic acid is a widely used industrial compound which has been broadly used in the past in various industries with various applications in, surfactants, oil, water repellant coating and more. One study has found a positive association between PFOA and reading ability in children aged 5 and 8 years [79]. Another study has found a relationship between increasing exposures to PFOA and decreased disturbing behavior such as hyperactivity in children [80]. PFOA has been seen to induce shortening of neurite length, together with increased spontaneous action potential independent release of neurotransmitter [81]. Prenatal low-level exposure to PFOA has been linked with adverse effects on cognitive function, language processing and social developmental abilities of infants at 6 months of age, as well as perturbing the fine and gross motor abilities of the children [82]. One study looking at the effects of PFOA exposure in mice found that the levels of CaMKII and GAP-43 was significantly increased in the hippocampus, and the level of synaptophysin and Tau was significantly upregulated in both the hippocampus and the cerebral cortex, causing perturbation of regular neurodevelopmental processes [75]. In another related study, it was found that PFOA induced perturbation of the spontaneous behavior of the animals, causing both hypoactivity and hyperactivity. Additionally, upregulation of the cholinergic system was observed, leading to higher sensitivity to stimulation [76].

Perfluorononanoic acid (PFNA), Perfluorodecanoic acid (PFDA), and Perfluoroundecanoic acid (PFUnDA)

Perfluorononanoic acid is a POP commonly used as an intermediate in processes related to industrial synthesis of fluoropolymers [83]. Prenatal exposure to PFNA has been shown to decrease scores in tests related to verbal reasoning in children at 8 years of age [84]. Additionally, one study has linked PFNA with disturbances related to impulsivity [85]. Studies conducted in zebrafish found PFNA to induce increased swimming speeds, a sign of hyperactivity [86].

Both perfluorodecanoic acid and perfluoroundecanoic acid have been widely used in a large range of products and industries and have been commonly found in human blood samples. PFDA has been seen induce cell death and accumulate in cerebellar granule neurons harvested from rat pups [87]. Similarly, PFUnDA has been shown to induce cell

death and accumulate in clusters in the cell membrane of the same type of cerebellar granule cells [87].

1.3 Neurodevelopment

1.3.1 Neuron Formation and Development

The development of the brain starts already 3 weeks after fertilization and the formation of the embryo. In the early stages of neurodevelopment, a large number complex and dynamic processes take place in an organized matter in which ultimately leads to the formation of a network of interconnected cells and supportive structures that is the human brain. By the end of gastrulation (E24, 24 days after conception), a small number of neural progenitor cells (neural stem cells) has formed in a region that is named the ventricular zone. These will go through a process of massive symmetrical cell proliferation, meaning that every cell will produce two duplicate neural progenitor cells, leading to a major increase in neural progenitor cells before the process starts shifting towards cell differentiation. The differentiation process starts at E42 and continues until about halfway into the pregnancy, at this point cell proliferation will become asymmetrical producing one neuron and one neural progenitor cell. Neurons are post-mitotic cells incapable to further cell proliferation. From this point on the neurons will migrate, and interact with each other and the environment to facilitate the development of the brain in a process that carries on until early adulthood, if not the entire life span [88].

Following the induction of neurons, the neurons will start migrating from the ventricular zone and out into the cortex where they will start interacting with each other to form neural networks. In order to communicate with other neurons, the neurons will start expressing different sorts of neurites, namely axons and dendrites. The neurons will extend one axon away from the cell which will mediate all signaling from the cell to the exterior environment. In order to guide the growth of the axon, the tip of the axon have a "growth cone" which senses the environment and helps the axon reach its target location. Upon reaching its target location, often in vicinity of dendrites of other neurons, the axon will form synapses in which neurotransmitters will be released to mediate the signaling from the cell. Dendrites on the other is the site for which the neuron receives signals from

other neurons in its vicinity, one neuron may have many thousands of dendrites which form synapses with many thousands of different neurons [88].

1.3.2 Synaptogenesis and Neurite Formation

Synapses are the neurons main tools for communicating with other neurons and are essential in neural networks ability to process information and for the functioning of the nervous system as a whole. A synapse is composed of two neurons in which neurotransmitters move from one (the presynaptic neuron) across the synaptic cleft and binds to receptors on the other (the postsynaptic neuron) [89]. Synapses continues rearrange and change throughout life, and one neuron may at any one point be interconnected and actively communicate with thousands of other cells [9]. Synaptogenesis is the name of the process in which the formation of synapses occurs, and is guided by a growth cone, which is located on the tip of the neuronal axon. The growth cone is a specialized structure in the axon which senses other cells and signaling molecules located in its proximity in order to find the correct spot to initiate synaptogenesis [90]. Upon contact between the pre- and post-synaptic neurons is initiated, signaling mediated by voltage gated ion channels in the pre-synaptic neuron initiates. This leads to upregulation of neurotransmitter receptor related genes in the post-synaptic neuron, which subsequently leads to an upregulation and clustering of receptors in the synaptic area [91]. Early synapse formation is usually characterized by the emergence of a dendritic spine in the postsynaptic neuron. Dendritic spines are membrane structures which protrudes from the surface of the neurons, and functions as the main site for synaptic transmission [92]. Shortly after spine formation, postsynaptic density protein 95 (PSD95) is recruited to the surface of the spine. PSD95 is a family of scaffolding proteins associated with a number of processes thought to be associated with synapse function. Among these being the recruitment of neurotransmitter receptors and ion channels. Therefore, PSD95 is thought to be highly involved in the postsynaptic neurons ability to establish contact with new axons and decrypt neurotransmitter signaling [89, 93].

Other factors thought to be heavily involved in the process of synapse formation is neurotrophic factors, which are signaling molecules crucial for the survival and differentiation of neurons [94, 95]. These types factors bind to and activate tropomyosin-related kinase (trk) receptors, which are tyrosine kinases that upon binding will dimerize

and phosphorylate each other [96]. This leads to the creation of docking sites in which adaptor molecules can bind and further the intracellular signaling transduction to signaling pathways such as the Ras/extracellular signal regulated kinase (ERK) pathway, the phosphatidylinositol-3-OH (PI3K)/Akt kinase pathway and phospholipase C-γ1 (PLC-γ1) [97, 98]. One such neurotrophic factor is the brain-derived neurotrophic factor (BDNF), which binds and activates the trkB transduction pathway which is thought to be heavily involved in the survival and morphogenesis of neurons located in the central nervous system, actively promoting survival and protecting against various insults that may be inflicted upon the neurons of the CNS. This may positively affect the pharmacokinetics in the brain by modulating the function of the blood-brain-barrier [99-101]. One of the prominent ways in which BDNF promotes neuronal survival is through activation of the ERK/cAMP-response element binding protein (CREB) [101, 102]. BDNF has also been shown to be involved in the synaptic plasticity of the CNS, playing key roles in the modulation of synaptic transmission and in long term potentiation (LTP) [103]. LTP being the observed increase in synaptic strength following earlier synaptic activity or stimulus. A process believed to be vital for a range of neuronal functions, such as memory [104, 105]. Additionally, neurotrophic factors such as BDNF has been shown to be directly involved in neurite outgrowth, neuronal excitability and the stimulation and maintenance synapse formation [89, 106, 107].

A protein thought to be heavily involved in synapse formation is the synaptic vesicle protein synaptophysin (SYP) which has been seen to be highly expressed both before and during synaptogenesis [108, 109]. Synaptophysin has been seen to accumulate in the axons and growth cones before the formation of the synapse, indicating that vesicles are specifically transported to the axons. SYP has also been shown to cluster in areas of contact between axons and dendrites [109], and is generally considered a marker for synapses [110]. Upon clustering it is thought that SYP form a complex with vesicle-associated membrane protein 2 (VAMP2) which then continues to mediate the release of neurotransmitter from the pre-synaptic neuron through electrostatic and hydrophobic forces, allowing the synaptic vesicle to rapidly fuse with the membrane [111]. Knockdown of the SYP gene has been linked with altered behavior and impaired learning and memory in mice, causing poorer object recognition and spatial learning [112].

Microtubule associated protein 2 (MAP2) is a commonly found protein in the brain, being primarily expressed in neurons and some astrocytes and oligodendrocytes [113, 114]. In the neurons, MAP2 has been found to mainly be distributed in the dendrites and not in the axons [115], where it is thought to bind and stabilize microtubules [116]. MAP2 has been found to play a key role in neurite induction through interaction with F-actin leading to the bundling and stabilization of the microtubules [117, 118]. MAP2 is further believed to be important for the correct extension and branching of neurites [119], as well as being involved in the remodeling of dendrites and damage response in the post-synaptic area [120].

Microtubules are cytoskeletal structures making up the internal structure of the cells, being composed of α-tubulin and β-tubulin dimers [121]. A common tubulin found in the microtubules of the brain is β-III-tubulin, which has been shown to be incorporated in the neurites when they have matured into axons and dendrites. β-III-tubulin is thought to be involved in the perseverance and elongation of matured neurites [122]. Knockdown of β-III-tubulin has been linked to decreased viability upon oxidative insults, consequently it is thought that β-III-tubulin contributes to the stress tolerance of the cells towards free radicals and reactive oxygen species [123].

1.4 *In Vitro* Models

1.4.1 PC12

Pheochromocytoma (PC12) cells were isolated from a tumour found in the adrenal medulla of a rat and established as a clonal cell line when characterized by Greene and Tischler in 1976. Though not being neuronal in nature, these cells exhibit a large number of characteristics that make them physiologically similar to neurons. Upon treatment with nerve growth factor (NGF), the cells will stop proliferating and start adopting a morphology that closely resembles that of primary sympathetic neurons, with associated neuronal processes. Upon withdrawal from NGF, the cells will revert to their former morphology and start proliferating again or die by apoptosis [124, 125].

PC12 cells have been found capable of producing and storing the neurotransmitters dopamine, norepinephrine, and acetylcholine. Upon triggering of either nicotinic or muscarinic acetylcholine receptors depolarization of the cell occurs, in which subsequently leads to the release of these neurotransmitters [126]. The depolarization processes are largely governed by the function of Na^+, K^+, and Ca^{2+} ion channels which coats the membranes of the PC12 cells. The composition of these ion channels works in unison to achieve a membrane potential that can be modulated in much the same way as human neuronal stem cells [127].

The cellular processes of the PC12 cell line are well understood and has been extensively studied in regard to neuroscientific research. This cell line is therefore a good model system to use for the exploration of the adverse mechanistic outcomes following exposure to potentially toxic compounds. PC12 cells are easy to culture and handle and can easily be modulated to exhibit different relevant characteristics depending on the goal of the inquiry. This makes the PC12 cell line a suitable model system for the *in vitro* investigation of the neurotoxic effects of potentially toxic compounds and mixtures [127]. Though some concerns about the reliability of using PC12 for neurotoxic testing has been raised. Among these being that they do not express complete axons or create proper synapses [128]. Another concern may be the fact that the cells are of a non-human and a non-neural origin, which may cause problems when trying to extrapolate toxicological effects [7, 127].

1.4.2 Human Induced Pluripotent Stem Cells (hiPSCs)

The discovery that terminally differentiated fibroblasts could be reprogrammed to form pluripotent stem cells in mice by introducing the transcriptional factors Oct2/4 and Sox2, performed by Kazutoshi Takahashi and Shinya Yamanaka in 2006 has paved the way for the application of these types of cells for in a wide range of application [129]. Pluripotent stem cells (PSCs) in the form of human embryonic stem cells (hESCs) and human induced pluripotent stem cells (HiPSCs) is currently being used increasingly more in areas of basic research and within research related to regenerative medicine. One appealing factor which set PSCs apart from other human derived cell lines, like those deriving from cancer cells, is that they to a very large degree exhibit the same internal environment as one would expect of the cells in their natural state within the human body, though some concerns has

been raised in regard to how reprogramming might change the internal state of hiPSCs in relation to hESCs [130-132].

Undifferentiated hiPSCs are generally round with big nucleoli (see "Figure 1.1"), generally exhibiting (more than 80%) typical markers for pluripotency, such as Oct4, SSEA3, SSEA4, and Tra1-60. At this stage, the level of neuronal markers nestin and β-III-tubulin is low (below 8% and 3%, repectively). The process of inducing hiPSCs into neuronal precursor cells is initiated by cutting the IMR90 colonies into fragments, causing the formation of embryoid bodies (EB). The formation of EBs is accompanied with the formation of three germ layers signified by the increased expression of mesodermal (NPPA and brachyury), ectodermal (Pax6, Sox1, and nestin), endodermal (AFP, KRT18) genes. Plating of the embryoid bodies unto laminin coated dishes which are then set to incubate with neural induction medium cause the formation of rossettes. The formation of rosettes can be characterized by expression of the nestin marker (usually around 90%) and low expression of the β-III-tubulin marker [133].

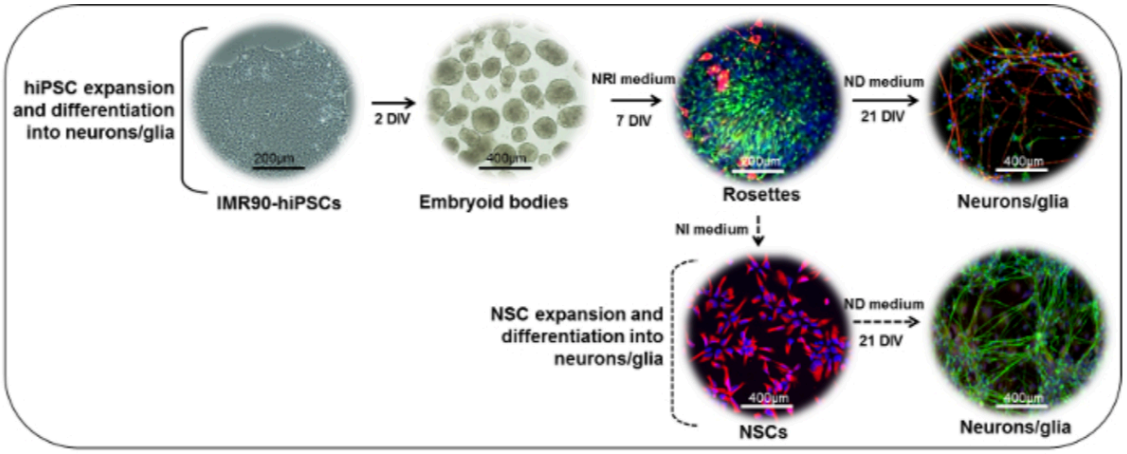

Figure 1.1: Overview of methodical steps in the induction and differentiation of neural stem cells (NSCs) from IMR90-hiPSCs. Showing the different steps in the protocol used for induction of IMR90 fibroblasts to hiPSCs, and further induction and differentiation of hiPSCs into neural stem cell (NSCs). At 2 days *in vitro* (DIV), cells are cut into fragments and plated unto laminin coated dishes, inducing the formation go embryoid bodies. Embryoid bodies may be incubated with neuroepithelial induction medium (7 DIV) in order to initiate the formation of rosettes expressing nestin (green) and β-III-tubulin (red). The rosettes can then either be set to incubate with either neural induction (NI) medium or neural differentiation (ND) medium giving rise to neural stem

cells expressing nestin (red), or neurons (NF200, green) and glia (GFAP, red) following 21 DIV, respectively. Figure is adapted from Pistollato et al. (2017) [133].

Differentiation of the rosettes is initiated upon incubation with neural differentiation medium, which will lead to the formation of a mixed culture containing both neurons and glia. Over time (approximately 21 DIV), the neurons will start to interconnect through neurites and form larger clusters of cells. Over time the expression the neuronal markers β-III-tubulin, NF200, Tau, and MAP2 will increase, signifying determination towards neuronal cells. The emergence of determined neurons will normally also be accompanied by cells expressing glia specific markers, such as glial fibrillary acidic protein (GFAP), maintaining a base layer expression of 20-30% nestin. At this point in differentiation, the overall composition of cells will be compromised of different subpopulations of GABAergic neurons (15-20%), dopaminergic neurons (13-20%), and glutamatergic neurons (35-42%). Each group, respectively, being signified by the expression of gamma-aminobutyric acid (GABA), tyrosine hydroxylase (TH), and vesicular glutamate transporter 1 (VGlut1). The differentiation can further be evaluated through analysis of genes and proteins related to these subpopulations, such as, the expression of microtubule-associated protein 2 (MAP2); the expression of synaptophysin (SYP), a presynaptic marker; Tyrosine hydroxylase (TH), a dopaminergic marker; GABRA1, a GABAergic marker; and more. The presence of glutamatergic and GABAergic cells indicates the cultures expressing features resembling those found in the forebrain and in the cerebrum, the presence of dopaminergic neurons may exhibit features resembling those found in the midbrain. This knowledge may be used to evaluate toxicological effects of chemicals upon the development of the nervous system [133].

During the process of induction and differentiation the different genes and proteins will change dynamically depending on the number of days *in vitro* (DIV) the culture has been allowed to differentiate, ultimately leading a mature cell culture containing neurons and glia (Figure 1.2) [133].

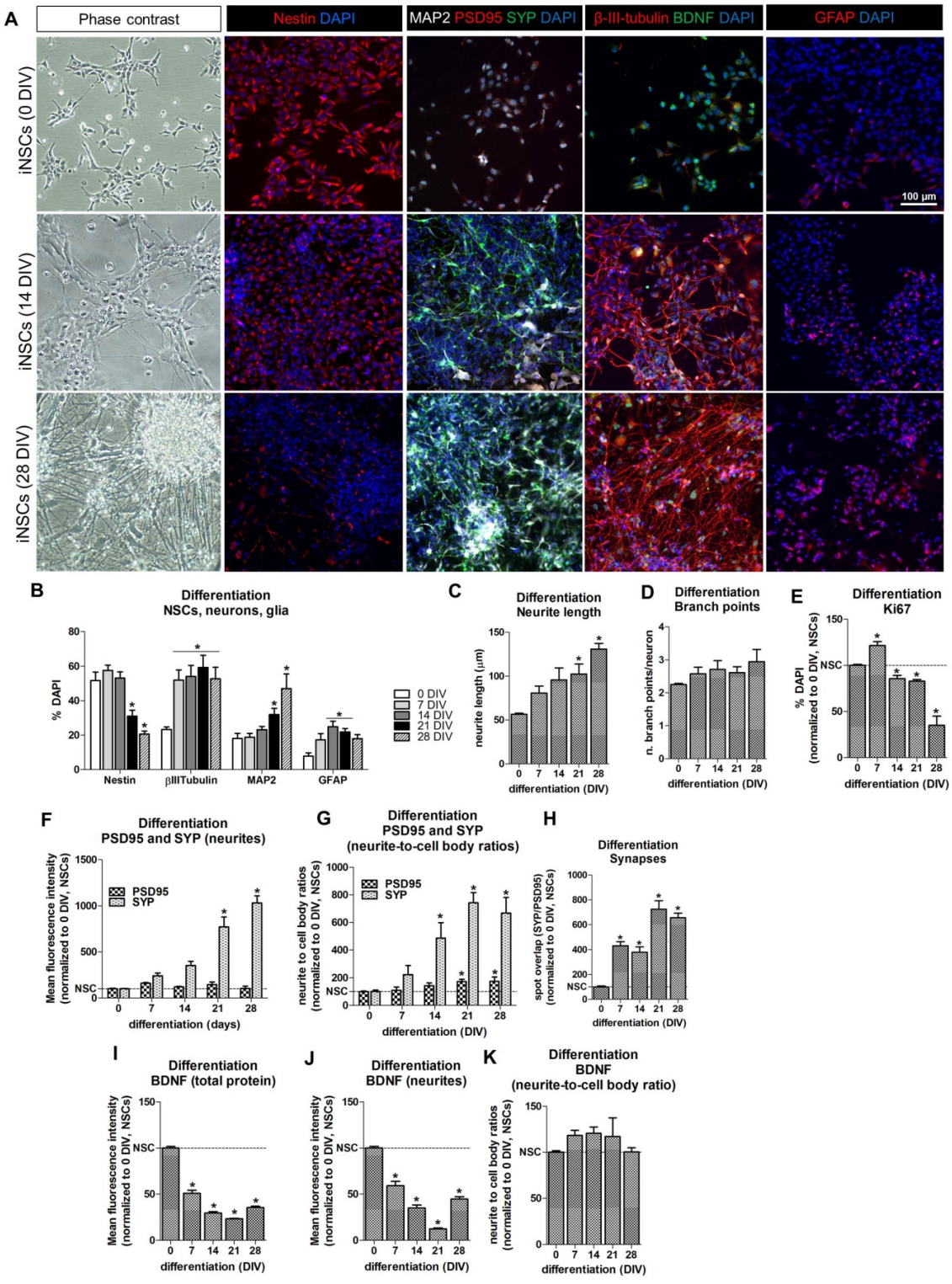

Figure 1.2: The Characterisation of IMR90-derived Neural Stem Cells (iNSCs) undergoing differentiation toward neurons and astrocytes. (A) Showing a representative phase contrast and immunocytochemical (IC) images of iNSCs (0 DIV, upper row), iNSCs following 14 days (14 DIV, middle row) and 28 days of differentiation (28 DIV, lower row). Immunocytochemical images display cells stained for nestin (red),

microtubule-associated protein-2 (MAP2, white) with postsynaptic density protein 95 (PSD95, red) and synaptophysin (SYP, green), β-III-tubulin (red) and brain derived neurotrophic factor (BDNF, green), and glial fibrillary acidic protein (GFAP, red). **(B)** The quantification of nestin, β-III-tubulin, MAP2 and GFAP expressing cells shown as a percentage of DAPI stained cells, comparing cells at 7, 14, 21 and 28 DIV with differentiation, to NSCs (0 DIV) (this graph was adapted from Fig. 1B graph in Pistollato et al. Neurochem. Int. 2017 Sep;108:457-471). Analysis was performed using immunofluorescence and high content imaging (HCI), using the Array Scan vTi platform and the Neuronal profiling V.4 BioApplication. **(C, D)** Neurite length analysis (C, adapted from Fig. 1D graph in Pistollato et al. Neurochem. Int. 2017 Sep;108457-471) and number of branch points per neurite **(D)** was evaluated by using β-III-tubulin staining and the Neurite Outgrowth V.4 BioApplication (same conditions as in B). **(F-H)** Shows the quantification of the levels PSD95 and SYP mean average intensity localized in neurites identified by MAP2 staining **(F)**, PSD95 and SYP mean average intensities in regard to neurite to cell body ratios (G), and number of SYP/PSD95 overlapping spots (indicating synapses) (all values have been normalized to undifferentiated NSCs, 0 DIV). **(I-K)** Showing the quantification of the total level of BDNF mean average intensity **(I)**, levels of BDNF mean average intensity specifically localized in neurites signified by β-III-tubulin staining **(J)**, and BDNF mean average intensities in respect to cell body ratio **(K)** (all values are normalized to undifferentiated NSCs, 0 DIV). Quantification of PSD95/SYP/MAP2 and BDNF/β-III-tubulin stained cells were done by using the Array Scan vTi platform and the Neuronal profiling V.4 BioApplication. Statistically significant results are presented with *$p<0.05$ as standard error mean based on three replicates, as validated by one-way ANOVA with Dunnett´s Multiple Comparison Test as Post Test, comparing all columns with undifferentiated cell column (NSCs, 0 DIV). Bars grouped by lines indicates a significant difference with NSCs (0 DIV). Figure is adapted from Pistollato et al. Neurochem. Int. 2017 Sep;108457-471 [133].

1.4.3 Adverse Outcome Pathways (AOPs)

The majority of human risk assessments conducted of chemicals is based on the documented effects following single compound treatment of animal models according to regulatory guidelines (e.g. OECD test no 426: Developmental neurotoxicity study),

measuring endpoints related to cognitive and other emergent behaviors, while offering little explanation to the fundamental mechanistic understanding of the observed toxicity [134]. These guidelines studies are expensive and highly time consuming, often amounting to outcomes that gives uncertain extrapolations towards human consequences of exposure [7]. With the discovery of new novel technologies and recent development of alternative test methods, efforts have been put forward to change the current paradigm of risk assessment in toxicology. Aiming to increase the over certainty and predictability of the toxicological outcomes, while additionally being more cost-efficient and ethically reduce animal testing [135].

A model that has been developed to accommodate this reformation of the risk assessment field in toxicology is the introduction of the Adverse Outcome Pathway (AOP) framework (See "Figure 1.3"), which builds upon all current literature describing toxicological modes of action by outlining categorical pathways of toxicology and which may be applied to all sub-fields of toxicology (e.g. neurological, developmental, cancer) [136]. This framework takes into account the different levels of biological organization and gives a clear more simplistic outline of the key events (KE) and key event relationships (KER) leading up to a deleterious toxicological event, which in the AOP framework is referred to as an adverse outcome (AO). An adverse outcome pathway will generally start with a molecular initiation event (MIE) that signifies the first interaction between the chemical and the biological system which leads to a key event [134, 137]. A framework of this sort can more easily rely on *in vitro* methods such as hiPSCs [133], and can easily be synergized with computational models [136].

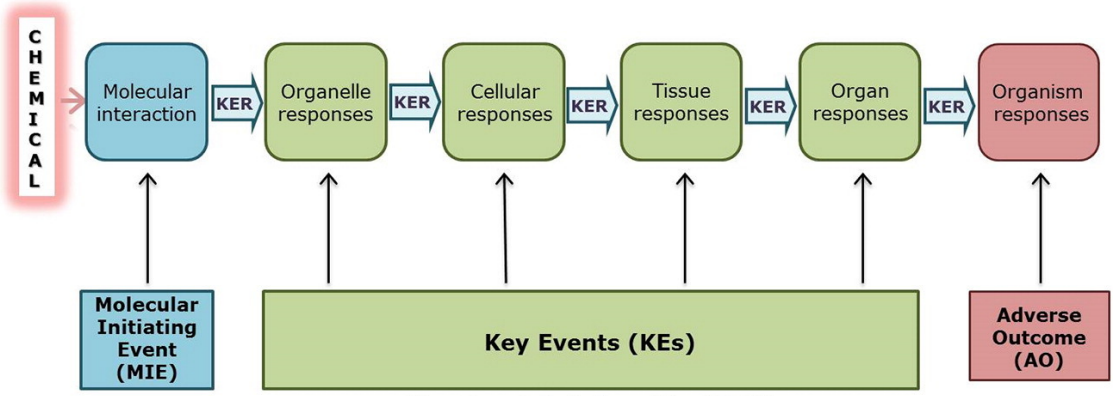

Figure 1.3: The Fundamental Concept of the AOP framework. Outlining the AOP framework following a chemical initiating a molecular initiating event (MIE) leading to a

series of key events (KEs) that are connected by a key event relationship (KER) leading to adverse outcome on the organism level. Figure is modified and adapted from Bal-Price et. al. 2017 [7].

When applying the AOP framework to developmental neurotoxicity the apparent complexity of nervous development has to be accounted for. The diverse nature exhibited by the function and structure of the nervous system suggests that the underlying mechanisms leading to neurotoxic outcomes might not be overtly simple. As the pathways of toxicity may not always be completely linear, having multiple MIEs leading to one KE and being that multiple mechanisms may function co-dependently and adjust according to each other. One solution to this apparent problem has been to identify converging KEs that specific to common MIEs [136, 138, 139]. One such model has been proposed by Sachana et. al. 2016 [140], which highlights the relationship from the binding of agonists to ionotropic glutamate receptors (MIE) leading to the overactivation of NMDA receptor (KE), which is followed by a series of key events amounting to reduced release of BDNF, causing decreased synaptogenesis, which manifests as decreased neuronal function which will ultimately cause impairment in the learning and memory capabilities of the organism (Figure 1.4) [140].

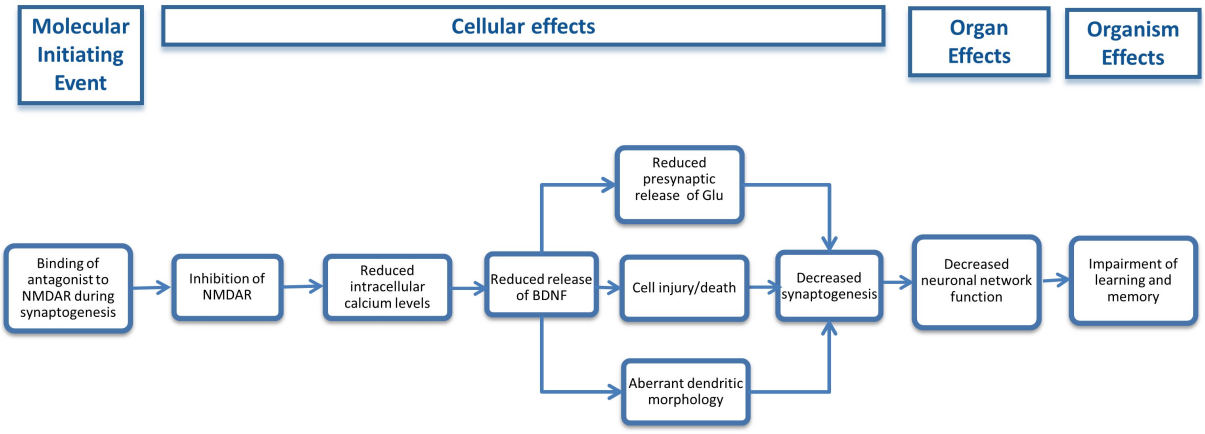

Figure 1.4: The AOP following antagonist binding to NMDA receptor during synaptogenesis. Neurotoxicity adapted to the AOP framework, showing the series of key events (KE) following the molecular initiating event (MIE) ultimately leading to decreased neuronal function and impairments in learning and memory. Figure is adapted from Sachana et. al. 2016 [140].

Though simple, the AOP framework is not completely without criticism. Common criticism being that the framework offered gives a too simplistic view on biological systems by not truly reflecting the complexity of toxicity upon biological systems. Presenting toxicological pathways as linear events, rather than parallel cascades may give a too simplistic view on how toxicological outcomes may develop [134]. Another concern is the general lack of understanding of the relationship between the triggering MIEs and KEs amounting to AOs. Additionally, there is still a big lack of fundamental and mechanistic understanding on how many common neurodevelopmental disorders develop, which complicates the development of relevant AOPs [7].

1.5 Aims of the Study

The harmful and toxicological effects of the accumulation of POPs upon humans and the environment has been widely observed. As they have been documented to induce harmful effects such as, cancer, damage the nervous system, induce birth defects, and modulate the immune and reproductive system [2]. At this point the understanding on how all these chemicals may interact with each other in mixtures is largely unknown, which in reality is how the populace are exposed to these compounds.

The main aim was to investigate how mixtures of POPs may induced developmental neurotoxic effects in neuronal stem cell cultures at concentrations relevant to human exposure and link these with health outcomes by use of the AOP framework.

The specific aims are:

- Evaluate how a complex mixture of 29 POPs may affect cell viability in PC12 cells.
- Investigate how these POP mixtures affects cell viability and neurodevelopmental processes in cell cultures derived from hiPSCs through assessment of the expression of proteins and genes related to neuronal development.
- Clarify interactions between chemically similar sub-mixtures in causing perturbations of neurodevelopmental outcomes.

- Attempt to link neurodevelopmental outcomes of *in vitro* studies with the MIEs and KEs of the AOP framework to elucidate the mechanisms behind neurodevelopmental effects.

2. Materials and Methods

2.1 PC12 Cells

Table 2.1: Products and Reagents Table for PC12 cells

Product/Reagent	Serial number	Supplier
Dimethyl sulfoxide	41639-500mL	Sigma
BioWhittaker DMEM	BE12-700F	Lonza Walkersville inc
Fetal bovine serum	10270	Gibco by Life Technologies
Horse serum	1131917	Gibco by Life Technologies
Sodium pyruvate	11360-070	Gibco by Life Technologies
L-Glutamine	BE17-605	Lonza
Pencillin Streptemycin	15140-122	Gibco by Life Technologies
Thiazolyl Blue Tetrazonium Bromide (MTT)	M5655-500MG	Sigma
SDS (Natrium dodecyl sulfate)	L4509	Sigma-Aldrich
Precision Plus Protein Standards	161-0374	Bio-Rad
2-merceptoetanol	M3148	Sigma-Aldrich
Trypan blue	T6146	Sigma-Aldrich
Leupeptin	L9783	Sigma
Pepstatin A	P5318	Sigma
PMSF	P-7626	Sigma
Na3VO4	S-6508	Sigma
Glycerol 87%	24 385.295	NORMAPUR
Luminata HPR substrate	WBLUF	Millipore
Luminata Classico Western	WBLUC	Biocompare
DMSO		Sigma Aldrich
Phosphate-buffered saline (PBS)		Universiry of Oslo
Dry milk		Local distributor, Norway
NaCl		
Tris-HCL		
Ethanol 96%		
Distilled Water		

Table 2.2: Equipment Table for PC12 Cells

Equipment	Manufacturer
CLARIOstar	BMG Labtech
Pipettes	Various
Pipette tips, 0.1-10 µL	Optifit
Pipette tips, 2-200 µL	Optifit
Pipette tips, 10-1000 µL	Optifit
Pippettes, 5 mL, 10 mL, 25 mL	Costar, Corning Inc.
96-well plate, Nucleon™ Delta Surface	NuncTM, Thermo Fisher
Nunc™ EasYFlask™ 75 cm2 Nucleon™ Delta Surface	NuncTM, Thermo Fisher
Cell culture plate, Nucleon™ Delta Surface	NuncTM, Thermo Fisher
Centrifuge Tube, 5 mL, 15 mL, 50 mL	Corning Incorporated
Cell scraper	Corning Incorporated
Cell temperature and CO2 incubator	Thermo Scietific
Gel electrophoresis machine (Power Pac 300)	Bio-Rad Labratories, Inc.
Light microscope	Nikon
Nitrocellulose membrane	Bio-Rad Labratories, Inc.
Blotting machine TransBlot® Turbo	Bio-Rad Labratories, Inc.
Developing Casette	Simes
Gel documentation system	Syngene
Pipetboy	Integra Biosciences Zizers
Fridge	Electrolux
Counting chamber	Bürcher
Excel	Microsoft
GraphPad Prism 5	Graphpad Prism Inc.
JMP Pro 13	SAS Institute

Table 2.3: Antibodies and Staining solutions Table for PC12 Cells

Antibodies and staining solutions	Cat no.	Supplier	Dilutions
Proliferating Cell Nuclear Antigen (PCNA) (Mouse)	MO879	DAKO	1:1000
Anti-Beta-Actin (Mouse)	A5441	Sigma Aldrich	1:5000
Anti-Mouse IgG (Goat)	A2304	Sigma Aldrich	1:10000

2.1.1 Storage and Culture

All the PC12 cells used in this experiment was supplied to us from the lab of Ragnhild Paulsen at the University of Oslo. Cells were kept in 75 cm^3 flasks with PC12 cell medium (as described in "Table 2.4") in an incubator at 37°C and 5% CO_2. Cells were split one to two times a week, approximately every 5 days, depending on level of confluency.

Table 2.4: Contents of PC12 cell medium.

Component:	Volume:
Dulbecco's MEM	500 mL
Fetal bovine serum (10%)	50 mL
Horse serum (5%)	25 mL
Pyruvate	5 mL
Streptomycin penicillin	5 mL
Glutamine	10 mL

2.1.2 Splitting of PC12 Cells to Bottle

1. Cell medium (DMEM, as described in "Table 2.4") is heated to 37°C on water bath.
2. Flask containing PC12 cells are checked for confluency under a microscope.
3. The medium is removed from the flask and 10 mL of fresh cell medium is then added to the flask containing the confluent cells.

4. The flask is then repeatedly hit into the bench to loosen the confluent cells.

5. The medium containing the cells is then pipetted up and down (~8 times), separating lumps of aggregated cells. Check in microscope for aggregates. If cell aggregates are still found, do additional pipetting.

6. Distribute 1.5 mL of the medium into a new bottle. Add 20 mL of fresh medium.

7. Loosen the caps of the bottles and put them to incubate at 37°C and 5% CO_2.

2.1.3 Splitting of PC12 Cells to Wells/Dishes

Protocol

1. Perform step 1-6 as described in "2.1.2 Splitting of PC12 cells to bottle".

2. Determine amount of cell solution which is needed to seed the wells/dishes, 100 µL for well, 1 mL for small dishes, and 10 mL for big dishes

3. A small sample (10 µL) is taken out from the old bottle and applied to a Neubauer chamber, cells are counted in each gridded square using a light microscope. And an average from three different gridded squares is calculated.

4. Calculate the amount of cell solution needed to achieve $10*10^4$ cells/mL. Do the calculation based on the average amount of cells observed during counting using this formula:

$$Cell\ solution\ (mL) = \frac{Required\ final\ volume\ (mL) * (10 * 10^4\ cells/mL)}{Calculated\ average * 10^4 cells/mL}$$

5. Take the calculated cell solution out from the old bottle and add medium to get the required final volume.

6. Transfer cell solution to wells (100 µL/well), small dishes (1 mL/dish), big dishes (10 mL/dish).

7. Incubate at 37°C and 5% CO_2.

2.1.4 Exposure of PC12 Cells

The stock mixtures of POPs were prepared and given to us from the lab of Erik Ropstad at the School of Veterinary Medicine at the Norwegian University of Life sciences. The original stock mixture used was at 1000 000x that of the concentrations found in human samples. Dilutions 1x, 10x, 100x, 500x, and 1000x was prepared ("Table 2.5"), based on human values.

Table 2.5: Using the 1 000 000x POP stock solution, multiple sub stocks were made with concentrations 1000x, 10 000x, 100 000x, 500 000x, and 1 000 000x using DMSO. The sub mixtures were then diluted to the concentrations 1x, 10x, 100x, 500x, and 1000x using DMEM cell medium. In 1000 µL medium, 1 µL of sub stock is added.

Original stock with total POP mixture:	1 000 000x				
Sub stocks (DMSO dilute):	1000x	10 000x	100 000x	500 000x	1 000 000x
Final dilutions (DMEM dilute):	1x	10x	100x	500x	1000x

Protocol

1. Dilute the POPs stock solution to the desired concentration using DMEM (See "Table 2.5").
2. Remove medium from the PC12 cell cultures.
3. Add an equal amount of exposure mix to the cultures.
4. Incubate at 37°C and 5% CO_2 for the required exposure time.

2.1.5 MTT-Assay

MTT (3-[4,5-dimethylthiazol-2-yl]-2,5 diphenyl tetrazolium bromide) assay is a method used to measure the viability of cell cultures by reading the absorbance of dissolved formazan crystals at 570 nm. The conversion of the tetrazolium salt MTT to formazan crystals is dependent on the mitochondrial activity in living cells, the conversion rate is therefore proportional to the amount of living cells, assuming that the mitochondrial activity is constant. Based on this proportionality the relative viability of cells can be determined by comparing a control with treatments of different concentrations [141].

Protocol

1. Make a set up and determine number of wells in which will be used. Typically, a 96-well plate is used.
2. Calculate the required amount of MTT. There should be 10 µL MTT solution for each well with concentration 5 mg MTT/mL PBS.
3. Measure the required amount of MTT.
4. Dissolve the MTT in PBS.
5. Mix the MTT solution to DMEM with the ratio 1:10.
6. Add 100 µL of the MTT/DMEM-solution to each well.
7. Incubate at 37°C and 5% CO_2 for 3-4 hours.
8. Remove MTT from wells and add 100 µL DMSO. Incubate at room temperature while shaking for 30 min.
9. Read samples at 570 nm with a CLARIOstar plate reader.

2.1.6 Harvesting for Western Blotting

The cells are lysed using sodium dodecyl sulfate (SDS). The lysate is then treated with protease inhibitors in cold conditions to prevent degradation (see Table 2.6). Commonly the protein concentration is measured to prepare a dilution, in order to compare the samples on an equal basis [142].

Table 2.6: Components added to a single dish when harvesting for western blotting. 2% SDS with protease inhibitors.

Component:	Volume:
2% SDS	100 µL
Leupeptin P (5 mg/mL)	1:1000
Pepstatin A (1 mg/mL)	1:200
PMSF (100 mM)	3:1000
Na3VO4 (10 mM)	1:100

Protocol

1. Pour out the medium, pipette out the residues.
2. Wash two times with 3 mL cold PBS. Remove the PBS wash using a pipette.
3. In each single dish, add 100 µL of the 2% SDS solution as described in "Table 2.6".
4. Using a cell scraper, scrape the cells in two different directions, perpendicular to each other.
5. Transfer the solution following the scraping to an Eppendorf tube, put the Eppendorf tube on ice.
6. Boil the samples at 95°C for 5 minutes.
7. Freeze the samples at – 20°C.

2.1.7 Western Blotting

Western blotting is a technique commonly used to detect and quantify specific proteins in complex mixtures of proteins, like those found in cells or tissue samples. The proteins are then separated in regard to their size/weight, and by attachment of antibody. In the first step, gel electrophoresis is used to separate the proteins based on charge which is proportional to their size/weight. In the second step, the proteins following separation with gel electrophoresis are transferred to a membrane. The membrane is then incubated with antibodies specific for the protein that is to be detected and quantified. If no protein of

interest is present in the membrane, no antibody binding will occur. The membrane is then developed, and the relative amounts of protein can be quantified by comparing intensities of the bands produced from antibody binding [142].

In western blotting, it is common to use a loading control in order to determine that the sample contains protein. Typically, proteins originating from housekeeping genes will be selected as loading control. Housekeeping genes are genes that are constitutively being expressed regardless of cell type and cell state and should not be affected by the treatments inflicted to the cells. A protein originating from one such gene is β-actin.

Laemmli buffer (4x) is first prepared according to "Table 2.7" to be used as loading buffer with the samples, which is to be mixed with 2-Mercaptoethanol and sample with the ratio 1:3 as described in "Table 2.8". Before electrophoresis the Laemmeli buffer, 2-mercaptoethanol and sample mixture is heated to 90°C for 5 minutes.

Table 2.7: Composition of Laemmeli buffer (4x).

Component:	Volume:
20% SDS	25 mL
Glycerol 87%	14.7 mL
Tris-HCl - pH 6.8	9.4 mL
Distilled water	0.9 mL
Bromphenol blue	A few granules (enough to make the solution blue)

Table 2.8: Preparation of samples, components to be mixed.

Component:	Volume:
4 x Laemmlibuffer	5 µL
2-Metcaptoethanol	1 µL
Sample	14 µL
Total loading sample:	20 µL

Protocol

1. Using a readymade gel, remove the comb and the plastic attached under the gel.
2. The gel is placed in a tub containing Elfo-buffer (Elfo solution diluted in distilled water 1:10).
3. Apply 5 µL standard (Precision Plus Protein Standards ladder) for use as size marker.
4. Using the frozen samples prepare loading samples as described in "Table 2.8", before they are set to boil at 90°C for 5 minutes.
5. The gel is set to run at 150 V for approximately 60 minutes.
6. Blotting paper and nitrocellulose membrane is moisturized with blotting buffer (made from 5x transferbuffer). The gel is packed as a sandwich between the blotting paper and the nitrocellulose membrane and put in the blotting machine for 10 minutes.
7. When the blotting is done, the nitrocellulose membrane (containing the proteins) is stained with Ponceau, before washing with distilled water. Put the membrane in a plastic container.
8. Picture is taken of the gel using a gel documentation system.
9. Place the membrane with the protein side facing inward in a 50 mL tube.
10. Add 5 mL TBS tween with 5% dry milk blocking solution to the tube and incubate it while rolling in room temperature for 1 hour minimum.
11. Dispose of the blocking solution and add primary antibody (PCNA) with ratio 1:1000 in 5 mL blocking solution.
12. Put the tube to incubate rolling overnight in a cold room.
13. The following day, dispose of the antibody solution and wash 3 x 10 minutes with TBS tween.
14. Add secondary antibody (goat anti-mouse) with ratio 1:10000 in 5 mL blocking solution.

15. Incubate at room temperature for 1 hour while rolling.

16. Wash the membrane with 5 mL PBS while rolling for 10 minutes at room temperature, repeat twice.

17. Remove the washing solution, dry the membrane by placing it on absorbing paper.

18. Put the membrane on a glass plate with the protein side facing up. Then develop the membrane by adding 1,5 mL classico developing solution (cover the entire membrane) and let it incubate for 5 minutes.

19. Wash membrane in 5 mL PBS while rolling for 10 minutes at room temperature.

20. Remove wash solution by putting it on absorbing paper.

21. Put the membrane protein side down in detection reagent Luminate HPR substrate for 4 minutes.

22. Put the membrane in a plastic bag and put it in a developing cassette.

23. The membrane is read using gel documentation system (Syngene).

24. Protein levels are quantified using ImageJ.

2.1.8 Trypan Blue Staining and Counting

Trypan blue counting is based on the uptake of the trypan blue dye that occurs in dead cells. This uptake is due to the loss of cell membrane integrity that occurs when the cell dies, making it possible for the trypan blue dye to diffuse into the cell. Living cells will have an intact cell membrane and will not take up dye from its surroundings. The difference between cells that has not taken up dye (unstained) and cells that has taken up dye (blue) can be distinguished and counted using a light microscope [143].

Table 2.9: Trypan blue staining is performed by combining the two stock solutions 2% trypan blue and 1.8 g NaCl solution, with a ratio 1:1.

2% Stock solution trypan blue	
Component:	Volume:
Trypan blue	1.0 g
Distilled water	50 mL
NaCl Stock solution (1.8g/ 100mL)	
Component:	Volume:
NaCl	1.8 g
Distilled water	100 mL

Protocol

1. Prepare the Trypan blue stock solution as shown in "Table 2.9", heat up until boiling while stirring. Cool to room temperature.
2. Filter the solution, and store at room temperature.
3. Mix trypan blue stock solution with NaCl stock solution (1.8g/100 mL) with the ratio 1:1.
4. Remove old medium from the plates.
5. Add trypan blue solution and cell medium with the ratio 1:4 (the plates were added 250 µL trypan blue solution, and 1000 µL cell medium).
6. Plates is set to incubate at 37°C for 30 minutes.
7. Remove trypan blue-medium solution.
8. Examine plates in the microscope using 40x magnification, count blue and unstained cells separately. Do this 4-5 places, counting up about 100 cells in total. Calculate ratio of the blue and unstained cells in relation to each other.

2.1.9 Statistics

Cell Viability

Averages were calculated for each concentration in each plate. The results were then normalized in regard to the control containing DMSO in medium (ratio 1:1000). Data was then visualized, and statistically significant results were determined by using one-way ANOVA with Dunnett´s Multiple Comparison Test, with a significance of *$p<0.05$. The software used to do this was Excel (Microsoft) and GraphPad Prism 5.

Western Blotting

All samples were normalized according to β-actin by comparing the intensity of each individual band using ImageJ software. Statistically significant results were determined by using one-way ANOVA with Dunnett´s Multiple Comparison Test, with a significance of *$p<0.05$. The software used to do this was Excel (Microsoft) and GraphPad Prism 5.

2.2 HiPSC-derived Neural Stem Cells

The human induced pluripotent stem cells (hiPSCs) used in this experiment were provided to us from the European Union Reference Laboratory for Alternatives to Animal Testing (EURL-ECVAM) under supervision of Dr. Anna Price and Dr. Francesca Pistollato.

The original hiPSCs used in this experiment was induced from IMR90 fibroblasts collected from lung tissue of a 16-week-old fetus, using the transcription factors Oct4 and Sox2 by viral transduction with pMIG vectors at I-Stem in France [132].

Table 2.10: Products and Reagents Table for HiPSCs

Product/ Reagent	Cat No.	Supplier
hiPSCS (reprogrammed IMR90 fibroblasts)		I-Stem, France
B27 Serum-Free Sumplement (50X), withouth vitamin A	12587010	Thermo-Fisher
B27 Serum-Free Sumplement (50X)	12587010	Gibco/Invitrogen
BDNF	PHC7074	Invitrogen
BSA (7.5% solution)	A8412	Sigma
GDNF	PHC7045	Thermo-Fisher
bFGF	13256-029	Thermo-Fisher
Defined Trypsin Inhibitor	R-007-100	Invitrogen

DMEM/F12	3133-038	Invitrogen
DMSO	M81802	Sigma-Aldrich
EGF Recombinant Human Protein, Animal-Origin Free	PHG6045	Invitrogen
Heparin Grade I-A, ≥180 USP units/mg	H3149-100KU	Sigma-Aldrich
L-Glutamin 200 mM Solution	25030-081	Gibco
Matrigel® Basement Membrane Matrix	354234	Corning
N2 Supplement	17502-048	Thermo-Fisher
NEAA: Non-Essential Amino Acids	11140-035	Thermo-Fisher
2-Propanol	190764	Sigma
P/S: Penicillin/ Streptomycine	15140-122	Thermo-Fisher
Sterile-Filtered Water	W3500	Sigma
Trypan Blue (0.4%)	T8154	Sigma-Aldrich
Trypsin-EDTA (0.5%), no phenol red	15400-054	Gibco
mTeSR™ 1 Basal Medium	05851	Stem Cell Technologies
MteSR™ 1 5X Supplements	05852	Stem Cell Technologies
Formaldehyde 37%	252549	Sigma-Aldrich
PBS 1x without Ca2+ and Mg2+	14190144	Thermo-Fisher
Triton-X-100	Sigma-Aldrich	93443-100ML
BSA 35%	Sigma-Aldrich	A7979-50ML
CryoStor cell cryopreservation medium	SIgma-Aldrich	C2874-100ML
Laminin	L2020	Sigma-Aldrich
Poly-di-Ornithine	P0671-25MG	Sigma-Aldrich
Neurobasal Medium	21103049	Thermo-Fisher
Sealing Tape, Black	236703	Thermo Scientific
RNAaqueous®-Micro Kit	AM1931	Life Technologies
High Capacity cDNA Reverse Transcription Kit	4368814	Thermo-Fisher
TaqMan Gene Expression Master Mix	4369016	Thermo-Fisher
TaqMan Gene Expression Assay	4331182	Thermo-Fisher

Table 2.11: Equipment Table for HiPSCs

Equipment	**Supplier**
15 mL conical plastic tubes	TPP
50 mL conical plastic tubes	TPP
25 cm2 cell culture flasks with filtered cap (T-25)	Corning
5 mL plastic pipettes (Dispenser)	TPP
10 mL plastic pipettes (Dispenser)	TPP
60 mm Petri dishes	TPP
Countess Cell Counting Chamber	Invitrogene
Cryovials Nalgene®	Sigma

Eppendorf tubes	Eppendorf
Gibson 20 µL dualfilter pipette tips	Eppendorf
Gibson 300 µL dualfilter pipette tips	Eppendorf
Gibson 20-200 µL filter pipette tips	Diamond
Poly-D-Lysine coated 96 well plates	Corning
Sterile Deep Well plates for serial dilution	Eppendorf
Multi-well Fluorimetric Reader	Tecan
Cellomics ArrayScan VTI high content imaging instrument	Thermo-Fisher
Cellomics iDEV-High Content intelligent acquisition software	Thermo-Fisher
7900HT Fast Real-Time PCR System	Thermo-Fisher
NALGENE Mr. Frosty™ freezing container	Sigma-Aldrich
Benchtop centrifuge	
Countess® Automated Cell Counter	
Fridge (4 °C)	
Freezer (-20 °C and -80 °C)	
Humidified incubator (37 °C, 5 % CO2 in air)	
Ice machine	
Laminar flow hood for sterile atmosphere (type II classified)	
Liquid nitrogen storage	
Micropipettes	
Milli-Q water dispenser	
pH meter	
Stereoscopic (dissecting) microscope	
Water bath	
Powder-free Nitrile Gloves (Microflex)	

Table 2.12: Antibodies and Staining Solutions for HiPSCs

Antibodies and staining solutions	**Cat no.**	**Supplier**	**Dilutions**
B-III-tubulin (Tuj1)	Covance	MMS-435P	1:500
MAP2	Abcam	AB5392	1:5000
GFAP	Thermo-Fisher	PA1-10004	1:500
Nestin	Sigma-Aldrich	N5413	1:200
synaptophysin (SYN)	Abcam	AB14692	1:400
PSD95 [7E3-1B8]	Abcam	AB13552	1:300
Goat Anti-Chicken IgY H&L (DyLight® 488) preadsorbed	Abcam	ab96951	1:500
Goat Anti-Rabbit IgG H&L (DyLight® 650) preadsorbed	Abcam	ab96902	1:500
Goat Anti-Mouse IgG H&L (DyLight®	Abcam	ab96880	1:500

550) preadsorbed			
Ki67	Thermo-Fisher	MAB4190	1:200
BDNF	Thermo-Fisher	PA5-15198	1:50
Donkey anti-Rabbit IgG (H+L) Cross Adsorbed Secondary Antibody, DyLight 594 conjugate	Thermo-Fisher	SA5-10040	1:500
Donkey anti-Mouse IgG (H+L) Cross Adsorbed Secondary Antibody, DyLight 488 conjugate	Thermo-Fisher	SA5-10166	1:500
DAPI Solution (1 mg/ml)	Thermo-Fisher	62248	1:1000

Table 2.13: Primers Table for HiSPCs

Gene	Cat no.	Category	Supplier
PAX6	Hs01088112_m1	Neural Stem Cells	Thermo Fisher
GFAP	Hs00909233_m1	Astrocytes	Thermo Fisher
MAP2	Hs00258900_m1	Commited and mature Neurons	Thermo Fisher
SYP	Hs00300531_m1	Commited and mature Neurons	Thermo Fisher
NTRk2	Hs00178811_m1	Commited and mature Neurons	Thermo Fisher
GPHN	Hs00982840_m1	Commited and mature Neurons	Thermo Fisher
DLG4	Hs01555373_m1	Commited and mature Neurons	Thermo Fisher
GAPDH	Hs02758991_g1	Reference gene	Thermo Fisher
ACTB	Hs99999903_m1	Reference gene	Thermo Fisher

2.2.1 Preparation of Flask and Thawing of HiPSC-derived Neural Stem Cells

Cell vials to be thawed are collected from the liquid nitrogen freezer holding -80 °C, where the cells are preserved in the vapor phase of the liquid nitrogen. The thawed cells are stored in an incubator maintaining 37°C and 5% CO_2.

Table 2.14: Neural induction (NI) medium with all necessary components and mitogens.

Neural Induction (NI) Medium	Final Concentration	Volume 500 mL
DMEM/F12	1x	490 mL
NEAA	1x	5 mL

N2 Supplement	1x	5 mL
Penicillin/ Streptomycin	50 U/mL	2.5 mL
Heparin	2 µg/mL	1 mL
B27 supplement (50x)	1x	10 mL
L-Glutamine	2 mM	5 mL
Mitogens to be added before use:		
bFGF	10 ng/mL	500 µL
EGF	10 ng/mL	500 µL
BDNF	2.5 ng/mL	125 µL

Protocol

1. Sterilize the hood and the working space, find required equipment and disinfect.
2. Dilute Matrigel in cold DMEM/F12 medium with the ratio 1:100 using chilled tips and pipettes, as Matrigel will solidify at approximately 20 °C.
3. Transfer 3 mL of the Matrigel/DMEM solution to a 75 cm^2 bottle, leave flask to incubate for 1 hour at 37°C, take it so out and leave it to incubate at room temperature for 30 min.
4. Take frozen neural stem cells (NSCs) (stored at -80 °C in liquid nitrogen) and thaw them by transferring them to a water bath at 37 °C for about 1-2 minutes. Mix gently with 6 mL pre-warmed NI medium (37 °C).
5. Centrifuge at 1000 rpm for 4.5 minutes in order to remove DMSO.
6. Remove the supernatant keeping the pellet intact. Then resuspend the pellet by adding 2 mL NI medium.
7. Carefully dilute the cell suspension by adding 4-5 mL of pre-heated (37 °C) complete NI medium.

8. Determine the number of cells by taking out 20 µL from the cell suspension and mixing it with 20 µL trypan blue (maintaining 1:1 ratio). Count the cells using an automated cell counter.

9. Remove the Matrigel/DMEM solution from the 75 cm^2 flask. Add approximately $3.5*10^6$ cells to the bottle.

10. Incubate at 37°C and 5% CO_2, replace NI complete medium every 48 hours.

2.2.2 Changing Medium of Flask

Protocol

1. Pre-warm NI medium to 37°C.

2. Open the sterile hood and disinfect working space.

3. Take the flask out the incubator, flip flask over to the side and aspire all but 1 mL of the old medium from the wall of the flask.

4. Add approximately 17 mL of fresh pre-heated NI medium.

5. Put flask with the cells and fresh medium back in the incubator at 37°C and 5% CO_2.

6. Change medium three times a week, every 48 hours.

2.2.3 Passaging of HiPSC-Derived Neural Stem Cells

Passaging is performed whenever the cell culture in the flask reaches confluency, which happens when the cells are allowed incubate and proliferate until covering 100% of the coated surface of the flask.

$$Needed\ volume\ of\ medium = (96\ wells\ x\ number\ of\ plates\ x\ 150\ \mu L) + 20\%\ extra\ volume$$

+

$$Number\ of\ cells\ needed = (\frac{Needed\ volume\ of\ medium}{150 \mu L\ medium\ per\ well})\ \text{x 6000 cells per well}$$

Figure 2.1: Calculations to be done for seeding of NSCs to 96-well plates. The equation on top shows the needed volume given a certain number of 96-well plates being seeded with 150 µL medium in each well added 20% for safe measure. The second equation shows the required number of cells to be added to the medium in order to seed the required number of wells with 6000 cells.

Protocol

1. Add 10 mL of pre-diluted Matrigel (as described in section "2.2.1 Preparation of Flask and Thawing of HiPSC-derived Neural Stem Cells", step 1-3) to a 75 cm^2 flask in order to coat it.

2. For splitting to 96-well plates, prepare plates by coating the wells with 100 µL matrigel diluted in DMEM/F12 medium (1:100) and incubate for 37 °C for 1 hour.

3. 1 mL 0.5% Trypsin-EDTA is mixed with 9 mL PBS to dilute the trypsin.

4. Aspire old medium from the flask containing confluent cells.

5. Add 6 mL of the diluted trypsin solution by flushing it over the cells. Put so the flask in the incubator for 2 minutes.

6. Aspire the Trypsin solution containing the cells and transfer them to a falcon tube.

7. Add 6 mL Defined Trypsin Inhibitor to the falcon tube to neutralize the trypsin.

8. Transfer the cell solution to a falcon tube, and centrifuge for 4.5 minutes at 1000 rpm.

9. Aspirate the supernatant without touching the pellet.

10. Resuspend the pellet with 10 mL NI medium (complete). Homogenize the cell suspension by gentle mixing.

11. Take 21 µL of the cell suspension and mix it with 21 µL Trypan Blue dye and quantify them by loading the mixture to a Countess counting chamber slide and mounting it in a Countess® Automated Cell counter to find the number of cells per milliliter.

12. Determine needed amount of cell suspension needed to seed 6000 cells per well using the equation (as seen in "Figure 2.1) with 150 µL medium in each well.

13. Aspire the DMEM/matrigrel solution from the new flask and transfer $3.5*10^6$ cells from the cell suspension. Mix with approximately 15 mL NI medium.

14. Incubate plates and flask at 37 °C and 5% CO_2.

2.2.4 Treatment of Neural Stem Cells

For treatment of the neural stem cells, dilutions were set up with the concentrations 0.1x, 0.5x, 1x, 10x, 100x, 500x, and 1000x for each of the mixtures. Using each original stock at 1 000 000x human blood concentration, dilutions were prepared so that they would be diluted 1:1000 when added to the cell medium (see "Table 2.15"). Treatments are done with different time intervals, varying time of differentiation and time of exposure. The NSCs are treated at 1 and 14 days of differentiation with 3 and 14 days of exposure.

Table 2.15: Set up of dilutions done for treatment of the NSCs. From the original stock of 1 000 000x, 100 µL was initially taken and transferred to the tube to be used as stock for 1000x when diluted with cell medium. Subsequently, 40 µL was taken from this and transferred to the tube to be used as stock for 500x, in which additionally 40 µL of DMSO was added. This was done in accordance with the table for all concentrations. The same set up was used for all 4 mixtures.

Original stock:	1 000 000x						
Sub stocks:	1 000 000x	500 000x	100 000x	10 000x	1 000x	500x	100x
POP solution added from previous:	100 µL (from Original stock)	40 µL	15 µL	10 µL	10 µL	40 µL	15 µL
DMSO added:	0 µL	40 µL	60 µL	90 µL	90 µL	40 µL	60 µL
Medium to be added (ratio):	1:1000	1:1000	1:1000	1:1000	1:1000	1:1000	1:1000
Concentration in medium:	1000x	500x	100x	10x	1x	0.5x	0.1x

POPs	1000x (µM)	500x (µM)	100x (µM)	10x (µM)	1x (µM)
PFOA	10.922	5.461165049	1.09223301	0.1092233	0.01092233
PFOS (potassium salt)	54.671	27.3354762	5.46709524	0.54670952	0.05467095
PFDA	0.963	0.481442577	0.09628852	0.00962885	0.00096289
PFNA	1.724	0.861920359	0.17238407	0.01723841	0.00172384
PFHxS (potassium salt)	7.855	3.927416784	0.78548336	0.07854834	0.00785483

PFUnDA	0.993	0.496374692	0.09927494	0.00992749	0.00099275
BDE-209	0.011	0.005645212	0.00112904	0.0001129	1.129E-05
BDE-47	0.018	0.008827889	0.00176558	0.00017656	1.7656E-05
BDE-99	0.006	0.003113213	0.00062264	6.2264E-05	6.2264E-06
BDE-100	0.004	0.001912554	0.00038251	3.8251E-05	3.8251E-06
BDE-153	0.015	0.007635414	0.00152708	0.00015271	1.5271E-05
BDE-154	0.003	0.00137279	0.00027456	2.7456E-05	2.7456E-06
HBCD	0.038	0.019167835	0.00383357	0.00038336	3.8336E-05
PCB 138	0.615	0.307581468	0.06151629	0.00615163	0.00061516
PCB 153	1.003	0.501551762	0.10031035	0.01003104	0.0010031
PCB 101	0.024	0.011947431	0.00238949	0.00023895	2.3895E-05
PCB 180	0.491	0.245370839	0.04907417	0.00490742	0.00049074
PCB 52	0.033	0.016438919	0.00328778	0.00032878	3.2878E-05
PCB 28	0.050	0.024850509	0.0049701	0.00049701	4.9701E-05
PCB 118	0.196	0.098030206	0.01960604	0.0019606	0.00019606
p,p'-DDE	1.578	0.78923372	0.15784674	0.01578467	0.00157847
HCB	0.411	0.205421729	0.04108435	0.00410843	0.00041084
α - chlordane	0.026	0.013177803	0.00263556	0.00026356	2.6356E-05
oxy - chlordane	0.052	0.026195308	0.00523906	0.00052391	5.2391E-05
trans-nonachlor	0.092	0.045925259	0.00918505	0.00091851	9.1851E-05
α-HCH	0.021	0.010315304	0.00206306	0.00020631	2.0631E-05
β-HCH	0.181	0.090430836	0.01808617	0.00180862	0.00018086
γ-HCH (Lindane)	0.021	0.010315304	0.00206306	0.00020631	2.0631E-05
Dieldrin	0.063	0.031503505	0.0063007	0.00063007	6.3007E-05

Table 2.16: Neural differentiation (ND) medium with all necessary components and mitogens.

Neural Differentiation (ND) Medium	**Final Concentration**	**Volume 500 mL**
Neurobasal Medium	1x	490 mL
B-27 Supplement (50x)	1x	5 mL
N2 Supplement	1x	5 mL
Pencillin/ Streptomycin	50 U/mL	2.5 mL
L-Glutamin	2 mM	5 mL
Mitogens to be added before use:		
GDNF	1 ng/mL	50 µL
BDNF	2.5 ng/mL	50 µL

Laminin	1:1000	500 µL

Protocol

1. Prepare the required amount of neural differentiation (ND) medium by adding the necessary components and mitogens (as described in "Table 2.16"). 150 µL ND medium is to be added in each well (see section 2.2.3 Passaging of HiPSC-derived Neural Stem Cells). Warm up the medium to 37°C.
2. Prepare containers of appropriate size to be used for treatment of the cells.
3. Calculate the required amount of POP mixtures to be mixed with ND medium (see "Table 2.15").
4. Mix the required amounts of POP mixture with the required amount of neural differentiation (ND) medium for each concentration to be tested.
5. Aspire the old neural induction (NI) medium from plates previously seeded with NSCs (described in 2.2.3 Passaging of HiPSC-derived Neural Stem Cells).
6. Distribute the treatments in the 96-well plates according to a preplanned scheme.

2.2.5 Fixation of Neural Stem Cells using Formaldehyde

In the process of formaldehyde fixation, the cells die and become fixed in their current state upon treatment. Fixation is used to preserve the cell for analysis while maintaining the structural integrity of the cell, preserving protein, carbohydrates and other macromolecules central to the inner workings of the cell [144].

Protocol

1. Aspire cell medium from the cell cultures.
2. Add 30 µL formaldehyde (4 %) to each well. Incubate the cells for 10 minutes.
3. Add 100 µL PBS.

4. Aspire the formaldehyde and PBS from the wells.

5. Add 200 µL PBS solution to each well.

6. Wrap plates in parafilm and store at 4 °C.

2.2.6 CellTiter Blue Cell Viability Assay

CellTiter Blue Assay is an fluorometric analysis method used for quantifying cells in a sample. It measures the metabolic activity of cells through the reduction of the substrate resazurin to the product resorufin, a fluorescent molecule giving off light at 590nm. The conversion rate correlates with the number of cells in the well and will decrease with reduced viability, and is thought to be performed by enzymes of mainly mitochondrial origin, but also cytosolic, and microsomal origin [145].

Protocol

1. Add 30 µL of CellTiter Blue solution to each well containing 150 µL medium and cells.

2. Incubate the cells with the CellTiter Blue solution for minimally 3 hours.

3. Prepare an equal number of plates corresponding to the ones that have been treated with CellTiter Blue, these are to be used for reading the result. To one column in each new plate, add 150 µL ND cell medium and 30 µL CellTiter Blue to be used as blank.

4. After incubation, Transfer 100 µL from each well of the treated plates, to the newly prepared plates.

5. Read samples using a Multi-Well Fluorimetric Reader (Tecan), reading luminescence at 530-560 nm (excitation) 590 nm (emission).

2.2.7 Immunocytochemistry

Immunocytochemistry can be used to detect and quantify different proteins in tissue and cell samples based on binding of a specific primary antibody. The primary antibody will bind directly to the antigen that is to be investigated in the sample. Secondary antibodies

specific for the primary antibodies with attached fluorophores is then added in order to mark the primary antibodies. Using light microscopy and high content imaging (HCI) equipment, the fluorescent signal for a number of different endpoints can be analyzed. The primary antibody staining, and the subsequent fluorescent signal can be detected and quantified in order to determine relative amounts and distribution of protein in cells and/or tissues [132, 146].

	1	2	3	4	5	6	7	8	9	10	11	12
A	Ctrl	x0.5	x1	x1000	Ctrl	x0.5	x1	x1000	Ctrl	x0.5	x1	x1000
B	Ctrl	x0.5	x1	x1000	Ctrl	x0.5	x1	x1000	Ctrl	x0.5	x1	x1000
C	Ctrl	x0.5	x1	x1000	Ctrl	x0.5	x1	x1000	Ctrl	x0.5	x1	x1000
D	Ctrl	x0.5	x1	x1000	Ctrl	x0.5	x1	x1000	Ctrl	x0.5	x1	x1000
E	Ctrl	x0.5	x1	x1000	Ctrl	x0.5	x1	x1000	Ctrl	x0.5	x1	x1000
F	Ctrl	x0.5	x1	x1000	Ctrl	x0.5	x1	x1000	Ctrl	x0.5	x1	x1000
G	Ctrl	x0.5	x1	x1000	Ctrl	x0.5	x1	x1000	Ctrl	x0.5	x1	x1000
H	Ctrl	x0.5	x1	x1000	Ctrl	x0.5	x1	x1000	Ctrl	x0.5	x1	x1000

I II III

Figure 2.2: Treatment scheme of 96-well plates as done for analysis with immunocytochemistry. Each set (annotated I, II, III) of treatments were analyzed with different primary antibodies, in order to identify different proteins relevant to neurodevelopment. I: Synaptogenesis (SYP, PSD95, MAP2), II: New Neurites and BDNF (βIII-Tubulin, GFAP, and BDNF), III: Nestin and Ki67. All nuclei were stained using DAPI. All diluted in 3.5% PBS.

The samples are read with high content imaging (HCI) techniques using a Thermo Scientific Cellomics ArrayScan vTi. Quantification of the proteins were done by calculating mean average intensity of the fluorescent signal and relative percentages of cells were calculated using a specific ArrayScan algorithm (Cytotoxicity V.4 BioApplication) which masks the cells with the help of DAPI staining and discards invalid nuclei. A wide range of Thermo Scientific Cellomics ArrayScan vTi algorithms (V.4 BioApplication) were used in order to have automated plate handling, and analysis of different endpoints [132].

Protocol

1. Aspirate PBS covering the cells.

2. Treat the cells with 1% Triton X-100 in PBS (1x) for 10-15 minutes in order to permeabilize the cells.

3. Treat the cells with 3.5% BSA in PBS blocking solution, incubate 15 minutes.

4. Treat cells with 40 µL primary antibody.
5. Incubate the treated cells in 4°C over night.
6. Recover primary antibodies the following day.
7. Wash cells with PBS 1x, repeat 2 times.
8. Add secondary antibody and DAPI diluted in 3.5% BSA in PBSAX for 40-45 minutes.
9. Remove secondary antibody solution.
10. Wash cells with PBS 1X, repeat 2 times.
11. Add 200 µL PBS 1X in each well. Seal with black sealing tape.
12. Store at 4°C.
13. The samples were then read with HCI techniques using a Thermo Scientific Cellomics ArrayScan vTi.

2.2.8 Gene Expression Analysis Using QR-PCR

The process of QR-PCR is reliant on multiple processes. Firstly, the reverse transcription using a reverse transcriptase that converts extracted RNA to cDNA. Secondly, PCR to amplify the cDNA created form the RNA. And third, the quantification of the signal using fluorescent probes like the ones used in the Taqman assay. Taqman assays make use of the 5'-3' exonuclease activity of the Taq polymerase [147] and the ability of specifically designed dual-labeled fluorogenic oligonucleotide probes to release a fluorescent signal through fluorescent resonance energy transfer upon cleavage [148].

The Taqman probe is designed to anneal to a target sequence located in between the forward and reverse primers. The probe is labelled with a fluorochrome at the 5'end and with a quencher dye located on the 3' end. When intact the quencher dye will absorb all signal coming from the fluorochrome. The melting point of the probe is at 70 °C, which is about 10 degrees higher than the primers used in PCR. The exonuclease activity of the Taq polymerase will however destroy the probe during the extension phase of the PCR. Every time a probe is broke, the fluorochrome and the quencher dye will be separated, and

fluorescent signal will occur. The amount of fluorescent signal is therefore proportional to the amount DNA that is produced for every cycle of PCR. This can be used to quantify the amount of specific cDNA, and consecutively the amount of mRNA [149]. The probes can bind to different types of sequences, as well as being labelled with different types of fluorochrome, which will release different types of fluorescent signal. Based on this, different genes can be quantified in a single reaction and also seen in relation to other genes. The point in which a fluorescent signal increases and go beyond the set threshold for background fluorescence is known as the "Threshold cycle" (C_t). The more starting material there is of a certain target, the lower the value of the C_t will be [150].

Samples of 200-500 ng RNA were prepared (depending on the concentration of RNA in the read samples). Retrotranscription was then performed using High Capacity cDNA Reverse Transcription Kits from Applied Biosystems.

Table 2.17: Components and volumes to be added in each sample before performing retrotranscription.

Component	µL/sample
10x RT Random P	2
10 RT Buffer	2
dNTPs Mix	0,8
H2O	0,2
RNAse inhibitor	1
RT enzyme	1

Table 2.18: Components and volumes to be added in each well of a PCR plate for Taq-Man Probe RQ-PCR.

Component	Volume (Volume/well)
20x primers/probe mix	1 µL
2x Master mix	10 µL
endonuclease free H20	8 µL
cDNA sample (from retro transcription)	1 µL

Table 2.19: Loading scheme for PCR plate to be used with the Taq-Man Probes RQ-PCR. Every two columns contain the same sample (denoted with "# number of sample"),

column 11 and 12 contain H2O. All wells are loaded with the primers shown in column 12, each primer for each row.

	1	2	3	4	5	6	7	8	9	10	11	12
A	#1	#1	#2	#2	#3	#3	#4	#4	#5	#5	H2O	BDNF
B	#1	#1	#2	#2	#3	#3	#4	#4	#5	#5	H2O	DLG4
C	#1	#1	#2	#2	#3	#3	#4	#4	#5	#5	H2O	SYP
D	#1	#1	#2	#2	#3	#3	#4	#4	#5	#5	H2O	GPHN
E	#1	#1	#2	#2	#3	#3	#4	#4	#5	#5	H2O	MAP2
F	#1	#1	#2	#2	#3	#3	#4	#4	#5	#5	H2O	PAX6
G	#1	#1	#2	#2	#3	#3	#4	#4	#5	#5	H2O	β-actin
H	#1	#1	#2	#2	#3	#3	#4	#4	#5	#5	H2O	GAPDH

The qPCR reactions were run in duplicates using TaqMan® Gene Expression Master Mix from Applied Biosystems and TaqMan Gene Expression Assays. The fluorescent discharge was real-time recorded using Sequence Detection System 7000HT from Applied Biosystems [132].

Protocol

1. Warm a heat block to 75 °C. To be used for heating the elution buffer.
2. Add 50 µL of 100% ethanol for each 100 µL of lysate. Mix, and centrifuge shortly (13200 rpm).
3. Load half of the ethanol/solution in an RNA extraction column with a mounted collection tube.
4. Centrifuge the column for 10 seconds at 13200 rpm.
5. Collect flow through and reapply to the same column, centrifuge again.
6. Remove flow through and dry the edge with a paper towel. RNA is now fixed in the filter.
7. Add 180 µL prepared “Wash Solution I” to the column. And spin the column for 10 seconds at 13200 rpm.
8. Add 180 µL of “Wash Solution 2/3”.
9. Centrifuge the column for 10 seconds at 13200 rpm.
10. Add “Wash Solution 2/3” again.

11. Centrifuge for 10 seconds again.

12. Remove flow through.

13. Centrifuge column for 1 minute at 13200 rpm.

14. Prepare new 1.5 mL Eppendorf tube for the RNA to be eluted in.

15. Add 10 µL heated elution buffer to the column mounted in the Eppendorf tube.

16. Centrifuge the column and Eppendorf tube for 30 seconds at 13200 rpm.

17. Again, add 10 µL elution buffer.

18. Centrifuge for 30 seconds at 13200 rpm.

19. Prepare a blank sample by adding a small amount of elution buffer in an Eppendorf tube.

20. Remove the column from the Eppendorf tube, close lid quickly.

21. Load 1 µL sample on a nucleic acid quantifier (NanoDrop 2000) in order to quantify amount of RNA. Set the blank before loading sample, then wipe the reader a paper towel between each reading.

22. Based on readings, the RNA samples were mixed with water to produce new samples containing 200-500 ng RNA (depending on the amount of RNA that is available) in a total volume of 13 µL.

23. Prepare a retrotranscription mixture containing the components as seen in "Table 2.17" and add 7 µL of the retrotranscription mixture to 13 µL of the RNA samples prepared in step 22.

24. Run retro-transcription of samples in order to produce cDNA.

25. Samples for Taq-Man Probes RQ-PCR are then prepared according to "Table 2.18". And loaded unto the PCR plate according to "Table 2.19", with primers added in each row.

26. Seal the plate and run PCR with the qPCR machine (ABI PRISM Sequence Detection System 7900HT) using 45 cycles with primer annealing happening at 60 °C. Read fluorescent emission.

2.2.9 Statistics

Viability Assays

Averages were calculated for each concentration in each plate. The results were then normalized in regard to the control containing DMSO in medium (ratio 1:1000). Data was then visualized, and statistically significant results were determined by using one-way ANOVA with Dunnett´s Multiple Comparison Test, with a significance of *$p<0.05$. The software used to do this was Excel (Microsoft) and GraphPad Prism 5.

RT-PCR

The quantitative real-time PCR (qPCR) reaction is run for 45 cycles and fluorescent emission is recorded every cycle. The Ct was recorder in each cycle through fluorescent emission. The average of two Ct values were calculated for each condition. ΔCt was then determined by subtracting the average Ct value for a given condition with the Ct value for the given condition in relation to a reference gene. The ΔΔCt was determined by subtracting the ΔCt of the given condition with the ΔCt of the control. The ΔΔCt method was then used to determine the fold change, which is done by calculating $2^{-\Delta\Delta Ct}$. The change was then visualized, and statistically significant results were determined by using one-way ANOVA with Dunnett´s Multiple Comparison Test, with a significance of *$p<0.05$. Software used was Excel (Microsoft) and GraphPad Prism 5.

3. Results

3.1 PC12 Cells

3.1.1 Cell Viability with MTT

A slight decrease in viability was observed upon exposure with the "Total mixture" containing the perfluorinated, brominated, and the chlorinated compounds for 24, 48, and 72 hours (Figure 3.1).

The cells treated for 24 hours, showed significant decrease in cell viability at all concentrations except for 100x (human blood). At 1x the viability was at about 90%, falling to approximately 65% when exposed to 1000x. In the cells treated for 48 hours, the only significant downregulation was observed at 10x the human blood concentration, amounting to about 75% downregulation. In cells treated for 72 hours there was also seen a significant decrease in cell viability starting at 1x to 1000x the human blood concentration, all except 100x. At 1x the viability fell to 80%, while at concentrations 10x and 500x, the viability increased slightly to about 85 % for both. Upon exposure to 1000x the human blood concentration, viability decreased to about 30%. The overall pattern following exposure, was similar across all graphs (though to a large degree not significant in the 48h graph).

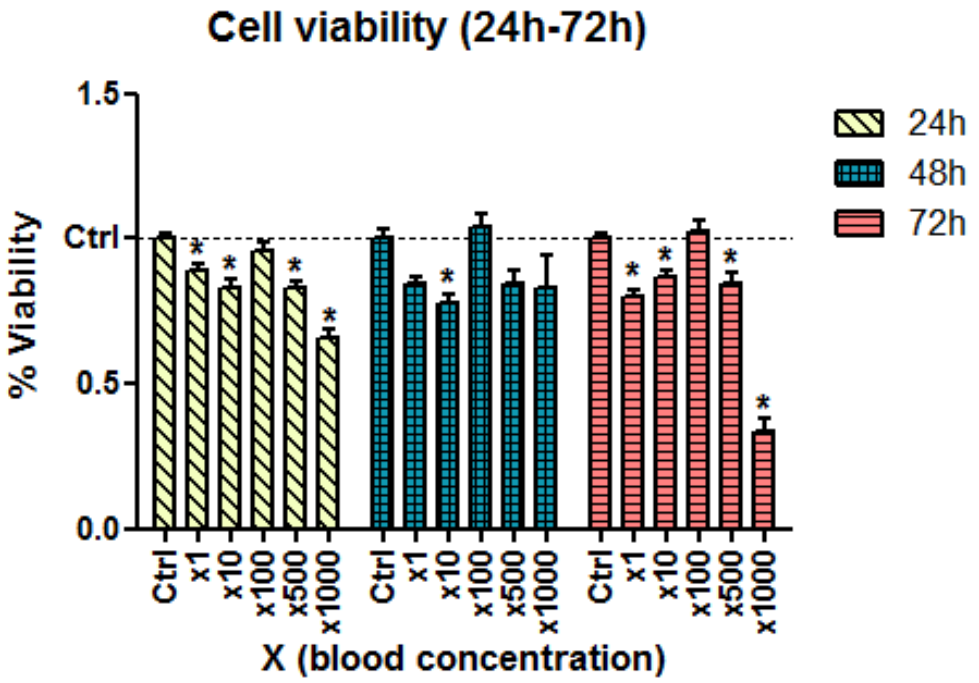

Figure 3.1: Cell viability assay with MTT of PC12 cells exposed to the "Total mixture" up to 72 hours. Undifferentiated PC12 cells were incubated with the total mixture for 24 (yellow), 48 (blue), and 72 (red) hours. Cells were treated with MTT and quantified with a plate reader. Samples were normalized to the DMSO control (Ctrl) which was set as 100% viability, shown as % viability on the y-axis. Concentrations are shown on the x-axis. For 24 hours, 9 replicates with either 8 or 16 parallels each were used. For 48 hours, 6 replicates with either 8 or 16 parallels each were used. For 72 hours, 5 replicates with either 8 or 16 parallels each were used. Statistically significant results are presented with *$p<0.05$, as validated by one-way ANOVA.

In another attempt to quantify the number of viable cells, Trypan Blue staining was performed. The experiment was run using 3 replicates with a blank and control for the concentrations 10x, 100x, 1000x the concentration of POPs found in blood. Too few dead cells were identified to be able to make a reliable estimate of the ratio between living and dead cells. Upon counting with microscope, almost all cells were identified as living.

3.1.2 Western Blotting

Based on the values seen initiating a response in the viability assay, the concentrations were chosen among those thought to be most interesting. But also, the ones initiating the

strongest response, in order to be able to possibly detect and quantify the proliferating cell nuclear antigen (PCNA, Figure 3.2, Table 3.1).

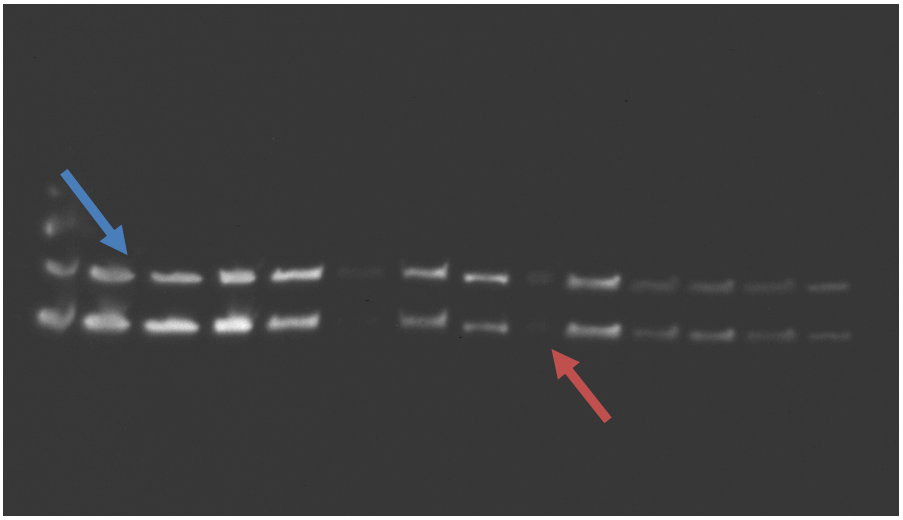

Figure 3.2: Results from western blotting after staining. The collected samples (Blank, DMSO, 10x, 100x, 1000x) were run in the same 15-well gel. PCNA (29 kDa) and β-actin (42 kDa) were identified using the "Precision Plus Protein Standards" ladder from Bio-Rad. The line of bands seen on the top was identified as B-actin (blue arrow), the bottom one was identified as PCNA (red arrow). Intensity of the signal was calculated using B-actin as reference this was done in each well.

Table 3.1: Results from quantification of western blottin,. showing values produced from the 3 replicates with Blank (medium, with no solvent), Ctrl (medium and DMSO), 10x (blood concentration), 100x (blood concentration), 1000x (blood concentration). Blank was not prepared in the first set of samples (#1).

Concentrations	#1	Normalized	#2	Normalized	#3	Normalized
Blank	*		0,811		0,943	
DMSO	1,740	1,000	0,328	1,000	1,020	1,000
10x	1,331	0,765	0,565	1,725	1,176	1,153
100x	1,598	0,918	0,470	1,435	0,937	0,918
1000x	1,330	0,764	0,702	2,142	0,488	0,478

The values were normalized for the control, and each condition (Table 3.1), and averages for each condition was calculated. The conditions were all tested against the control with

one-way ANOVA using $p < 0.05$, no condition was found to cause significant changes in the level of PCNA expression.

3.2 HiPSC-Derived Neural Stem Cells

3.2.1 CellTiter Blue (Cell Viability Assay)

During testing generally little or no cytotoxicity was observed. Surprisingly, upregulation rather than downregulation seems to generally be the norm across all concentrations, level of differentiation, and treatment with the mixtures. “Mix A” denotes the “Total Mixture” with all three groups of compounds, “Mix B” denotes the “Perfluorinated + Chlorinated Mixture”, “Mix C” denotes the “Brominated + Chlorinated mixture”, and “Mix D” denotes the “Chlorinated mixture”. The neural stem cells were treated following either 1 day (1 DIV) or 14 days (14 DIV) of differentiation, with treatments spanning either over 3 days or 14 days. Treatments were diluted in medium containing mitogens, and cells were treated twice a week. In total, the experiment was run with 5 replicates, using 6 parallels for each concentration. The readings were corrected using a blank, before being normalized to the DMSO control. Using one-way ANOVA analysis, the statistical significance of the results was determined.

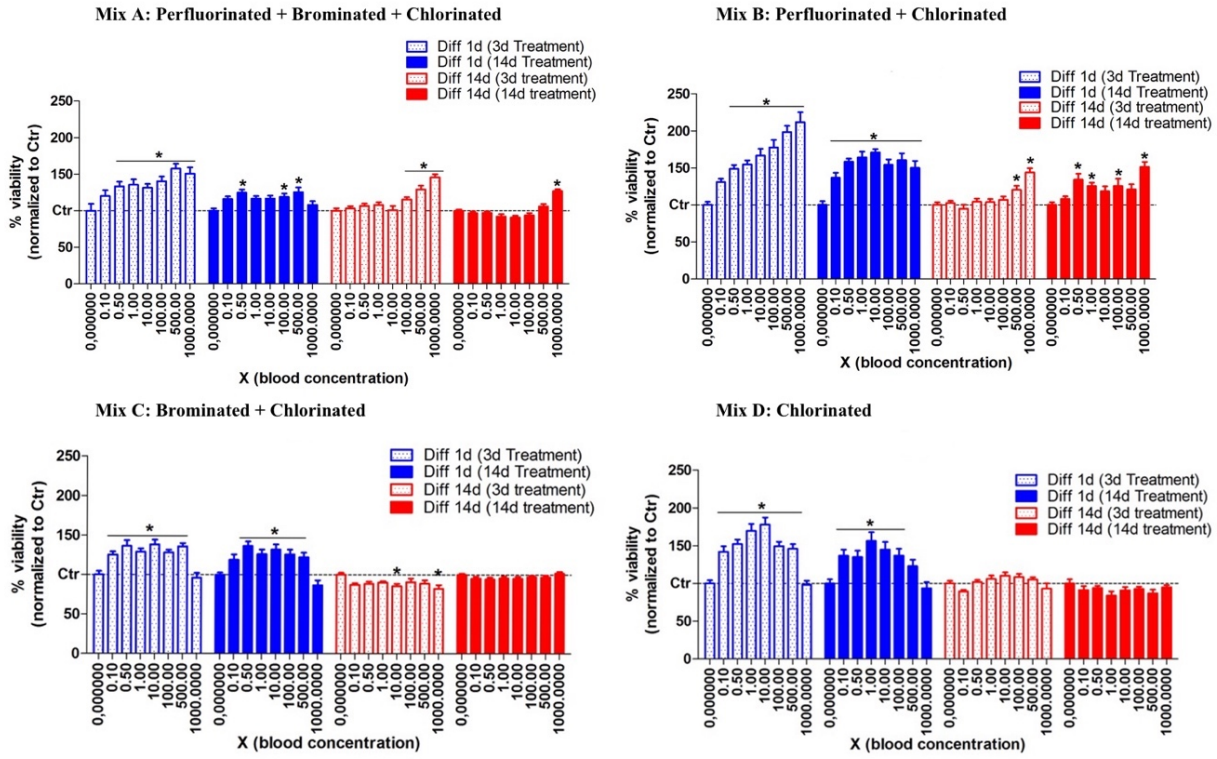

Figure 3.3: Cell viability assay of NSCs using CellTiter Blue with each POP mixture. Cells differentiated for 1 day (blue), with 3 days of treatments being shown with blue stippled filling and 14 days of treatments shown with fully blue filling. Cells differentiated for 14 days (red), with 3 days of treatments being shown with red stippled filling and 14 days of treatments shown with fully red filling. All samples have been normalized to the DMSO control (Ctrl) which is set as 100 % viability and samples are calculated as a percentage of this, % viability is seen in the y-axis. Concentrations is set on the x-axis. All mixtures have been tested in five replicates, with each concentration being tested with 6 parallels each. Statistically significant results are presented with *$p<0.05$, as validated by one-way ANOVA. **(A)** Graph for the total mixture containing all 29 of the perfluorinated, brominated, and chlorinated compounds. **(B)** Graph for the mixture containing the perfluorinated and chlorinated compounds. **(C)** Graph for the mixture containing the brominated and the chlorinated compounds. **(D)** Graph for the mixture containing the chlorinated compounds.

In the cells treated with the "Total Mixture", a general upregulation of viability was observed rather than mortality (Figure 3.3A). This effect is especially prominent in the undifferentiated cells (1 DIV) upon acute exposure for 3 days, with significant results showing at 0.5 times (0.5x) of that found in human blood attributing to approximately 30% upregulation. This general trend continues until the highest tested concentration

(1000x) which leads to 50-60% upregulation. 14 days of chronic exposure of immature cells (1 DIV) leads to modest upregulation at some concentrations (0.5x, 100x, 500x) without any apparent pattern. Differentiated cells which had matured for 14 days prior to treatment showed greater resistance to treatment than the immature cells. The acutely exposed cells did not have any significant response before being exposed to 100 times that of human blood, which resulted in approximately 10 % upregulation. Upon exposure to 1000 times that of human blood the upregulation goes up to about 50%. Chronic exposure (14 days) of mature cells (14 DIV) did only produce a significant response at the highest tested concentration (1000x), leading to approximately 20% upregulation.

The second mixture (Figure 3.3B) containing the perfluorinated compounds mixed with the chlorinated compounds produced an increasingly stronger response in acutely exposed (3 day) cells which had been standing 1 DIV prior to being exposed. In a dose-response manner, significant results started at 0.5 times the human blood concentration until the 1000 times concentration mark, going from approximately 50% to 110% upregulation. In the chronic exposed immature cells significant upregulation occurred already at 0.1 times human blood concentration, leading to approximately 40% increased perceived viability. With increasing concentrations, the upregulation appeared to stabilize at 50-70%. Acute exposure (3 days) of mature cells (14 DIV) produced no significant results at lower concentrations, upregulation was only seen in the two highest tested concentrations (500x and 1000x), causing at highest 50% upregulation. Chronic exposure (14 days) of matured cells (14 DIV) caused modest upregulation in some concentrations (0.5x, 1x, 100x, and 1000x). Causing at highest 50% upregulation upon 1000x exposure.

In the third mixture (Figure 3.3C) containing the brominated and chlorinated compounds, the undifferentiated cells (1 DIV) produced a bell shape looking response upon both acute and chronic exposure. Acute exposure (3 days) triggered a general upregulation in the concentrations 0.1x-500x, amounting to about 40-50% upregulation. The highest tested concentration (1000x) did not produce any significant result and was visually indistinguishable from the control. Chronic exposure (14 days) caused a similar acting response as acute exposure, producing 40-50% upregulation in the concentrations 0.5x-1000x. Cells that had been differentiating for 14 days expressed a slight downregulation upon acute exposure, with 10x and 1000x producing significant responses. When the

differentiated cells were chronically treated (14 days), no significant outcome was observed.

The fourth mixture (Figure 3.3D), containing only the chlorinated compounds caused strong upregulation when medial concentration was added to the immature cells (1 DIV). Upon acute exposure (3 days), concentrations 0.10x-500x caused 50-80% upregulation, with 10x being the concentration causing the strongest response. No significant effect was seen in 1000x. Chronic exposure (14 days) caused upregulation similar to that seen in acute exposure. Concentrations 0.1x-100x caused significant upregulation, amounting to about 40-50% upregulation. Concentration 1x seemed to instigate the strongest response, while concentrations 500x and 1000x caused no significant outcome. In the mature cells (14 DIV) neither acute (3 day) nor chronic (14 day) exposure prompted any significant outcome in relation to the control.

The cells were inspected with a microscopy during the proceedings of these experiments. Little to no morphological disturbance was noted. Generally, there were no apparent visual difference between the control and the different treatments, both in regard to apparent cell density or cell numbers.

3.2.2 Immunocytochemistry

The most prominent results from the viability study indicated that the lesser differentiated cells gave stronger responses to the treatments than the more developed cells. Additionally, it was shown that a wide range of concentrations were capable of eliciting a response. Based on this the less developed cells (1 DIV) were chosen for further study with immunocytochemistry. Treatment of the cells were chosen to be done with 0.5x, 1, and 1000x to cover both the relevant ranges as seen to elicit an effect, and to make evaluations relevant to human exposure.

Synaptogenesis

In the less mature cells acute exposure induced general upregulation of total amount of SYP in all mixtures (Figure 3.4A). Upregulation was observed starting at 0.5 times human blood concentrations in the mixtures B (Perfluorinated + Chlorinated) and C (Brominated and chlorinated), while significant results were first noted at 1x, and 1000x for, respectively, mixture A (Total mixture) and mixture D (Chlorinated). Upregulation was highest for mixture C, reaching 50% upregulation. While the ratio of the distribution of SYP in neurite compared to the cell body appeared to decrease with some concentrations, indicating accumulation of SYP in the cell body (Figure 3.4B). Concentrations that were observed to cause significant down regulation was 1000x in the "Total Mixture" and 0.5x and 1000x in the "Brominated and Chlorinated mixture". Downregulation appeared to generally be around 20%.

The more developed cells also exhibited general upregulation of total SYP with three out of four mixtures (Figure 3.4C). The strongest response was observed in the B (Perfluorinated + Chlorinated) and C mixtures (Brominated + Chlorinated), both eliciting upregulation of 25-30% at 0.5 the human blood concentration. The A mixture (Total) produced significant upregulation only at the human relevant concentration, while no significant effect was observed in the D mixture (Chlorinated). The distribution seemed to favour the cell body for the highest concentrations of the mixtures A, C, and D (Figure 3.4D).

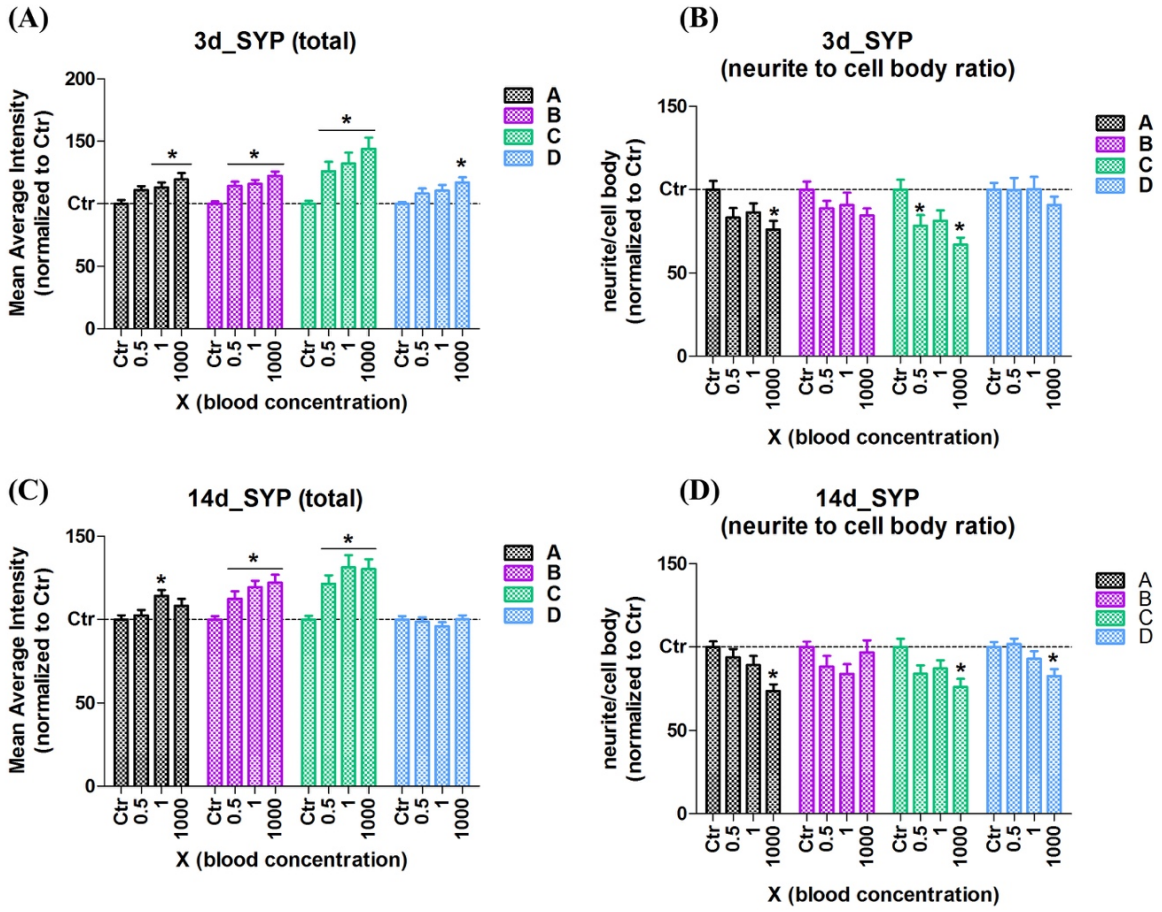

Figure 3.4.: Effects on the distribution of synaptophysin (SYP) upon acute and chronic exposure to mixtures of POPs. Graphs are shown as averages with standard error mean (SEM). Cells were treated for 3 and 14 days with the mixtures A: Total mixture (Black), B: Perfluorinated and Chlorinated mixture (Pink), C: Brominated and Chlorinated mixture (Green), D: Chlorinated mixture (Blue). Distribution of SYP was determined by use of immunostaining and HCI analysis software. All readings were normalized to the DMSO control (Ctrl), and the mean average intensity (y-axis) was calculated as a percentage of this. Concentrations are shown on the x-axis. All mixtures have been tested in six replicates, with each concentration being tested with 8 parallels each. Statistically significant results are presented with *$p<0.05$, as validated by one-way ANOVA. **(A) and (C)** Shows the effects of total amount of SYP found in the cells following acute (3 days) and chronic (14 days) exposure. **(B) and (D)** Shows the relative distribution between the amounts of SYP found in the neurites and in the cell body following acute (3 days) and chronic (14 days) exposure.

Acute exposure to the mixtures induced significant upregulation of total PSD95 in the mixtures A, B, and D (Figure 3.5A). In the A mixture significant upregulation was observed starting at 0.5x(blood concentration), amounting to about 30 % upregulation in all concentrations. A modest significant upregulation was observed in mixtures B and D as well. No significant results were observed in the C mixture. The distribution of PSD95 seemed to favour accumulation in the cell body upon exposure to all the mixtures, starting at 0.5x(blood concentration).

Upregulation of PSD95 was observed upon chronic exposure to mixtures A, C, and D. Starting at 1x (blood concentration) in mixtures C, and D, with 10-15% upregulation noted. At 1000x (blood concentration), a response was observed in mixture A, C, and D, amounting to approximately 15-20% upregulation. The distribution favoured accumulation in the cell body in all cases, though only significant at 1000x for mixture A and D, and significant starting at 0.5 for mixture C.

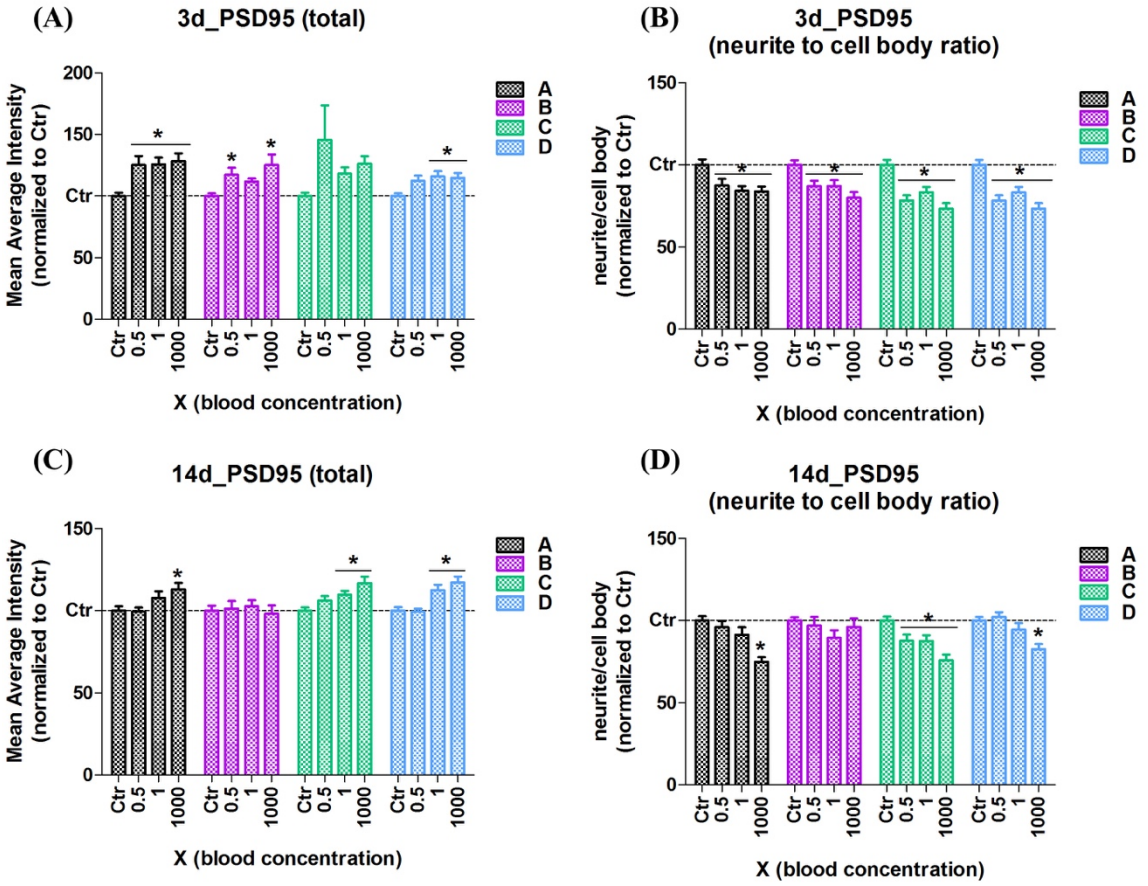

Figure 3.5: Effects on the distribution of PSD95 upon acute and chronic exposure to mixtures of POPs. Graphs are shown as averages with standard error mean (SEM). Cells

were treated for 3 and 14 days with the mixtures; A: Total mixture (Black), B: Perfluorinated and Chlorinated mixture (Pink), C: Brominated and Chlorinated mixture (Green), D: Chlorinated mixture (Blue). The graphs shown are depicted following immunostaining and analysis with HCI equipment and software. All samples were normalized in relation to the control (Ctrl), and % Mean Average Intensity is shown in relation to this (y-axis). Concentrations are depicted on the x-axis. All mixtures have been tested in six replicates, with each concentration being tested with 8 parallels each. Statistically significant results are presented with *p<0.05, as validated by one-way ANOVA. **(A) and (C)** Shows the effects of total amount of PSD95 found in the cells following acute (3 days) and chronic (14 days) exposure. **(B) and (D)** Shows the relative distribution between the amounts of PSD95 found in the neurites and in the cell body following acute (3 days) and chronic (14 days) exposure.

Acute exposure to the A mixture induced upregulation of expression of MAP2 positive cells starting at 0.5x and up to the highest tested concentration, amounting to approximately 25% upregulation (Figure 3.6A). In mixture B, a significant upregulation was observed only at concentration 1x (human blood). For mixture C, upregulation was seen in concentrations 0.5x and 1000x (human blood). In mixture D, concentrations 1x and 1000x were significant. Upon chronic exposure (Figure 3.6B), upregulation to about 10% were observed in mixture C starting at 0.5x (blood concentration). Significant upregulation was seen in mixture A and D when exposed to 1000x (blood concentration).

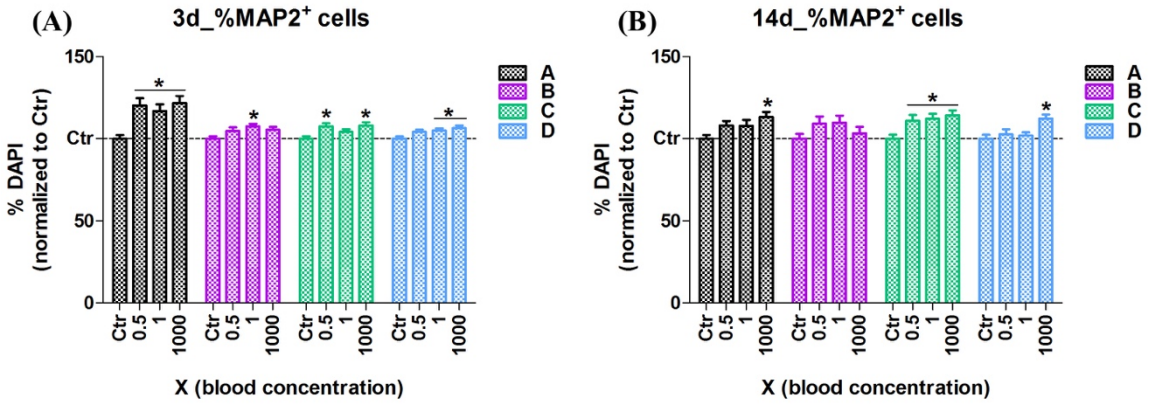

Figure 3.6: Quantification of % MAP2+ cells identified by immunostaining and DAPI following acute and chronic exposure to POP mixtures. Graphs are shown as averages with standard error mean (SEM). Cells treated for 3 and 14 days were probed for expression of MAP2. Tested with mixtures; A: Total mixture (Black), B: Perfluorinated

and Chlorinated mixture (Pink), C: Brominated and Chlorinated mixture (Green), D: Chlorinated mixture (Blue). Cells were stained with immunostaining and quantified using HCI software and equipment. Samples were normalized to the control (Ctrl), and relative amounts of MAP+ cells were calculated from this (y-axis) and validated using DAPI staining. Concentrations are located on the x-axis. Testing was done using 6 replicates and 8 parallels per condition. Statistically significant results are presented with *p<0.05, as validated by one-way ANOVA. **(A)** Effects following acute (3 day) exposure. **(B)** Effects following chronic (14 day) exposure.

The morphological changes following acute and chronic exposure to the POP mixtures can be observed in Figure 3.7. With the relative distributions and intensities showing for MAP2 (white), PSD95 (red), and SYP (green) in relation to DAPI (DNA, Blue).

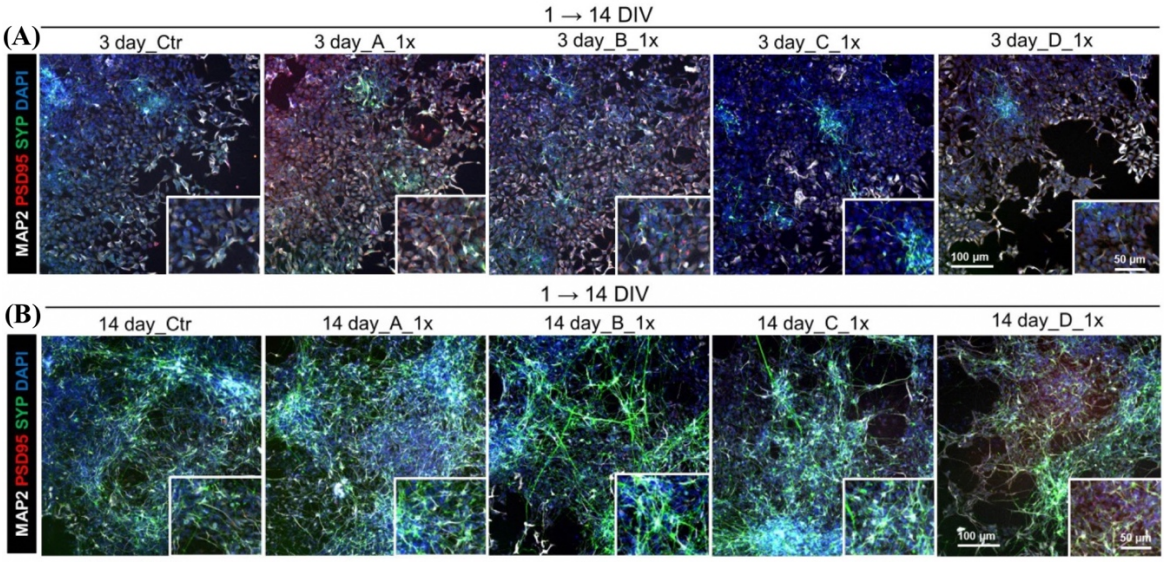

Figure 3.7: Immunochemical images showing the acutely and chronically treated cells stained with antibodies for synaptogenesis (MAP2, PSD95, SYP) following exposure to the different POP mixtures. Cells treated with 1x (the human blood concentration) of the different mixtures; A: Total mixture, B: Perfluorinated and Chlorinated mixture, C: Brominated and Chlorinated mixture, D: Chlorinated mixture, and stained with MAP2 (white), PSD95 (red), SYP (green), and DAPI (blue). Images were captured using Array Scan vTi platform and the Neuronal profiling V.4 bioapplication for immunofluorescence and high content imaging (HCI). **(A)** Showing the cells treated for 3 days (acute). **(B)** Showing the cells treated for 14 days (chronic).

New Neurites and BDNF

In the acutely treated cells, downregulation was only seen in mixture D (Chlorinated mixture) at concentration 1x (blood concentration). Chronic exposure caused significant downregulation at 1x (blood concentration) only in the total mixture (Figure 3.8).

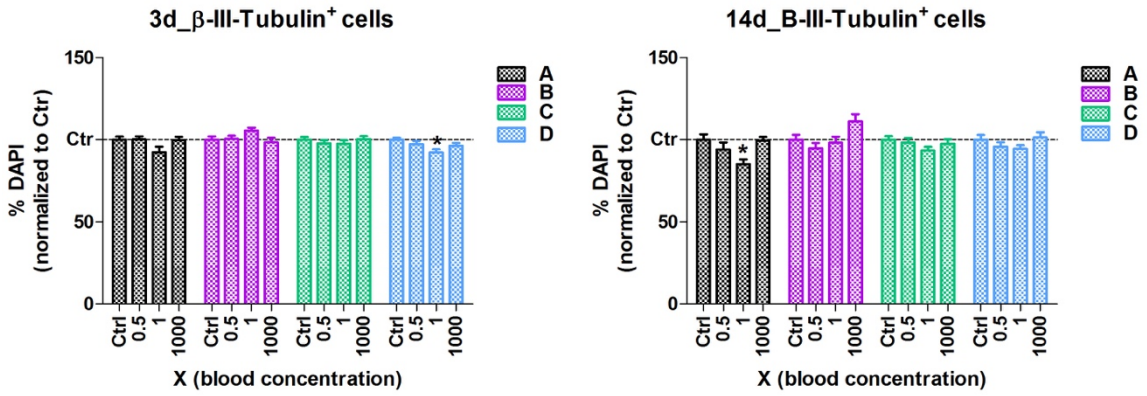

Figure 3.8: Quantification of % β-III-Tubulin+ cells identified by immunostaining and DAPI following chronic and acute exposure to mixtures of POPs. Graphs are shown as averages with standard error mean (SEM). Cells were treated for 3 and 14 days with mixtures; A: Total mixture (Black), B: Perfluorinated and Chlorinated mixture (Pink), C: Brominated and Chlorinated mixture (Green), D: Chlorinated mixture (Blue). Results were analyzed based on immunostaining and HCI. The relative amounts of β-III-Tubulin+ cells (y-axis) were determined by normalization to the control (Ctrl), and nuclei verification with DAPI. Concentrations are shown on the x-axis. The experiment was done using 5 replicates with 8 parallels for each condition. Statistically significant results are presented with *$p<0.05$ and was validated by one-way ANOVA. **(A)** Effects following acute (3 day) exposure. **(B)** Effects following chronic (14 day) exposure.

Acute exposure caused 50% upregulation of BDNF at all tested concentration when exposed to mixture D (Figure 3.9A). The distribution seemed to favour the neurites with concentration 1x (blood concentration) of the D mixture (Figure 3.9B).

In the chronically exposed cells (Figure 3.9C), downregulation was observed in concentration 1x (blood concentration) in mixture "Total mixture" (A mixture), and in concentration 1x and 0.5x (blood concentration) of the cells exposed to the chlorinated mixture (Mixture D). Distribution seemed to favour the neurites when exposed to mixture

A, B, and D (Figure 3.9D). The "Total mixture" initiated a change in the distribution at 0.5x (blood concentration), the perfluorinated and chlorinated mixture initiated a change in the distribution at 1x (blood concentration), and the chlorinated mixture induced changes in distribution at 0.5x and 1x the blood concentration.

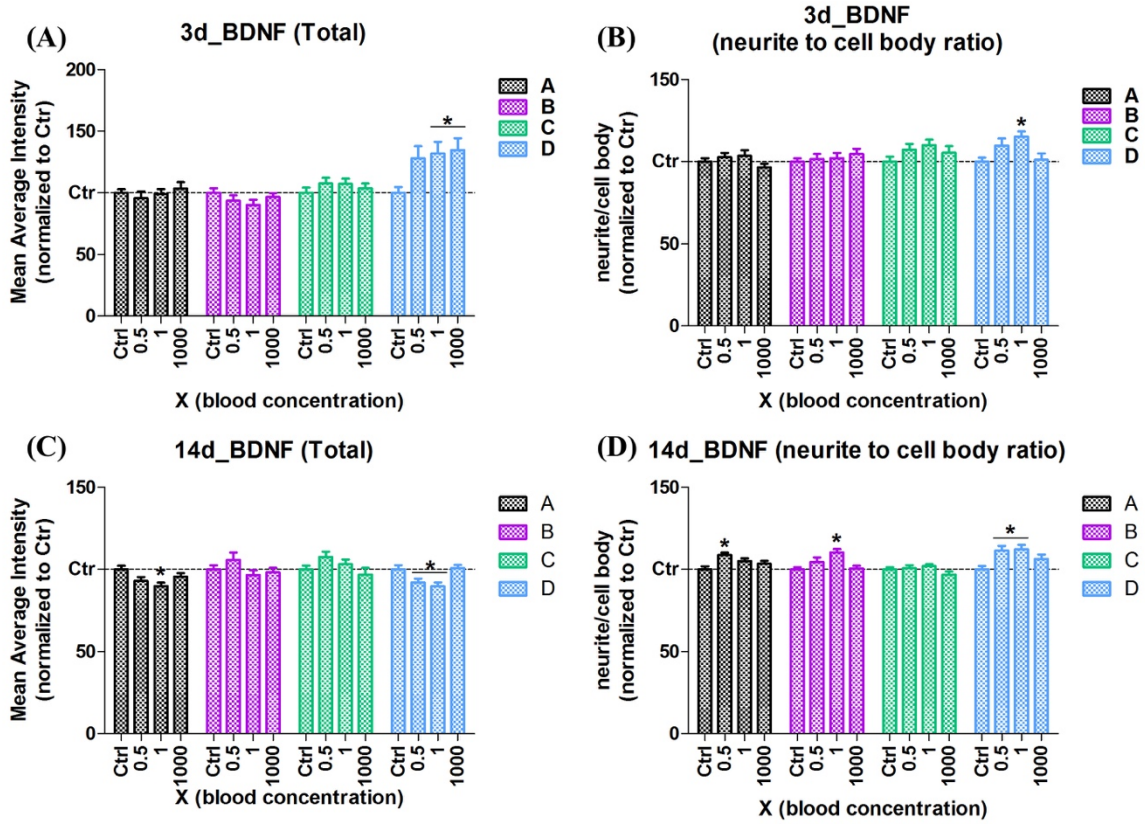

Figure 3.9: Effects on distribution of BDNF upon acute and chronic exposure to mixtures of POPs. Graphs are shown as averages with standard error mean (SEM). Treatments were done over 3 or 14 days with the POP mixtures; A: Total mixture (Black), B: Perfluorinated and Chlorinated mixture (Pink), C: Brominated and Chlorinated mixture (Green), D: Chlorinated mixture (Blue). The distribution of BDNF were determined with immunostaining and HCI. All readings were normalized in regard to the control, and % Mean Average Intensity (y-axis) is calculated from this. Concentrations are seen on the x-axis. The experiment was done with five replicates with 8 parallels for each condition. Statistically significant results are presented with *$p<0.05$ and was validated by one-way ANOVA. **(A) and (C)** Shows the effects of total amount of BDNF found in the cells following acute (3 days) and chronic (14 days) exposure. **(B) and (D)** Shows the relative distribution between the amounts of BDNF found in the neurites and in the cell, body following acute (3 days) and chronic (14 days) exposure.

Several changes were observed in the neurites when they were acutely exposed to POPs. An increase in the number of neurites were observed upon treatment with 1000x of the "Total mixture", and with 1x the chlorinated mixture (Figure 3.10A). There was a 50% increase in neurite length upon 1000x treatment with the "Total Mixture" (Figure 3.10B). For the brominated mixture, significant shortening of the neurite lengths was seen starting at concentration 0.5x, amounting to about 25-30% shortening of the neurites. Upon exposure to 0.5x and 1x of the chlorinated mixture, about 30% shortening was observed. Significant increase (70%) in the number of branch point per neurite was observed at 1000x of the "Total mixture" (Figure 3.10C). Decrease in the number of branch points was observed upon treatments starting with 0.5x of the brominated mixture. Decrease in the number of branch points was also seen upon exposure to 0.5x and 1x of the chlorinated mixture.

Chronical exposure only lead to a significant increase in the number of neurites in the cells treated with 1000x of the brominated mixture (Figure 3.10D). Neurite length was only significantly decreased upon treatment with 0.5x and 1x of the chlorinated mixture (Figure 3.10E). No significant effect was observed in the number of branch points following chronic exposure (Figure 3.10F).

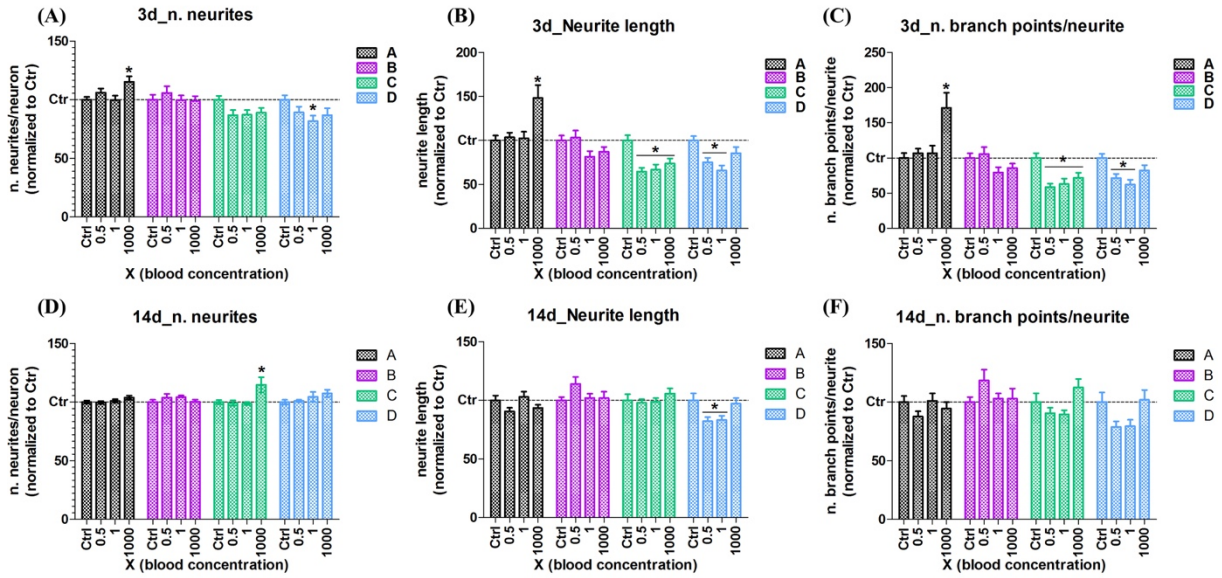

Figure 3.10: Determination of neurite outgrowth, length, and number of branch points (per neurite) following acute and chronic exposure to mixtures of POPs. Graphs are shown as averages with standard error mean (SEM). Treatments were done

over 3 and 14 days with the POP mixtures; A: Total mixture (Black), B: Perfluorinated and Chlorinated mixture (Pink), C: Brominated and Chlorinated mixture (Green), D: Chlorinated mixture (Blue). Number of neurites, neurite length, and number of branch points per neurite was determined using immunostaining and HCI software. The n. neurites, lengths, and n. branch point of the neurites were analyzed in relativity to the control (Ctrl). Concentrations are seen on the x-axis. The experiment was done with five replicates with 8 parallels for each condition. Statistically significant results are presented with *p<0.05 and was validated by one-way ANOVA. **(A) and (D)** Shows the number of neurites per neuron for acute and chronic exposure, respectively. **(B) and (D)** Shows the neurite lengths following acute and chronic exposure, respectively. **(C) and (D)** Shows the number of branch points per neurite following chronic and acute exposure, respectively.

The morphological changes following acute and chronic exposure to the POP mixtures can be observed in "Figure 3.11". With the relative distributions and intensities showing for β-III-Tubulin (red) and BDNF (green), in relation to DAPI (DNA, Blue).

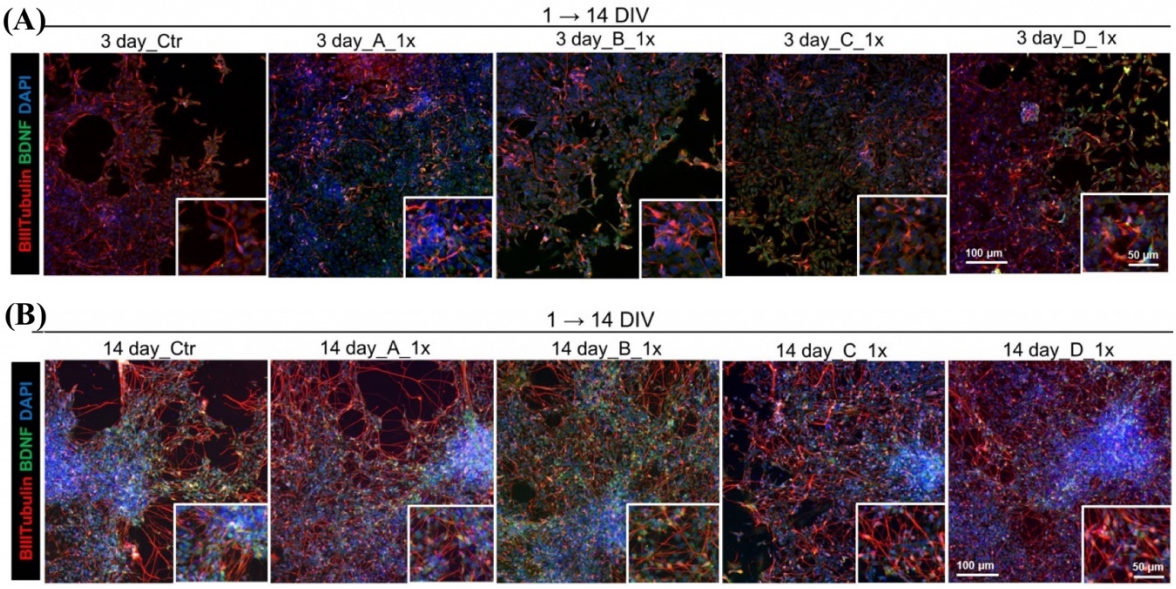

Figure 3.11: Immunochemical images showing the acutely and chronically treated cells stained with antibodies for neurites and BDNF (β-III-Tubulin and BDNF) following exposure to the different POP mixtures. Cells treated with 1x (the human blood concentration) of the different mixtures; A: Total mixture, B: Perfluorinated and Chlorinated mixture, C: Brominated and Chlorinated mixture, D: Chlorinated mixture, and

stained with β-III-Tubulin (Red), BDNF (green), and DAPI (blue). Images were captured using Array Scan vTi platform and the Neuronal profiling V.4 bioapplication for immunofluorescence and high content imaging (HCI). **(A)** Showing the cells treated for 3 days (acute). **(B)** Showing the cells treated for 14 days (chronic).

Neural Stem Cells and Astrocytes

No significant results were observed when the acutely exposed cells were treated with POP mixtures (Figure 3.12A). Upon chronic exposure to the POPs (Figure 3.12B), a decrease in the amount of GFAP expressing cells were observed in the cultures exposed to 1x of the human blood concentration.

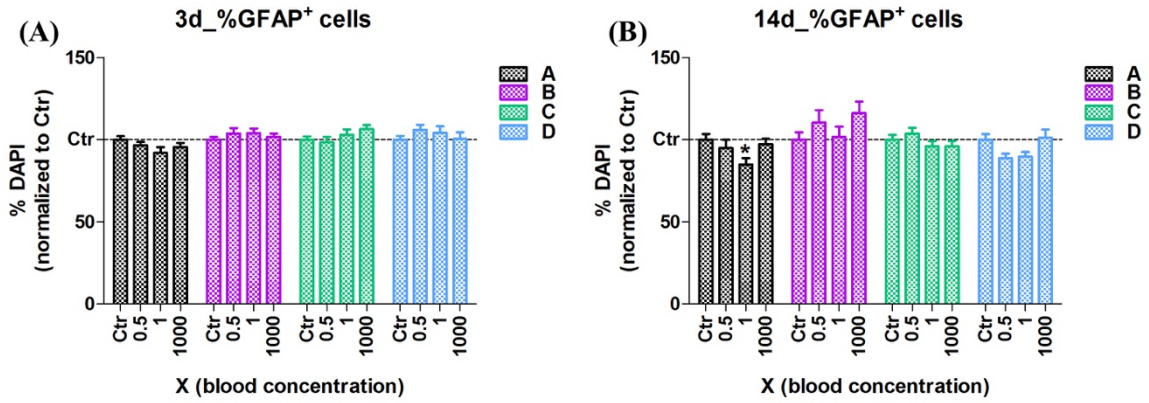

Figure 3.12: The quantification of % GFAP+ cells following acute and chronic exposure to POP mixtures. Graphs are shown as averages with standard error mean (SEM). Cells were exposed to the POP mixture for 3 and 14 days, with the mixtures being; A: Total mixture (Black), B: Perfluorinated and Chlorinated mixture (Pink), C: Brominated and Chlorinated mixture (Green), D: Chlorinated mixture (Blue). GFAP was visualized using immunostaining and HCI techniques. Samples were normalized to the control (Ctrl) and are shown on the y-axis as % DAPI, cells were identified using DAPI staining. Concentrations are shown on the x-axis. Experiments were done with five replicates using 8 parallels per condition. Statistically significant results are presented with *$p<0.05$ and was validated by one-way ANOVA. **(A)** Effects following acute (3 day) exposure. **(B)** Effects following chronic (14 day) exposure.

Acute exposure induced a significant decrease in the number of cells expressing nestin when exposed to 1000x of the mixtures A, B, C (Figure 3.13A). Following chronical

exposure, 70% upregulation of nestin positive cells were observed with 1x of the "Total mixture" (Figure 3.13B). Downregulation was noted for 1000x of the perfluorinated and chlorinated mix, amount to about 20% downregulation. The brominated mixture induced upregulation of nestin positive cells at 0.5x. The chlorinated mixture induced upregulation of cells expressing nestin at the concentration 0.5x and 1000x.

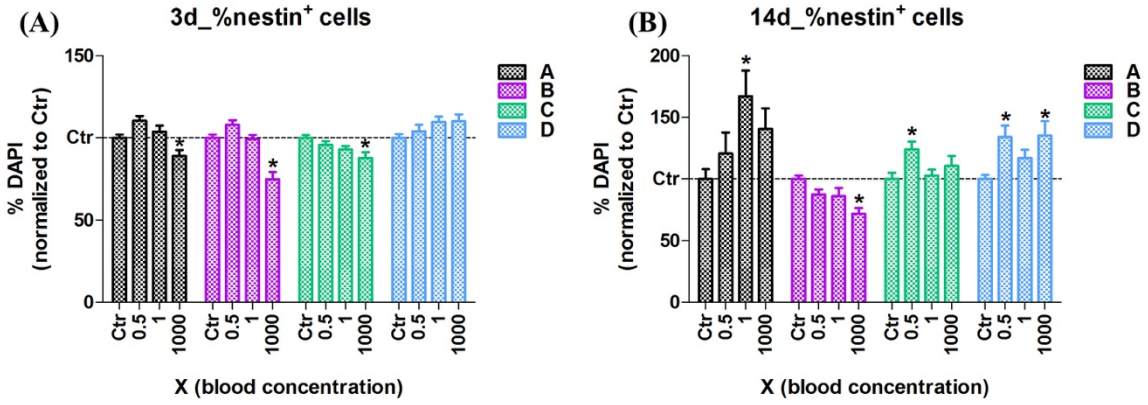

Figure 3.13: Quantification of % nestin+ cells following acute and chronic exposure to POP mixtures. Graphs are shown as averages with standard error mean (SEM). Treatments were performed for 3 and 14 days with the POP mixtures; A: Total mixture (Black), B: Perfluorinated and Chlorinated mixture (Pink), C: Brominated and Chlorinated mixture (Green), D: Chlorinated mixture (Blue). Visualization of nestin was done using immunostaining and HCI techniques. All samples have been normalized to a control (Ctrl) and are depicted in relation to this as shown on the y-axis (% DAPI). Cells were verified using DAPI staining. Experiments were done using five replicates with 8 parallels for each condition. Statistically significant results are presented with *$p<0.05$ and was validated by one-way ANOVA. **(A)** Effects following acute (3 day) exposure. **(B)** Effects following chronic (14 day) exposure.

The morphological changes following acute and chronic exposure to the POP mixtures can be observed in "Figure 3.14". As well as the relative intensities and distribution of nestin (green) and GFAP (green) with DNA (DNA, DAPI).

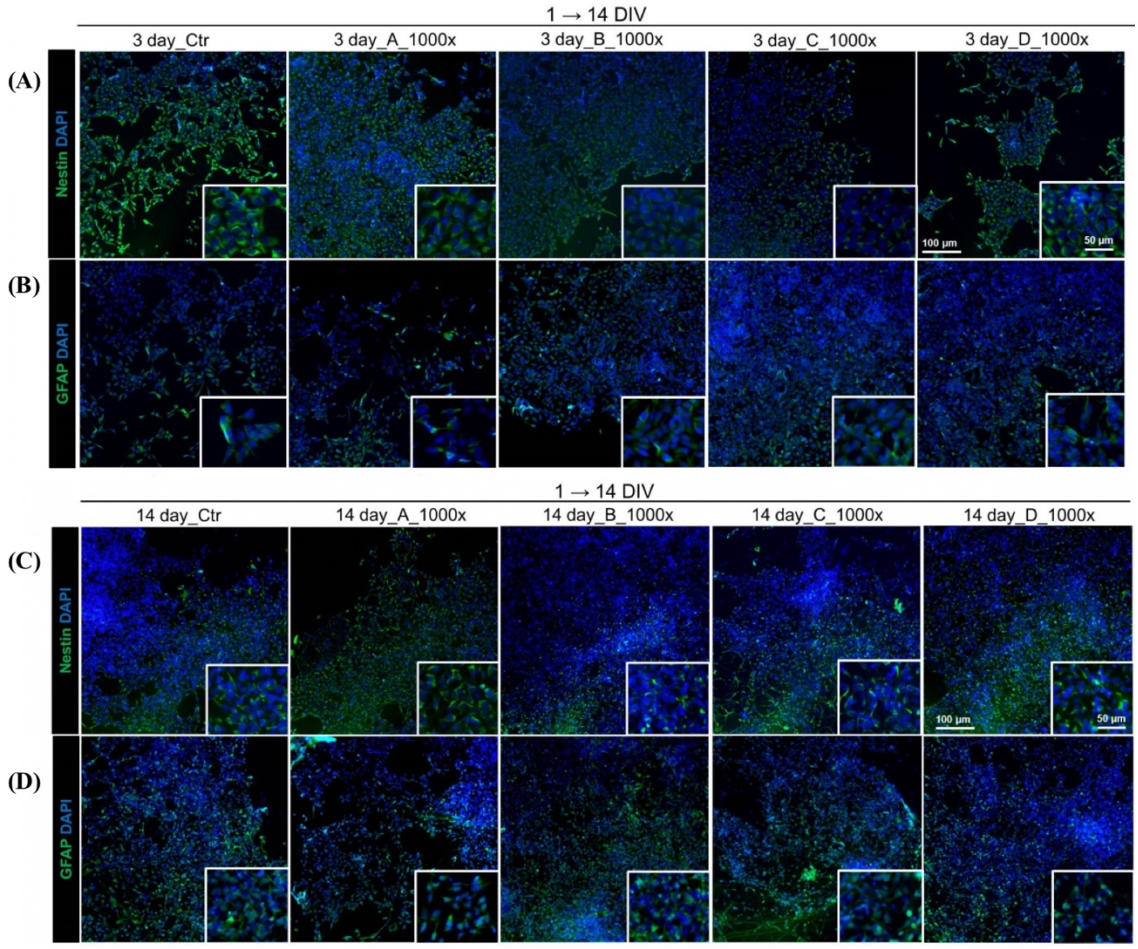

Figure 3.14: Immunochemical images showing the acutely and chronically treated cells stained with antibodies specific for neural stem cells and astrocytes (nestin and GFAP) following exposure to the different POP mixtures. Cells treated with 1000x (the human blood concentration) of the different mixtures; A: Total mixture, B: Perfluorinated and Chlorinated mixture, C: Brominated and Chlorinated mixture, D: Chlorinated mixture, and stained with antibodies for β-III-Tubulin and BDNF, and DAPI. Images were captured using Array Scan vTi platform and the Neuronal profiling V.4 bioapplication for immunofluorescence and high content imaging (HCI). **(A)** Showing nestin (green) and DAPI (blue) in the cells treated for 3 days (acute). **(B)** Showing GFAP (green) and DAPI (blue) in the cells treated for 3 days (acute). **(C)** Showing nestin (green) and DAPI (blue) in the cells treated for 14 days (chronic). **(D)** Showing GFAP (green) and DAPI (blue) in the cells treated for 14 days (chronic).

No significant effects in the expression of Ki67 were observed with any of the mixtures following acute and chronic exposure the POP mixtures (Figure 3.15).

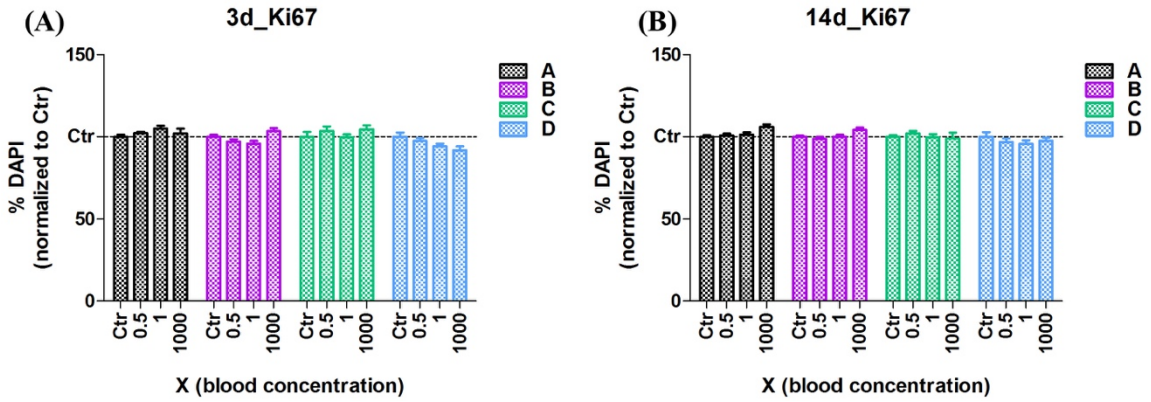

Figure 3.15: Quantification of Ki67 upon acute and chronic exposure to mixtures of POPs using immunostaining and DAPI. Graphs are shown as averages with standard error mean (SEM). Treatments were performed for 3 and 14 days with the POP mixtures; A: Total mixture (Black), B: Perfluorinated and Chlorinated mixture (Pink), C: Brominated and Chlorinated mixture (Green), D: Chlorinated mixture (Blue). Ki67 was visualized with immunostaining and HCI techniques. The experiment was done using 2-4 replicates, some replicates were dismissed due to faulty staining. Samples were all normalized to a control (Ctrl) and are shown as a percentage of this on the y-axis (% DAPI).

In the acutely exposed cells concentrations around the level of human exposure caused upregulation in the number of validated live cells (Figure 3.16A). Exposure to 1x (blood concentration) of the "Total mixture" (Mixture A) and the perfluorinated mixture (Mixture B) caused significant upregulation, amounting to respectively, 40% and 60% upregulation. Exposure to 0.5x and 1x (blood concentration) of the chlorinated mixture (Mixture D) induced significant upregulation amounting to 50-60% upregulation.

Chronic exposure induced a significant response when subjected to all the mixtures, amounting primarily to upregulation of living cells (Figure 3.16B). The cell cultures subjected to 0.5x and 1x the blood concentration of the "Total mixture" saw a significant increase in live cells. The perfluorinated mixture induced upregulation at all tested concentrations, inducing as much as 100% upregulation at 1x the blood concentration. The brominated mixture induced 10% significant downregulation at 1000x the blood concentration. The chlorinated mixture induced upregulation in concentration 0.5x and 1x, amounting to, respectively, 50% and 40% upregulation in live cells.

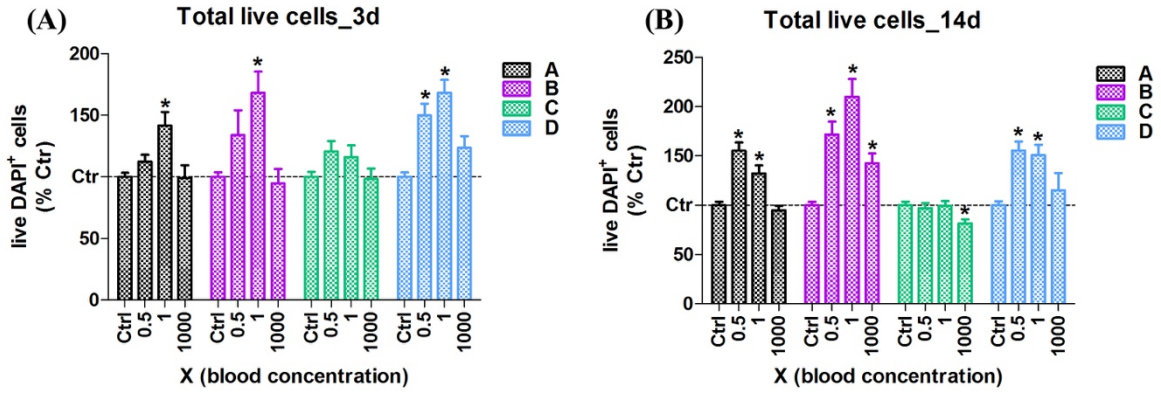

Figure 3.16: Viability quantification of validated cells using DAPI and cellomics following exposure to POP mixtures. Graphs are shown as averages with standard error mean (SEM). Treatments with the POP mixtures were performed for 3 days (acute) and 14 days (chronic). The mixtures; A: Total mixture (Black), B: Perfluorinated and Chlorinated mixture (Pink), C: Brominated and Chlorinated mixture (Green), and D: Chlorinated mixture (Blue), were used. Cells were validated and quantified using DAPI staining of the nucleuses and HCI. Samples were normalized to the control and are shown as a percentage of this. The experiment was done using 20-25 replicates with 8 parallels each for each condition. Statistically significant results are presented with *$p<0.05$ and was validated by one-way ANOVA. **(A)** Effects following acute (3 day) exposure. **(B)** Effects following chronic (14 day) exposure.

3.2.3 qPCR

Upon exposure to the POP mixtures, no significant response in regard to SYP, MAP2, DLG4 (PSD95), or GPHN (gephyrin I) was observed in either of the acutely or chronically treated cells (Figure 3.17). Though the appeared to be a non-significant upregulation generally occurring chlorinated mixture across all tested genes. No significant effects were seen perturbing the synaptogenesis at the gene expression level.

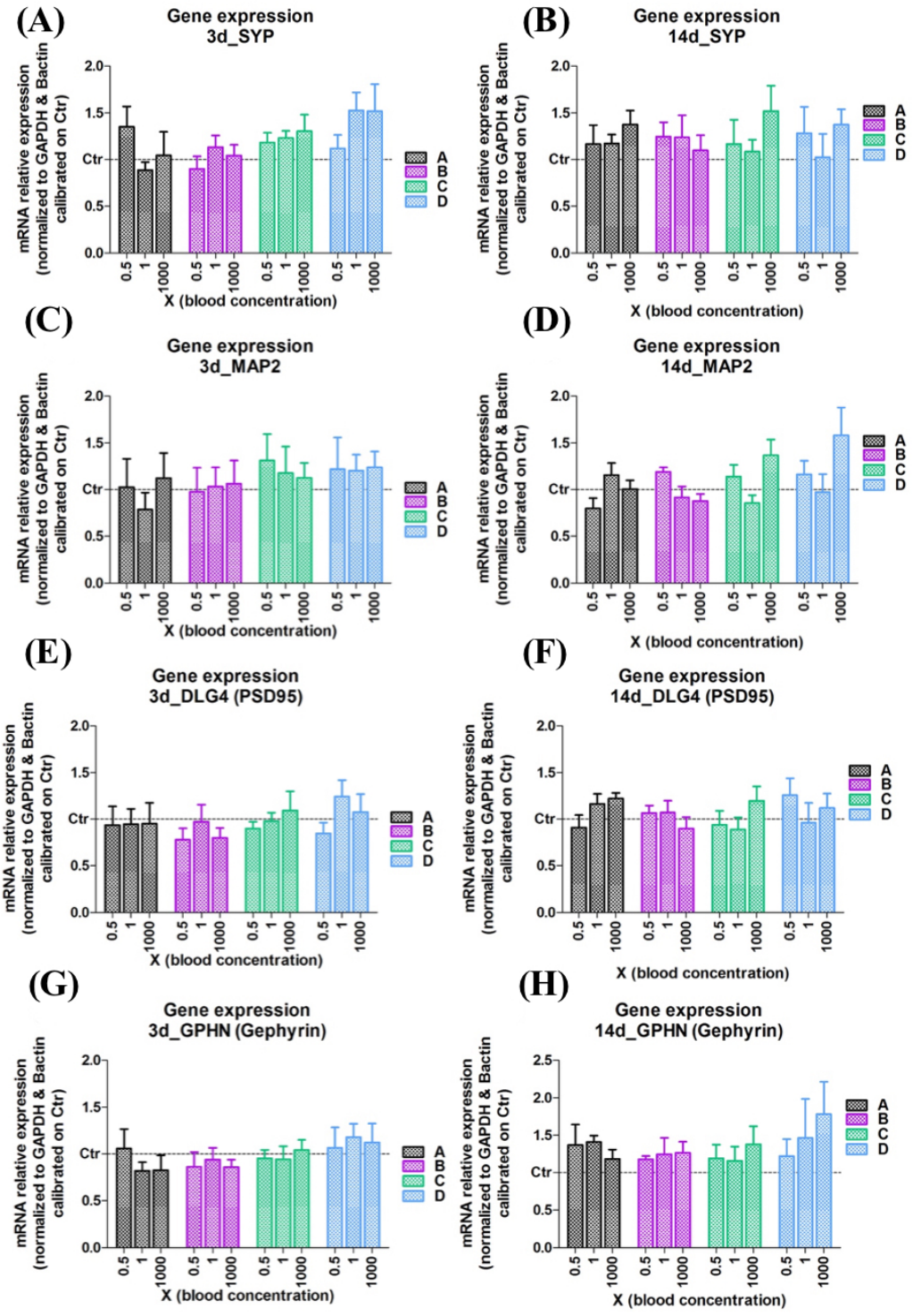

Figure 3.17: Quantitative PCR analysis displaying the gene expression of SYP, MAP2, DLG4, and GPHN following treatment with the POP mixtures. The graphs show the average expression level with standard error mean (SEM) for each condition following treatment with the POP mixtures for 3 days (acute) and 14 days (chronic). The mixtures; A: Total mixture (Black), B: Perfluorinated and Chlorinated mixture (Pink), C: Brominated and Chlorinated mixture (Green), and D: Chlorinated mixture (Blue), were

used. The expression levels were estimated and normalized based on the relative mRNA expression of the housekeeping genes GAPDH and β-actin, and calibrated to the control, the graphs are shown as a percentage of this. Statistically significant results are presented with *p<0.05 and was validated by one-way ANOVA. **(A)** Effects on the expression of SYP following acute (3 day) exposure. **(B)** Effects on the expression of SYP following chronic (14 day) exposure. **(C)** Effects on the expression of MAP2 following acute (3 day) exposure. **(D)** Effects on the expression of MAP2 following chronic (14 day) exposure. **(E)** Effects on the expression of DLG4 following acute (3 day) exposure. **(F)** Effects on the expression of DLG4 following chronic (14 day) exposure. **(G)** Effects on the expression of GPHN following acute (3 day) exposure. **(H)** Effects on the expression of GPHN following chronic (14 day) exposure.

No significant changes were seen in the gene expression of NTRK2 upon exposure to the POP mixtures for 3 and 14 days (Figure 3.18). Seemingly, the expression of the Trkβ BDNF receptor seem to be upregulated in the chlorinated mixtures, and partially in the total mixture, and the brominated and chlorinated mixture, though not significant.

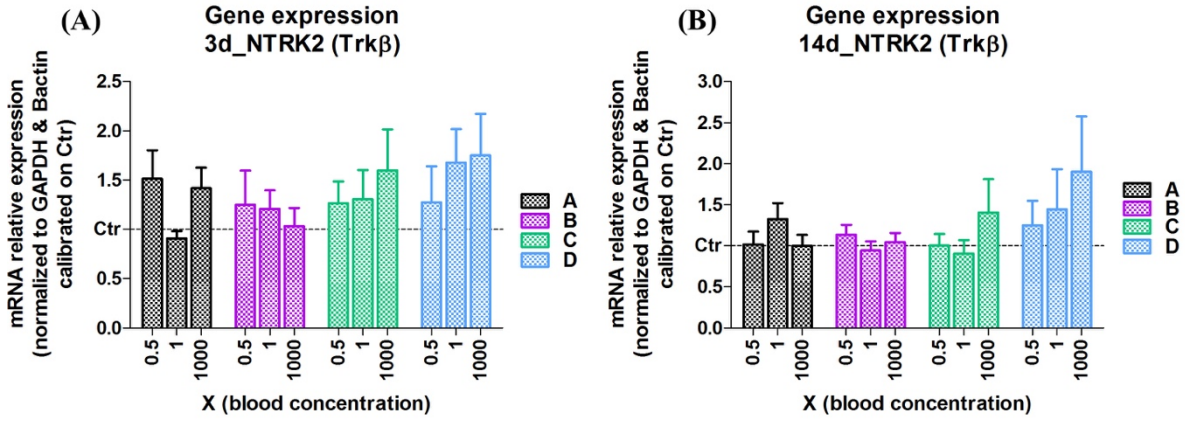

Figure 3.18: Quantitative PCR analysis of NTRK2 (Trkβ) gene expression following treatment with the POP mixtures. The graphs show the average expression level with standard error mean (SEM) for each condition following 3 days (acute) and 14 days (chronic) exposure to the POP mixtures; A: Total mixture (Black), B: Perfluorinated and Chlorinated mixture (Pink), C: Brominated and Chlorinated mixture (Green), and D: Chlorinated mixture (Blue). Expression levels were determined using GAPDH and β-actin for normalization, the control was used for calibration, the graphs are shown as percentages of the control (Ctrl). Statistically significant results are presented with

*p<0.05 and was validated by one-way ANOVA. **(A)** Effects following acute (3 day) exposure. **(B)** Effects following chronic (14 day) exposure.

There was not observed any significant changes in the expression PAX6 upon acute and chronic exposure with the POP mixtures (Figure 3.19). Seemingly treatments did not affect the expression of the neuroectodermal gene.

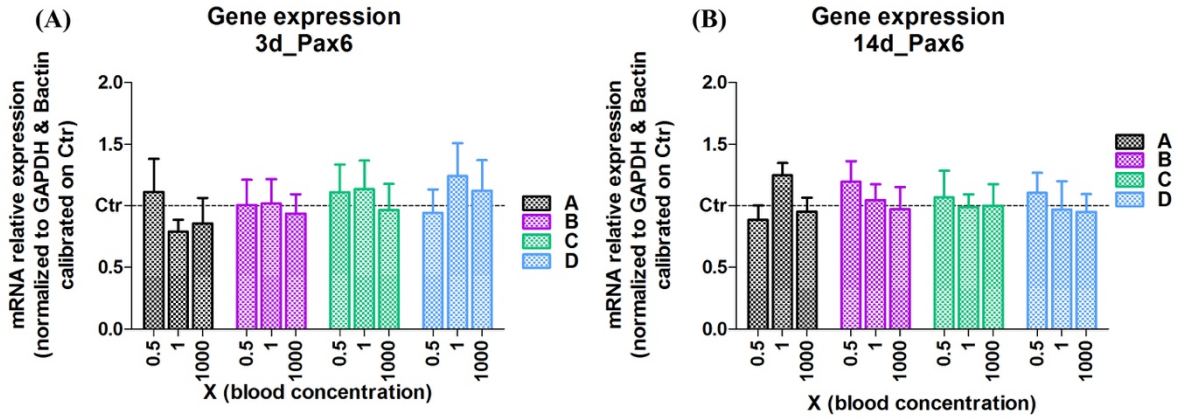

Figure 3.19: Quantitative PCR analysis of PAX6 gene expression following treatment with the POP mixtures. Graphs show the average expression level with standard error mean (SEM) for each condition following 3 days (acute) and 14 days (chronic) exposure to mixtures of POPs. The mixtures; A: Total mixture (Black), B: Perfluorinated and Chlorinated mixture (Pink), C: Brominated and Chlorinated mixture (Green), and D: Chlorinated mixture (Blue). The levels of expression were determined by normalization with GAPDH and β-actin, before being calibrated using the control (Ctrl). Statistically significant results are presented with *p<0.05 and was validated by one-way ANOVA. **(A)** Effects following acute (3 day) exposure. **(B)** Effects following chronic (14 day) exposure.

4. Discussion

4.1 PC12 cells

The PC12 cells were treated with the total mixture, containing all the 29 POPs, for 24, 48, and 72 hours, and viability was assed using the MTT assay. A general trend showing decreased viability at the concentrations 1x, 10x, 500x, and 1000x the human blood concentration was observed, though not statistically significant for the concentrations 1x, 500x, and 1000x at the 48-hour timepoint. The lowered viability occurring at 1x, 10x, and 500x are all more or less in the same range after both 24 hours and 72 hours. This may suggest that the cells are at some level able to tolerate the increasing concentrations of POPs, possibly by upregulating factors such as glutathione in order to mediate increased oxidative stress [151]. Overt toxicity becomes apparent at 1000x, which is especially pronounced at 72 hours of exposure. The same mixture has been tested *in vitro* on human hepatocarcinoma cell line at 48 hours of exposure in a previous study, where no cell death was observed at 1000x the human blood concentration [152]. This may reflect a higher vulnerability of neuronal cells as opposed to those from the liver.

Though it is impossible to determine which of the single compounds in the mixture that are responsible for the observed toxicity in our experiments, or whether interactions between the chemicals have occurred, some studies have shown that some of the compounds are toxic to different cell types *in vitro*. For example, the most prominent polychlorinated biphenyl in the mixture, PCB-153, is in the 1000x mixture present at 1,003 μM (Table 2.15) and has been found to induce significant decline in viability at 6,25 μM in cerebellar granule cells of rats [28]. Additionally, 5 μM PCB-153 induce loss of cell viability in chondrocytes when treated for 24 hours [153]. Another study found that the lethal concentration of PCB-153 causing 50% death (LC50) of the PC12 cells to be 47,8 μM, PC12 cells being the most insensitive neuron or neuron-like cell model tested [154]. PCB-101, which is present in the 1000x mixture at 0,024 μM has been shown to induce chondrocyte cell death at 10 μM after 24 hours of exposure, further was it found that 5 μM induced death at 48 hours of exposure [153]. PCB-180, present in the mixture at 0,491 μM has been found to induce chondrocyte cell death at 5 μM following 24 hours of exposure [153]. BDE-47 is present in the mixture at 0,018 μM, its metabolite 6-OH-BDE-

47 has been shown to reduce the cell viability of HepG2 cells when treated for 72 hours with 0,5 μM [155]. Reduced cell viability has also been observed in human adrenocortical carcinoma cells treated with 2,5 μM [156] and 0,5 μM [157] of 6-OH-BDE-47 for 24 and 48 hours, respectively. BDE-209, present in the 1000x mixture at 0,011 μM has been shown to induce loss in cell viability at 25 μM when exposed for 2 hours [158]. The most prominent brominated flame retardant in the mixture present at 0,038 μM in the 1000x mix, HBCD, has been shown to induce cell death in PC12 cells following 24 hours of incubation at 10 μM [159]. PFOS is the most prominent compound in the entire mixture being present at 54,671 μM, the only relevant study found in which PC12 cells had been tested with PFOS found significant loss in cell viability occurring at 250 μM, but only in differentiated PC12 cells [160]. Though, PFOS has been found to induce loss in cell viability at lower concentrations in other cell models; in cerebellar granule neurons from rat, loss in cell viability was observed starting at 20 μM [87]; in primary hippocampal neurons from rats, loss in cell viability was observed starting at 75 μM [74]. The second most prominent compound in the mixture, PFOA, which is present at 10,922 μM in the 1000x mixture has in a previous study not been found to induce cell death in PC12 cells at concentrations up to 250 μM at 24 hours of exposure [160]. PFHxS is another chemical present at a fairly high concentration in the 1000x mixture at 7,855 μM, this compound has been found to reduce cell viability starting at 100 μM [72].

Different cell models may react differently to the same concentrations of the same compound, leading to uncertainties when comparing and extrapolating the data [161]. However, it is apparent that the loss in viability using the mixture appears at lower concentrations compared to the single compounds. This may indicate that the simultaneous exposure to several POPs lowers the thresholds for toxicity, which could indicate antagonistic effects for each compound, either through additive or synergistic effects. However, it is possible that a few compounds present in the mixture is responsible for the cellular toxicity.

We suspected that the observed decrease in cell viability did not reflect actual cell death, but rather a direct or indirect interference with the ability of the cells to convert MTT to formazan, a process that is dependent on mitochondrial activity [141]. For example, BDE-99 has been shown to decrease DNA content, while also increasing overall protein in the cell and membrane, leading to a change in the determination of the cell from replication to

cell growth and enlargement [162]. This kind of interference has also been noted for multiple perfluorinated compounds [163]. This is supported by our results, with an apparent upregulation or lack of change at 100x, a trend that was seemingly consistent across all replicates, which may indicate a threshold before actual cell death is observed at the concentrations 500x, and 1000x. To evaluate whether the replication machinery was affected by the presence of POPs we decided to check whether proliferating cell nuclear antigen (PCNA), was down- or upregulated. PCNA is a commonly used replication marker [164] associated with significant upregulation during the S phase of replication [165], and it has been found to be necessary for DNA replication to occur [166]. No significant change was observed in regard to the control in the western blot analysis, indicating that the replication machinery was functioning normally, strengthening the belief that the mitochondrial machinery may be affected. However, the variation between each sample and each replicate was large. Additional replicates may give a more definite answer.

In an additional attempt to measure cell viability, we performed trypan blue staining in which the cells were counted manually. Dead cells will upon trypan blue staining take up the dye and become colored blue [143]. However, too few dyed cells were observed to be able to quantify cell death accurately, at all the tested concentrations. This may indicate that no cell death has occurred following the treatment with POPs. However, upon removing the cell titer blue solution in step 7 of the protocol (see section "2.4.1 Trypan Blue Staining and Counting"), dead cells may be aspired as the death of cells generally is accompanied by weakened adherence to the plate.

4.2 hiPSCs

4.2.1 Neuron Proliferation or Mitochondrial Dysfunction?

For the CellTiter blue cell viability assay, the cells were either differentiated for 1 or 14 days before 3 or 14 days of exposure prior to being analyzed (Figure 3.3). Generally, upregulation in the perceived viability seemed to be the norm, as opposed to the PC12 cells where downregulation was the apparent trend. The most notable difference in outcome can be observed between undifferentiated (1 DIV) and differentiated (14 DIV) cells, with the differentiated cells being seemingly more resistant to the POPs than the

undifferentiated. This resistance is possibly due to better developed detoxification mechanisms and general stress response exhibited by more mature neurons [167]. The presence of perfluorinated and chlorinated chemicals seems to induce upregulation in the apparent viability of the cells (Figure 3.3BD), while the presence of brominated chemicals may antagonize these effects (Figure 3.3AC), through downregulation. The perfluorinated compounds seems to be the only ones able to induce a notable response in the matured cells (Red graph, Figure 3.3AB). The upregulation in viability may be caused by an increased number of cells, or it may be the result of the POPs inducing an increased reduction of resazurin to the red fluorescent molecule resorufin [145], for example, through upregulation of mitochondrial and cellular dehydrogenases.

POPs such as PCBs and HCB have in some studies been linked to mitochondrial dysfunction, leading metabolic disease [168]. In fact, chronic exposure to PCBs such as Arocolor-1254 have been shown to induce mitochondrial toxicity and cause alterations in the energy metabolism of neuroblastoma cells, leading to changes in signaling pathways relevant for brain development [169]. Similarly, a large range of PCBs like these has been shown to act inhibitory upon the NADH-oxidase system and succinoxidase activity [170], in adipose tissue. PFOS has also been shown to cause structural changes to the mitochondria, and hinder mitochondrial function in cardiomyocytes [171]. In this study opposite was observed, as the perfluorinated and chlorinated mixtures appeared to invoke an upregulation of the mitochondrial activity (as reflected by the CellTiter blue assay). BDEs, such as BDE-49 has been shown to interfere with the mitochondrial function by uncoupling the electron transport chain and inhibiting ATP synthesis in brain mitochondria and neural progenitor cells [172], similar inhibition has also been observed in the mitochondria of the liver following exposure to BDE-154 [173]. This apparent inhibition of the mitochondria induced by BDEs is in line with what was observed in our present study (Figure 3.3C). Dysfunction of the mitochondria has been linked to a number of neurodegenerative outcomes. It has been reported that neurons are especially sensitive to metabolic, structural, and distributional changes of the mitochondria [174], and disturbances may affect the function of the synapses ultimately leading to diminished working memory [175]. Mitochondria are thought to play a central role in the development of the nervous system, by fueling the early stages of neural stem cell proliferation and neurite outgrowth. The need for energy starts falling as the cells starts focusing on synaptogenesis [176]. During NSC differentiation, mitochondrial DNA has

been found to be prone to oxidative damage, resulting in mutation. The subsequent accumulation of mutations has been found to impair the ability of NSCs to differentiate into neurons [177, 178]. Additionally, dysfunctional mitochondria have been linked to a long range of neurodegenerative diseases, such as Parkinson´s disease, Huntington´s disease, Alzheimer´s disease, and Amyotrophic lateral sclerosis (ALS) [179].

If in fact an upregulation in the number of living cells is observed, the effects upon neurodevelopment will be determined by which cellular processes that is perturbed. If the ability of the cell to control its own cell death has been disturbed, development of the nervous system can be affected, as studies show that healthy neurons will routinely die in an coordinated manner during neurodevelopment [180], and that the proper development of the neuronal network is dependent on neuron density [181, 182]. It has further been found a correlation between excess number of neurons in the prefrontal cortex and the occurrence of autism in children. Autistic children have been found to have as much as 67% more neurons in the prefrontal cortex than those who does not suffer from autism [183, 184]. One study using a mixture containing HCHs, Chlordanes, DDTs, PCBs, BDEs and HBCD on zebrafish embryos found that multiple genes involved in apoptosis was upregulated following exposure [185]. Similarly, studies looking at the effects of individual perfluorinated, brominated, and chlorinated compounds upon apoptosis, reported induction of apoptosis and related genes [63, 72, 74, 186-188], suggesting that the increase in viability observed in the current study is due to interference with the metabolic activity and not apoptosis. Additionally, no significant change from the control is observed in the mature cells (Red graphs, Figure 3.3), indicating a normalization in the cell count. This may suggest that mitochondrial dysfunction is the main contributor to the apparent increase in viability.

Ki67 is a marker of cell proliferation, which is expressed during the G_1, S, G_2 phases of the cell cycle, but absent in resting cells (G_0) [189, 190]. However, no significant increase in the expression of Ki67 after exposure to any of the mixtures was observed. This suggests that there is no increase in the proliferation rate of the cells. Conversely, the viability quantification done by the cellomics machine upon the immunocytochemical cells found a significant increase in the number of viable cells for cells exposed to 0,5-1x of the total, perfluorinated and chlorinated mixture, with the strongest response being exhibited by the 1x concentration.

4.2.2 Brain Development

For immunocytochemistry of neural development, different protein markers for neuronal development was selected to be used for staining, and later analysis with high content imaging (HCI). The markers SYP, PSD95, BDNF, MAP2, βIII-tubulin, GFAP, and nestin were chosen based on their relevance to key neurodevelopmental processes, such as neuronal differentiation and synaptogenesis. Considering the strong response observed in the undifferentiated cells (Blue graphs, Figure 3.3) compared to the more mature cells (Red graphs, Figure 3.3) they were chosen for further inquiry with immunocytochemistry. The exposure concentrations chosen for immunocytochemistry were chosen based on the concentrations known to provoke response in the cell viability assay, while covering the range of human relevant exposure [19].

Synaptogenesis

Exposure to POPs induced alterations in the presence and distribution of protein relevant to synaptogenesis. Synaptophysin was found to be significantly upregulated in all tested mixtures upon acute exposure (Figure 3.4A), though only for the highest concentrations (1000x) of the chlorinated mixture. Perturbation in the amount of SYP was observed starting at human relevant concentrations and below (1x ≥ blood concentration), with the strongest response being promoted by the perfluorinated and brominated mixtures, but seemingly downregulated when these two groups of compounds were combined. This apparent trend seemed to be strengthened following chronic exposure (Figure 3.4C), reflected by normalization in regard to the control in the total and chlorinated mixtures, and a slight strengthening of the response by the perfluorinated and brominated mixtures. The distribution of SYP seemed to favour the cell body, amounting to a slight decrease of SYP in the neurites, but primarily in the highest concentrations (Figure 3.4BD). Seen in context with the increased amounts of synaptophysin, homeostasis may be maintained by storing excess SYP in the cell body. Both PFOS and PFOA has been found to increase the protein levels of synaptophysin in hippocampus and cerebral cortex of neonatally exposed mice, which was linked to spontaneous behaviour and changes in the cholinergic system of the affected mice [75, 76]. For the BDEs, there are limited and conflicting reports regarding their effects on synaptophysin. BDE-209 has been found to be significantly increase [191] and decrease [192] the amount of synaptophysin in the brain. One study using a mixture containing PCB 28, 52, 101, 138, 153, and 180 was found to induce

downregulation of SYP in exposed mice [193], which does not correlate with what was observed in the current study (Blue graphs, Figure 3.4). The increase in observed SYP protein is not reflected in the gene expression which shows no significant increase in the expression of SYP (Figure 3.17AB), upregulation must therefore be through other mechanisms, possibly through altered break down of SYP. Synaptophysin is generally highly concentrated in the axon terminals, and have been used as markers for synapses, where they are believed to play key functions in the synaptic vesicle formation and cycling [108-110]. Upregulation of these mechanisms may induce increased or perturbed vesicle formation and cycling, leading to changes in synapse density, which again may adversely modulate neural network formation.

The amounts and distribution of PSD95 was significantly affected by the presence of all the mixtures. Generally amounting to the upregulation of protein, with associated accumulation in the cell body which was observed across all concentrations and all mixtures (Figure 3.5AB). The response was seemingly weakened with time, amounting to a weaker response with chronic exposure (Figure 3.5CD). The brominated compounds did, however, induce significant increase following chronic exposure as opposed to acute. In literature, acute and chronic PFOS exposure has been shown to decrease PSD95 clustering in the dendrites [73]. In one study, chronic BDE-47 exposure has not been shown to induce any significant changes in PSD95 levels [59], in the present study the brominated compounds induced significant changes only in the chronically exposed cells (Green graphs, Figure 3.5AC). Additionally, a mixture containing PCB 28, 52, 101, 138, 153, and 180, induced decreased expression of PSD95 [193], which contradict our observation which shows a slight increase in the amount of PSD95 aggravated by the chlorinated chemicals (Blue graph, 3.5). In relation to PSD95 there seems to be a great deal of contradicting reports regarding the effects of the different chemicals. There may be different causes for this, attributed to the complexity of the mixtures used or to different model systems. Similar to SYP, the expression of the PSD95 corresponding gene DLG4 was not altered following exposure, indicating that the POPs induce changes at the protein level. PSD95 is thought to be involved in a number of key mechanisms related to neuronal development, among these being the recruitment of neurotransmitter receptors and ion channels to the post-synaptic site [89, 93]. The vitality of PSD95 became evident when knockout mice with mutant PSD95 was generated, where the mice exhibited enhanced LTP, which upon stimuli caused exaggerated potentiation without the necessary

depression, leading to lowered ability of the animal to process and recall information [194]. Upregulation of PSD95 has been connected with Alzheimer's disease, possibly a compensatory mechanism for synapse degeneration [195]. Additionally, dysfunction of PSD95 has been linked to the development of schizophrenia and autism [196].

The occurrence of the dendritic marker MAP2 was modestly upregulated in all mixtures at human relevant concentrations, with the most upregulation occurring with acute exposure of the total mixture (Figure 3.6). This may indicate additive or synergistic effects between the different compounds. Notably, the response in the mature cells was less dramatic with the brominated mixture producing the most upregulation. The apparent upregulation was not reflected by significant increase in gene expression (Figure 3.17CD). Incidence of MAP2 positive cells will generally increase in line with the maturation of the cells (Figure 1.2), meaning that the observed upregulation may suggest an accelerated maturation. There are few publications investigating the effects of the relevant POPs upon MAP2, however, one study suggested that PFOS caused downregulation of MAP2 [197]. A connection between MAP2 interference and neurological disease is reported, decreased immunoreactivity of MAP2 without corresponding decrease in amount of protein has been linked to schizophrenia, and lowered expression of MAP2 has been found in patients suffering from bipolar disease [198].

New Neurites and BDNF

The POP treatments did not considerably alter the amount of β-III-tubulin expressing cells, a slight downregulation was observed upon acute exposure of the chlorinated mixture and chronic exposure to the total mixture at relevant human exposure (Figure 3.8). There are few studies on POPs and the cellular effects on β-III-tubulin. 6-OH-BDE-47, the metabolite of BDE-47, has been shown to lower the level of β-III-tubulin expressing cells dose-dependently [199]. The lowering of β-III-tubulin may lead to lower tolerance against free radicals and indicate a slowing of the maturation of the cell. [122, 123].

Acute exposure to the chlorinated mixture significantly caused upregulation of BDNF in the NSCs, with the distribution favouring the neurites in both the acutely and chronically treated cells (Figure 3.9). Considering the presence of the chlorinated compounds in all the mixtures, the lack of response observed for the other mixtures may indicate

antagonistic effects. PFOS has been found to induce downregulation of BDNF [77], something that is not observed in the current study. Similarly has chronic exposure to BDE-209 been found to decrease the level of BDNF [200], which is not found in the current study. There are lacking reports upon the effects of the relevant PCBs upon the expression and distribution of BDNF. However, there are a considerable amount of reports investigating the role of BDNF dysfunction in neurodevelopmental diseases. BDNF is thought to be involved in a large range of neurological functions, such as promoting survival and protection of the CNS, modulating the blood brain barrier, neurite outgrowth, excitability, and synapse plasticity and modulation [99-101, 103, 106]. Dysfunction of the distribution and occurrence of BDNF may therefore impact a large range of neurological functions. Schizophrenia patients have generally been found to have lower than normal levels of BDNF, which is thought to contribute to dysfunctional neural networks with altered neuroplasticity and synaptic function which amounts to altered brain function. Additionally, the lack of BDNF consequently makes the neural network more vulnerable to disturbances [201-203]. Lowered BDNF has been linked to Parkinson´s, Alzheimer´s, and Huntington´s disease [204]. BDNF is a common key event involved in multiples AOPs linked to disturbances in learning and memory [140, 205, 206]. In this current study, upregulation of BDNF is observed which may indicate a neuroprotective effect, similar to that associated with exercise [207]. Increased levels of BDNF has been linked with increased cognitive performance, which has been observed following exercise [207]. Upregulation may therefore reflect a protective response to the POP mixture. The upregulation of BDNF was, however, not accompanied by an increase in its receptor Trkβ at gene level (Figure 3.18).

At human relevant levels lower number of neurites, shorter neurite length and fewer branch points was observed following exposure to the chlorinated and brominated mixtures. The strongest response was elicited by the chlorinated compounds, in which case the perfluorinated compounds may demonstrate an upregulating or synergistic effect, as the total mixture induces upregulation of the number of neurites, neurite length, and number of branch point at 1000x the human concentration (Figure 3.10). The trend remains but subside in the chronically treated cells. PFOS and PFDA has been shown to decrease the average neurite length and neurite branching, while PFOA has been found to shorten neurites without affecting the average length [81]. BDE99 [162] and BDE-209 [208] are reported to cause shorter neurite length. There is little available literature

regarding the effects of PCBs on neurite outgrowth. Lindane has been found to cause significantly decrease neurite initiation, neurite length, and neurite branching [49]. Relating to neurodevelopmental diseases, autism is believed to be caused by abnormal circuit formation during development, suggesting upregulation of neurite formation between adjacent cells, and decreased long range neurite formation. This may alter the ability of the brain to integrate the information coming from various brain regions [209]. In the current study we do, however, observe a decrease in neurite outgrowth, length, and branchpoints, suggesting that the chlorinated and brominated do not induce increased circuit formation. Decreased circuit formation has, however, been linked to chronic temporal lobe epilepsy. Decreased neurite circuitry is believed to cause hyperexcitability, leading to epileptic seizures, affect learning and memory, and increase the risk of depression [210].

Neural Stem Cells and Astrocytes

Treatments of the cells with the POPs did not significantly affect the expression of the glial fibrillary acidic protein (GFAP), suggesting that the ratio between neurons and glia is to a large degree not affected. Neither does the treatments induce increased maturation of the neurons, as the emergence of glia is generally a feature exhibited by more mature cell cultures. The cells treated chronically with the human relevant blood concentration of the total mixture was found to significantly decline the amount of GFAP expressing cells. Studies has found linkage between dysfunctional glia and the emergence of disorders such as bipolar disease [211], Parkinson´s disease [212], and schizophrenia [213].

The expression of the neuronal stem cell marker nestin was significantly altered in the POP treated cells, causing downregulation at the highest concentrations in the immature cells, and mainly upregulation in the matured cells. The chlorinated and brominated mixtures exhibit upregulation of nestin at 0.5x the blood concentration. Considering the response observed in the acutely exposed cells, the upregulation may be attributed to the chlorinated compounds, with the perfluorinated working antagonistic upon these effects, possibly only at high concentrations. The strongest upregulation is observed in the cells treated chronically with 1x of the total mixture, which may be attributed to the chlorinated possibly working additively with the brominated mixture causing a significant upregulation. This upregulation, may however, be downregulated by the high concentrations of the perfluorinated compounds. Nestin is a neuronal stem cell marker,

generally associated with rosettes which are neuronal destined cells still exhibiting a great deal of pluripotency. The presence of increased nestin markers in the mature cells, may suggest latent or delayed differentiation.

4.2.3 Adverse Outcome Pathways

The AOP framework may be used to interpret the current findings by highlighting various key events. Which in this case may be the upregulation of neuronal viability, upregulation of SYP, PSD95, MAP2, and BDNF.

Reduced BDNF may be caused by upstream inhibition of the NMDA receptor (NMDAR), and reduced intracellular Ca^{2+} (Figure 1.4) [140]. This is linked with reduced presynaptic release of glutamate, leading to decreased synaptogenesis affecting neuronal function amounting to impairment in learning and memory [140]. In the current study, upregulation of BDNF is observed, which could indicate altered function of the NMDAR and subsequent intracellular Ca^{2+} levels, possibly through upregulation. Increased BDNF may subsequently induce increased presynaptic release of glutamate, cell injury, and dendritic aberrations, further upregulating synaptogenesis, which is reflected by the observed increase of SYP, PSD95, and MAP2, which may subsequently lead to increased neuronal network function affecting learning and memory. Another AOP outlining how inhibition of the Na+/I- symporter (NIS) leads to learning and memory impairment explains how reduction in BDNF occurs following decreased thyroxin (T4) synthesis, leading to a lowering of T4 in neuronal tissue, with subsequent decrease in GABAergic interneurons, decreased synaptogenesis, consequent decreased neuronal network formation, and ultimately learning and memory impairment [206]. However, although disturbed BDNF level is a key event also in this AOP which may be relevant to our findings, markers for disturbance of thyroid system was not elucidated in our system.

Agonistic binding to ionotropic glutamate receptors have been linked to overreaction of NMDAR and increased intracellular Ca^{2+}, both act upstream of and will upon downregulation cause lowered BDNF. Upregulation of these have been linked to mitochondrial dysfunction, subsequent cell death and neurodegeneration in the adult brain [205]. In the current study, both increased BDNF and mitochondrial dysfunction is observed, which may indicate that upregulation is caused by an overactive NMDA

receptor following direct or indirect interference by the POPs with the ionotropic glutamate receptor, ultimately leading to neuronal aberrations.

4.2.4 Further Studies

Further investigations should be carried out to evaluate whether the energy metabolism of the cells is affected, for example, by measuring the ATP in the cells, as the energy state of the cell is an important indicator of whether cells are capable of apoptosis or will die following necrosis [214]. Apoptosis related genes should also be examined to probe for interference. Further mitochondrial dysfunction should be investigated. This could possibly be done by measuring intracellular Ca^{2+}, which is linked with mitochondrial dysfunction as described in "4.2.3 Adverse Outcome Pathways" [205]. Additionally, one could probe for upregulation of mitochondrial proteins and genes.

Considering the KEs of the AOPs (section 4.3.2), measuring the release of glutamate and examining dendritic morphology following increased levels of BDNF may be an option. Additionally, one could measure changes in NMDAR recruitment and activity as well in order to find the cause for BDNF upregulation. Further, the expression of GABAergic interneurons could be probed by checking for the expression of GAD1, as BDNF has been linked with this.

The immunocytochemistry experiments could additionally be carried out on the matured cells, starting exposure at 14 days *in vitro*. Exposure to POPs over longer timeframes than 14 days could additionally be tested to evaluate the effects upon synaptogenesis and neuronal network formation over longer periods of time [214], additionally, the activity of the neuronal circuits could be measured using the micro electrode array (MEA). Furthermore, experiments could be performed using even more complex neuronal/glia models, for example, 3D brain organoids, which are thought to reflect the complex interactions of neurons and glia better than monolayer cultures [215].

The same experiments performed in the current study, could be carried out on the single compounds of the mixture, to determine whether the observed response is due to interactions in the mixture or single compounds dominating the toxicity.

5. Conclusions

Mixtures of POPs has been found to induce downregulation in PC12 cells and upregulation in NSCs derived from hiPSCs at relevant human blood concentrations, without associated changes in cell proliferation. One of the most notable findings in the present study is that concentrations below that of the average human blood concentration can be seen to provoke a response in the function of key neurodevelopmental endpoints, through the upregulation of proteins such as SYP, PSD95, MAP2, and MAP2.

Toxicity was observed in the PC12 cells even though each individual compound in the mixtures are present at concentrations lower than concentrations shown to cause toxicity in earlier studies, suggesting additive effects. In the NSCs, a major increase in cell viability was observed in the immature cells. This increase was however generally not reflected in the mature cells, except for the perfluorinated compounds. The mechanisms for the cell viability effects are therefore unclear, possibly causing mitochondrial dysfunction.

The present results suggest that current day populations are continuously being exposed to chemicals at concentrations that may interfere with neurological function, and that children are at risk of neurodevelopment defects due to high blood levels of POPs. The current study shows POPs to be involved in specific key events related to AOPs leading to impaired learning and memory, indicating disturbances of a large range of biological systems relevant to neurodevelopment and function. This may contribute to the prevalence of various neurological and neurodevelopmental disorders. Whether these findings can be buffered by the brains ability to maintain homeostasis must be evaluated with further studies, looking at the effects of even longer periods of exposure, and periods of development, and possibly through functional studies of the neuronal networks.

Sources

1. Jones, K.C. and P. de Voogt, *Persistent organic pollutants (POPs): state of the science.* Environ Pollut, 1999. **100**(1-3): p. 209-21.
2. UNEP. *Overview*. 2008; Available from: http://chm.pops.int/TheConvention/Overview/tabid/3351/Default.aspx.
3. (ECHA), E.C.A. *Understanding REACH*. 2006; Available from: https://echa.europa.eu/regulations/reach/understanding-reach.
4. Ratcliffe, D.A., *Decrease in Eggshell Weight in Certain Birds of Prey.* 1967.
5. Kavlock, R.J., et al., *Research needs for the risk assessment of health and environmental effects of endocrine disruptors: a report of the U.S. EPA-sponsored workshop.* Environ Health Perspect, 1996. **104 Suppl 4**: p. 715-40.
6. Boekelheide, K., et al., *Predicting later-life outcomes of early-life exposures.* Environ Health Perspect, 2012. **120**(10): p. 1353-61.
7. Bal-Price, A. and M.E.B. Meek, *Adverse outcome pathways: Application to enhance mechanistic understanding of neurotoxicity.* Pharmacol Ther, 2017. **179**: p. 84-95.
8. Hogberg, H.T., et al., *Gene expression as a sensitive endpoint to evaluate cell differentiation and maturation of the developing central nervous system in primary cultures of rat cerebellar granule cells (CGCs) exposed to pesticides.* Toxicol Appl Pharmacol, 2009. **235**(3): p. 268-86.
9. Rodier, P.M., *Developing brain as a target of toxicity.* Environ Health Perspect, 1995. **103 Suppl 6**: p. 73-6.
10. Ek, C.J., et al., *Barriers in the developing brain and Neurotoxicology.* Neurotoxicology, 2012. **33**(3): p. 586-604.
11. Vizcaino, E., et al., *Transport of persistent organic pollutants across the human placenta.* Environ Int, 2014. **65**: p. 107-15.
12. Berghuis, S.A., et al., *Developmental neurotoxicity of persistent organic pollutants: an update on childhood outcome.* Arch Toxicol, 2015. **89**(5): p. 687-709.
13. Khezri, A., et al., *A Mixture of Persistent Organic Pollutants and Perfluorooctanesulfonic Acid Induces Similar Behavioural Responses, but Different Gene Expression Profiles in Zebrafish Larvae.* Int J Mol Sci, 2017. **18**(2).
14. Gill, S., et al., *Effects of environmentally relevant mixtures of persistent organic pollutants on the developmental neurobiology in rats.* Toxicol Pathol, 2013. **41**(1): p. 38-47.
15. Hudecova, A.M., et al., *A human exposure based mixture of persistent organic pollutants affects the stress response in female mice and their offspring.* Chemosphere, 2018. **197**: p. 585-593.
16. Harris, A. and J. Seckl, *Glucocorticoids, prenatal stress and the programming of disease.* Horm Behav, 2011. **59**(3): p. 279-89.
17. Liggins, G.C., *The role of cortisol in preparing the fetus for birth.* Reprod Fertil Dev, 1994. **6**(2): p. 141-50.
18. Olsen, G.W., et al., *Half-life of serum elimination of perfluorooctanesulfonate,perfluorohexanesulfonate, and perfluorooctanoate in retired fluorochemical production workers.* Environ Health Perspect, 2007. **115**(9): p. 1298-305.

19. Berntsen, H.F., et al., *The design of an environmentally relevant mixture of persistent organic pollutants for use in in vivo and in vitro studies.* J Toxicol Environ Health A, 2017. **80**(16-18): p. 1002-1016.
20. Fromberg, A., et al., *Estimation of dietary intake of PCB and organochlorine pesticides for children and adults.* Food Chemistry, 2011. **125**(4): p. 1179-1187.
21. Liem, A.K., P. Furst, and C. Rappe, *Exposure of populations to dioxins and related compounds.* Food Addit Contam, 2000. **17**(4): p. 241-59.
22. Fromme, H., et al., *Perfluorinated compounds--exposure assessment for the general population in Western countries.* Int J Hyg Environ Health, 2009. **212**(3): p. 239-70.
23. Darnerud, P.O., et al., *Dietary intake estimations of organohalogen contaminants (dioxins, PCB, PBDE and chlorinated pesticides, e.g. DDT) based on Swedish market basket data.* Food Chem Toxicol, 2006. **44**(9): p. 1597-606.
24. Urabe, H., H. Koda, and M. Asahi, *Present state of yusho patients.* Ann N Y Acad Sci, 1979. **320**: p. 273-6.
25. Schantz, S.L., *Developmental neurotoxicity of PCBs in humans: what do we know and where do we go from here?* Neurotoxicol Teratol, 1996. **18**(3): p. 217-27; discussion 229-76.
26. Park, H.Y., et al., *Neurodevelopmental toxicity of prenatal polychlorinated biphenyls (PCBs) by chemical structure and activity: a birth cohort study.* Environ Health, 2010. **9**: p. 51.
27. Winneke, G., et al., *Developmental neurotoxicity of polychlorinated biphenyls (PCBS): cognitive and psychomotor functions in 7-month old children.* Toxicol Lett, 1998. **102-103**: p. 423-8.
28. Mariussen, E., et al., *The polychlorinated biphenyl mixture aroclor 1254 induces death of rat cerebellar granule cells: the involvement of the N-methyl-D-aspartate receptor and reactive oxygen species.* Toxicol Appl Pharmacol, 2002. **179**(3): p. 137-44.
29. Korrick, S.A. and S.K. Sagiv, *Polychlorinated Biphenyls (PCBs), Organochlorine Pesticides, and Neurodevelopment.* Curr Opin Pediatr, 2008. **20**(2).
30. Tan, Y., et al., *Ortho-substituted but not coplanar PCBs rapidly kill cerebellar granule cells.* Toxicol Sci, 2004. **79**(1): p. 147-56.
31. Bemis, J.C. and R.F. Seegal, *PCB-induced inhibition of the vesicular monoamine transporter predicts reductions in synaptosomal dopamine content.* Toxicol Sci, 2004. **80**(2): p. 288-95.
32. Mariussen, E. and F. Fonnum, *The effect of polychlorinated biphenyls on the high affinity uptake of the neurotransmitters, dopamine, serotonin, glutamate and GABA, into rat brain synaptosomes.* Toxicology, 2001. **159**(1-2): p. 11-21.
33. Eskenazi, B., et al., *In utero exposure to dichlorodiphenyltrichloroethane (DDT) and dichlorodiphenyldichloroethylene (DDE) and neurodevelopment among young Mexican American children.* Pediatrics, 2006. **118**(1): p. 233-41.
34. Ribas-Fito, N., et al., *Breastfeeding, exposure to organochlorine compounds, and neurodevelopment in infants.* Pediatrics, 2003. **111**(5 Pt 1): p. e580-5.
35. Torres-Sánchez, L., et al., *Prenatal p,p´-DDE Exposure and Neurodevelopment among Children 3.5–5 Years of Age.* Environ Health Perspect, 2013. **121**(2): p. 263-8.
36. Wnuk, A., et al., *The Crucial Involvement of Retinoid X Receptors in DDE Neurotoxicity.* Neurotox Res, 2016. **29**(1): p. 155-72.
37. Hatcher, J.M., et al., *Disruption of dopamine transport by DDT and its metabolites.* Neurotoxicology, 2008. **29**(4): p. 682-90.
38. UNEP. *All POPs listed in the Stockholm Convention*. 2008; Available from: http://chm.pops.int/TheConvention/ThePOPs/ListingofPOPs/tabid/2509/Default.aspx.

39. Ribas-Fitó, N., et al., *Exposure to Hexachlorobenzene during Pregnancy and Children's Social Behavior at 4 Years of Age.* Environ Health Perspect, 2007. **115**(3): p. 447-50.
40. Peters, H.A., et al., *Epidemiology of hexachlorobenzene-induced porphyria in Turkey: clinical and laboratory follow-up after 25 years.* Arch Neurol, 1982. **39**(12): p. 744-9.
41. Addae, C., H. Cheng, and E. Martinez-Ceballos, *Effect of the Environmental Pollutant Hexachlorobenzene (HCB) on the Neuronal Differentiation of Mouse Embryonic Stem Cells (†).* Int J Environ Res Public Health, 2013. **10**(10): p. 5244-56.
42. Kilburn, K.H. and J.C. Thornton, *Protracted neurotoxicity from chlordane sprayed to kill termites.* Environ Health Perspect, 1995. **103**(7-8): p. 690-4.
43. Fishman, B.E. and G. Gianutsos, *Inhibition of 4-aminobutyric acid (GABA) turnover by chlordane.* Toxicol Lett, 1985. **26**(2-3): p. 219-23.
44. Hrdina, P.D., D.A. Peters, and R.L. Singhal, *Role of noradrenaline, 5-hydroxytryptamine and acetylcholine in the hypothermic and convulsive effects of alpha-chlordane in rats.* Eur J Pharmacol, 1974. **26**(2): p. 306-12.
45. Alvarez-Pedrerol, M., et al., *Thyroid disruption at birth due to prenatal exposure to beta-hexachlorocyclohexane.* Environ Int, 2008. **34**(6): p. 737-40.
46. Ribas-Fito, N., et al., *Organochlorine compounds and concentrations of thyroid stimulating hormone in newborns.* Occup Environ Med, 2003. **60**(4): p. 301-3.
47. Richardson, J.R., et al., *beta-Hexachlorocyclohexane levels in serum and risk of Parkinson's disease.* Neurotoxicology, 2011. **32**(5): p. 640-5.
48. Muller, D., et al., *Electroneurophysiological studies on neurotoxic effects of hexachlorocyclohexane isomers and gamma-pentachlorocyclohexene.* Bull Environ Contam Toxicol, 1981. **27**(5): p. 704-6.
49. Ferguson, C.A. and G. Audesirk, *Non-GABA(A)-mediated effects of lindane on neurite development and intracellular free calcium ion concentration in cultured rat hippocampal neurons.* Toxicol In Vitro, 1995. **9**(2): p. 95-106.
50. Anand, M., et al., *Role of GABA receptor complex in low dose lindane (HCH) induced neurotoxicity: neurobehavioural, neurochemical and electrophysiological studies.* Drug Chem Toxicol, 1998. **21**(1): p. 35-46.
51. Slotkin, T.A. and F.J. Seidler, *Diverse Neurotoxicants Converge on Gene Expression for Neuropeptides and their Receptors in an In Vitro Model of Neurodifferentiation: Effects of Chlorpyrifos, Diazinon, Dieldrin and Divalent Nickel in PC12 Cells.* Brain Res, 2010. **1353**: p. 36-52.
52. Richardson, J.R., et al., *Developmental exposure to the pesticide dieldrin alters the dopamine system and increases neurotoxicity in an animal model of Parkinson's disease.* Faseb j, 2006. **20**(10): p. 1695-7.
53. Kitazawa, M., V. Anantharam, and A.G. Kanthasamy, *Dieldrin-induced oxidative stress and neurochemical changes contribute to apoptopic cell death in dopaminergic cells.* Free Radic Biol Med, 2001. **31**(11): p. 1473-85.
54. de Wit, C.A., *An overview of brominated flame retardants in the environment.* Chemosphere, 2002. **46**(5): p. 583-624.
55. Gascon, M., et al., *Effects of pre and postnatal exposure to low levels of polybromodiphenyl ethers on neurodevelopment and thyroid hormone levels at 4 years of age.* Environ Int, 2011. **37**(3): p. 605-11.
56. Herbstman, J.B., et al., *Prenatal Exposure to PBDEs and Neurodevelopment.* Environ Health Perspect, 2010. **118**(5): p. 712-9.
57. Cowell, W.J., et al., *Prenatal exposure to polybrominated diphenyl ethers and child attention problems at 3-7 years.* Neurotoxicol Teratol, 2015. **52**(Pt B): p. 143-50.

58. Koenig, C.M., et al., *Maternal Transfer of BDE-47 to Offspring and Neurobehavioral Development in C57BL/6J Mice.* Neurotoxicol Teratol, 2012. **34**(6): p. 571-80.
59. Dingemans, M.M., et al., *Neonatal exposure to brominated flame retardant BDE-47 reduces long-term potentiation and postsynaptic protein levels in mouse hippocampus.* Environ Health Perspect, 2007. **115**(6): p. 865-70.
60. Glazer, L., et al., *Developmental exposure to low concentrations of two brominated flame retardants, BDE-47 and BDE-99, causes life-long behavioral alterations in zebrafish.* Neurotoxicology, 2017.
61. Viberg, H., A. Fredriksson, and P. Eriksson, *Investigations of strain and/or gender differences in developmental neurotoxic effects of polybrominated diphenyl ethers in mice.* Toxicol Sci, 2004. **81**(2): p. 344-53.
62. Dach, K., et al., *BDE-99 impairs differentiation of human and mouse NPCs into the oligodendroglial lineage by species-specific modes of action.* Sci Rep, 2017. **7**.
63. Zhang, H., et al., *Lactation exposure to BDE-153 damages learning and memory, disrupts spontaneous behavior and induces hippocampus neuron death in adult rats.* Brain Res, 2013. **1517**: p. 44-56.
64. Sun, W., et al., *PBDE-209 exposure damages learning and memory ability in rats potentially through increased autophagy and apoptosis in the hippocampus neuron.* Environ Toxicol Pharmacol, 2017. **50**: p. 151-158.
65. Eriksson, P., et al., *Impaired behaviour, learning and memory, in adult mice neonatally exposed to hexabromocyclododecane (HBCDD).* Environ Toxicol Pharmacol, 2006. **21**(3): p. 317-22.
66. Miller-Rhodes, P., et al., *Prenatal exposure to the brominated flame retardant hexabromocyclododecane (HBCD) impairs measures of sustained attention and increases age-related morbidity in the Long-Evans rat.* Neurotoxicol Teratol, 2014. **45**: p. 34-43.
67. Pham-Lake, C., et al., *Impairment in the mesohippocampal dopamine circuit following exposure to the brominated flame retardant, HBCDD.* Environ Toxicol Pharmacol, 2017. **50**: p. 167-174.
68. Genskow, K.R., et al., *Selective damage to dopaminergic transporters following exposure to the brominated flame retardant, HBCDD.* Neurotoxicol Teratol, 2015. **52**(Pt B): p. 162-9.
69. Karrman, A., et al., *Perfluorinated chemicals in relation to other persistent organic pollutants in human blood.* Chemosphere, 2006. **64**(9): p. 1582-91.
70. Lee, I. and H. Viberg, *A single neonatal exposure to perfluorohexane sulfonate (PFHxS) affects the levels of important neuroproteins in the developing mouse brain.* Neurotoxicology, 2013. **37**: p. 190-6.
71. Viberg, H., I. Lee, and P. Eriksson, *Adult dose-dependent behavioral and cognitive disturbances after a single neonatal PFHxS dose.* Toxicology, 2013. **304**: p. 185-91.
72. Lee, Y.J., S.Y. Choi, and J.H. Yang, *NMDA receptor-mediated ERK 1/2 pathway is involved in PFHxS-induced apoptosis of PC12 cells.* Sci Total Environ, 2014. **491-492**: p. 227-34.
73. Liao, C.Y., et al., *Acute enhancement of synaptic transmission and chronic inhibition of synaptogenesis induced by perfluorooctane sulfonate through mediation of voltage-dependent calcium channel.* Environ Sci Technol, 2008. **42**(14): p. 5335-41.
74. Li, Z., et al., *Evaluation of PFOS-mediated neurotoxicity in rat primary neurons and astrocytes cultured separately or in co-culture.* Toxicol In Vitro, 2017. **38**: p. 77-90.
75. Johansson, N., P. Eriksson, and H. Viberg, *Neonatal exposure to PFOS and PFOA in mice results in changes in proteins which are important for neuronal growth and synaptogenesis in the developing brain.* Toxicol Sci, 2009. **108**(2): p. 412-8.

76. Johansson, N., A. Fredriksson, and P. Eriksson, *Neonatal exposure to perfluorooctane sulfonate (PFOS) and perfluorooctanoic acid (PFOA) causes neurobehavioural defects in adult mice.* Neurotoxicology, 2008. **29**(1): p. 160-9.
77. Guo, X.X., et al., *Brain-Derived Neurotrophic Factor Mediated Perfluorooctane Sulfonate Induced-Neurotoxicity via Epigenetics Regulation in SK-N-SH Cells.* Int J Mol Sci, 2017. **18**(4).
78. Gilbert, M.E. and S.M. Lasley, *Developmental thyroid hormone insufficiency and brain development: a role for brain-derived neurotrophic factor (BDNF)?* Neuroscience, 2013. **239**: p. 253-70.
79. Zhang, H., et al., *Prenatal and childhood perfluoroalkyl substances exposures and children's reading skills at ages 5 and 8years.* Environ Int, 2018. **111**: p. 224-231.
80. Quaak, I., et al., *Prenatal Exposure to Perfluoroalkyl Substances and Behavioral Development in Children.* Int J Environ Res Public Health, 2016. **13**(5).
81. Liao, C., et al., *Changes in synaptic transmission, calcium current, and neurite growth by perfluorinated compounds are dependent on the chain length and functional group.* Environ Sci Technol, 2009. **43**(6): p. 2099-104.
82. Goudarzi, H., et al., *Prenatal exposure to perfluorinated chemicals and neurodevelopment in early infancy: The Hokkaido Study.* Sci Total Environ, 2016. **541**: p. 1002-1010.
83. Kudo, N. and Y. Kawashima, *Toxicity and toxicokinetics of perfluorooctanoic acid in humans and animals.* J Toxicol Sci, 2003. **28**(2): p. 49-57.
84. Wang, Y., et al., *Prenatal exposure to perfluroalkyl substances and children's IQ: The Taiwan maternal and infant cohort study.* Int J Hyg Environ Health, 2015. **218**(7): p. 639-44.
85. Gump, B.B., et al., *Perfluorochemical (PFC) exposure in children: associations with impaired response inhibition.* Environ Sci Technol, 2011. **45**(19): p. 8151-9.
86. Jantzen, C.E., et al., *PFOS, PFNA, and PFOA sub-lethal exposure to embryonic zebrafish have different toxicity profiles in terms of morphometrics, behavior and gene expression.* Aquat Toxicol, 2016. **175**: p. 160-70.
87. Berntsen, H.F., et al., *Time-dependent effects of perfluorinated compounds on viability in cerebellar granule neurons: Dependence on carbon chain length and functional group attached.* Neurotoxicology, 2017. **63**: p. 70-83.
88. Stiles, J. and T.L. Jernigan, *The Basics of Brain Development.* Neuropsychol Rev, 2010. **20**(4): p. 327-48.
89. Munno, D.W. and N.I. Syed, *Synaptogenesis in the CNS: An Odyssey from Wiring Together to Firing Together.* J Physiol, 2003. **552**(Pt 1): p. 1-11.
90. Mueller, B.K., *Growth cone guidance: first steps towards a deeper understanding.* Annu Rev Neurosci, 1999. **22**: p. 351-88.
91. Sanes, J.R. and J.W. Lichtman, *Development of the vertebrate neuromuscular junction.* Annu Rev Neurosci, 1999. **22**: p. 389-442.
92. Nimchinsky, E.A., B.L. Sabatini, and K. Svoboda, *Structure and function of dendritic spines.* Annu Rev Physiol, 2002. **64**: p. 313-53.
93. Kim, E. and M. Sheng, *PDZ domain proteins of synapses.* Nat Rev Neurosci, 2004. **5**(10): p. 771-81.
94. Levi-Montalcini, R., et al., *Nerve growth factor: from neurotrophin to neurokine.* Trends Neurosci, 1996. **19**(11): p. 514-20.
95. Levi-Montalcini, R., *The nerve growth factor 35 years later.* Science, 1987. **237**(4819): p. 1154-62.
96. Patapoutian, A. and L.F. Reichardt, *Trk receptors: mediators of neurotrophin action.* Curr Opin Neurobiol, 2001. **11**(3): p. 272-80.

97. Pawson, T. and P. Nash, *Protein-protein interactions define specificity in signal transduction.* Genes Dev, 2000. **14**(9): p. 1027-47.
98. Kaplan, D.R. and F.D. Miller, *Neurotrophin signal transduction in the nervous system.* Curr Opin Neurobiol, 2000. **10**(3): p. 381-91.
99. Wu, D. and W.M. Pardridge, *Neuroprotection with noninvasive neurotrophin delivery to the brain.* Proc Natl Acad Sci U S A, 1999. **96**(1): p. 254-9.
100. Schabitz, W.R., et al., *Intravenous brain-derived neurotrophic factor reduces infarct size and counterregulates Bax and Bcl-2 expression after temporary focal cerebral ischemia.* Stroke, 2000. **31**(9): p. 2212-7.
101. Numakawa, T., et al., *BDNF function and intracellular signaling in neurons.* Histol Histopathol, 2010. **25**(2): p. 237-58.
102. Hetman, M., et al., *Neuroprotection by brain-derived neurotrophic factor is mediated by extracellular signal-regulated kinase and phosphatidylinositol 3-kinase.* J Biol Chem, 1999. **274**(32): p. 22569-80.
103. Patterson, S.L., et al., *Recombinant BDNF rescues deficits in basal synaptic transmission and hippocampal LTP in BDNF knockout mice.* Neuron, 1996. **16**(6): p. 1137-45.
104. Bliss, T.V. and G.L. Collingridge, *A synaptic model of memory: long-term potentiation in the hippocampus.* Nature, 1993. **361**(6407): p. 31-9.
105. Lomo, T., *The discovery of long-term potentiation.* Philos Trans R Soc Lond B Biol Sci, 2003. **358**(1432): p. 617-20.
106. Poo, M.M., *Neurotrophins as synaptic modulators.* Nat Rev Neurosci, 2001. **2**(1): p. 24-32.
107. Heerssen, H.M. and R.A. Segal, *Location, location, location: a spatial view of neurotrophin signal transduction.* Trends Neurosci, 2002. **25**(3): p. 160-5.
108. Tarsa, L. and Y. Goda, *Synaptophysin regulates activity-dependent synapse formation in cultured hippocampal neurons.* Proc Natl Acad Sci U S A, 2002. **99**(2): p. 1012-6.
109. Fletcher, T.L., et al., *The distribution of synapsin I and synaptophysin in hippocampal neurons developing in culture.* J Neurosci, 1991. **11**(6): p. 1617-26.
110. Calhoun, M.E., et al., *Comparative evaluation of synaptophysin-based methods for quantification of synapses.* J Neurocytol, 1996. **25**(12): p. 821-8.
111. Adams, D.J., C.P. Arthur, and M.H.B. Stowell, *Architecture of the Synaptophysin/Synaptobrevin Complex: Structural Evidence for an Entropic Clustering Function at the Synapse.* Sci Rep, 2015. **5**.
112. Schmitt, U., et al., *Detection of behavioral alterations and learning deficits in mice lacking synaptophysin.* Neuroscience, 2009. **162**(2): p. 234-43.
113. Menezes, J.R. and M.B. Luskin, *Expression of neuron-specific tubulin defines a novel population in the proliferative layers of the developing telencephalon.* J Neurosci, 1994. **14**(9): p. 5399-416.
114. Papasozomenos, S.C. and L.I. Binder, *Microtubule-associated protein 2 (MAP2) is present in astrocytes of the optic nerve but absent from astrocytes of the optic tract.* J Neurosci, 1986. **6**(6): p. 1748-56.
115. De Camilli, P., et al., *Distribution of microtubule-associated protein 2 in the nervous system of the rat studied by immunofluorescence.* Neuroscience, 1984. **11**(4): p. 817-46.
116. Cleveland, D.W., S.Y. Hwo, and M.W. Kirschner, *Physical and chemical properties of purified tau factor and the role of tau in microtubule assembly.* J Mol Biol, 1977. **116**(2): p. 227-47.
117. Roger, B., et al., *MAP2c, but not tau, binds and bundles F-actin via its microtubule binding domain.* Curr Biol, 2004. **14**(5): p. 363-71.

118. Dehmelt, L. and S. Halpain, *The MAP2/Tau family of microtubule-associated proteins.* Genome Biol, 2005. **6**(1): p. 204.
119. Matus, A., N. Delhaye-Bouchaud, and J. Mariani, *Microtubule-associated protein 2 (MAP2) in Purkinje cell dendrites: evidence that factors other than binding to microtubules are involved in determining its cytoplasmic distribution.* J Comp Neurol, 1990. **297**(3): p. 435-40.
120. Caceres, A., et al., *An immunocytochemical and biochemical study of the microtubule-associated protein MAP-2 during post-lesion dendritic remodeling in the central nervous system of adult rats.* Brain Res, 1988. **427**(3): p. 233-46.
121. Downing, K.H. and E. Nogales, *Tubulin and microtubule structure.* Curr Opin Cell Biol, 1998. **10**(1): p. 16-22.
122. Ferreira, A. and A. Caceres, *Expression of the class III beta-tubulin isotype in developing neurons in culture.* J Neurosci Res, 1992. **32**(4): p. 516-29.
123. Guo, J., C. Walss-Bass, and R.F. Ludueña, *The β isotypes of tubulin in neuronal differentiation.* Cytoskeleton (Hoboken), 2010. **67**(7): p. 431-41.
124. Greene, L.A. and A.S. Tischler, *Establishment of a noradrenergic clonal line of rat adrenal pheochromocytoma cells which respond to nerve growth factor.* Proc Natl Acad Sci U S A, 1976. **73**(7): p. 2424-8.
125. Westerink, R.H. and A.G. Ewing, *The PC12 cell as model for neurosecretion.* Acta Physiol (Oxf), 2008. **192**(2): p. 273-85.
126. Greene, L.A. and G. Rein, *Release of (3H)norepinephrine from a clonal line of pheochromocytoma cells (PC12) by nicotinic cholinergic stimulation.* Brain Res, 1977. **138**(3): p. 521-8.
127. Shafer, T.J. and W.D. Atchison, *Transmitter, ion channel and receptor properties of pheochromocytoma (PC12) cells: a model for neurotoxicological studies.* Neurotoxicology, 1991. **12**(3): p. 473-92.
128. G Banker, K.G., *Types of nerve cell cultures, their advantages and limitations*. Culturing Nerve Cells, ed. K.G. G Banker. Vol. 2nd edition. 1998, Massachusetts: MIT Press.
129. Takahashi, K. and S. Yamanaka, *Induction of pluripotent stem cells from mouse embryonic and adult fibroblast cultures by defined factors.* Cell, 2006. **126**(4): p. 663-76.
130. Ho, P.J., et al., *Current applications of human pluripotent stem cells: possibilities and challenges.* Cell Transplant, 2012. **21**(5): p. 801-14.
131. Drews, K., et al., *Human induced pluripotent stem cells--from mechanisms to clinical applications.* J Mol Med (Berl), 2012. **90**(7): p. 735-45.
132. Pistollato, F., et al., *Development of a pluripotent stem cell derived neuronal model to identify chemically induced pathway perturbations in relation to neurotoxicity: effects of CREB pathway inhibition.* Toxicol Appl Pharmacol, 2014. **280**(2): p. 378-88.
133. Pistollato, F., et al., *Protocol for the Differentiation of Human Induced Pluripotent Stem Cells into Mixed Cultures of Neurons and Glia for Neurotoxicity Testing.* J Vis Exp, 2017(124).
134. Vinken, M., *The adverse outcome pathway concept: a pragmatic tool in toxicology.* Toxicology, 2013. **312**: p. 158-65.
135. Krewski, D., et al., *TOXICITY TESTING IN THE 21ST CENTURY: A VISION AND A STRATEGY.* J Toxicol Environ Health B Crit Rev, 2010. **13**(0): p. 51-138.
136. Bal-Price, A., et al., *Putative adverse outcome pathways relevant to neurotoxicity.* Crit Rev Toxicol, 2015. **45**(1): p. 83-91.
137. OECD, *Proposal for a template and guidance on developing and assessing the completeness of adverse outcome pathways.* 2012.

138. Crofton, K.M., et al., *Developmental neurotoxicity testing: recommendations for developing alternative methods for the screening and prioritization of chemicals.* Altex, 2011. **28**(1): p. 9-15.
139. Bal-Price, A.K., et al., *In vitro developmental neurotoxicity (DNT) testing: relevant models and endpoints.* Neurotoxicology, 2010. **31**(5): p. 545-54.
140. Sachana, M., A. Rolaki, and A. Bal-Price, *Development of the Adverse Outcome Pathway (AOP): Chronic binding of antagonist to N-methyl-d-aspartate receptors (NMDARs) during brain development induces impairment of learning and memory abilities of children.* Toxicol Appl Pharmacol, 2018.
141. van Meerloo, J., G.J. Kaspers, and J. Cloos, *Cell sensitivity assays: the MTT assay.* Methods Mol Biol, 2011. **731**: p. 237-45.
142. Mahmood, T. and P.C. Yang, *Western Blot: Technique, Theory, and Trouble Shooting.* N Am J Med Sci, 2012. **4**(9): p. 429-34.
143. Louis, K.S. and A.C. Siegel, *Cell viability analysis using trypan blue: manual and automated methods.* Methods Mol Biol, 2011. **740**: p. 7-12.
144. Fox, C.H., et al., *Formaldehyde fixation.* J Histochem Cytochem, 1985. **33**(8): p. 845-53.
145. Corporation, P., *CellTiter-Blue Cell Viability Assay Technical Bulletin, TB31.* 2013.
146. Brooks, S.A., *Basic Immunocytochemistry for Light Microscopy.* Metastasis Research Protocols. Methods in Molecular Biology (Methods and Protocols), 2012. **878**.
147. Holland, P.M., et al., *Detection of specific polymerase chain reaction product by utilizing the 5'----3' exonuclease activity of Thermus aquaticus DNA polymerase.* Proc Natl Acad Sci U S A, 1991. **88**(16): p. 7276-80.
148. Cardullo, R.A., et al., *Detection of nucleic acid hybridization by nonradiative fluorescence resonance energy transfer.* Proc Natl Acad Sci U S A, 1988. **85**(23): p. 8790-4.
149. Overbergh, L., et al., *The use of real-time reverse transcriptase PCR for the quantification of cytokine gene expression.* J Biomol Tech, 2003. **14**(1): p. 33-43.
150. Nolan, T., R.E. Hands, and S.A. Bustin, *Quantification of mRNA using real-time RT-PCR.* Nat Protoc, 2006. **1**(3): p. 1559-82.
151. Chen, Z.H., et al., *Induction of adaptive response and enhancement of PC12 cell tolerance by 7-hydroxycholesterol and 15-deoxy-delta(12,14)-prostaglandin J2 through up-regulation of cellular glutathione via different mechanisms.* J Biol Chem, 2006. **281**(20): p. 14440-5.
152. Wilson, J., et al., *Effects of defined mixtures of persistent organic pollutants (POPs) on multiple cellular responses in the human hepatocarcinoma cell line, HepG2, using high content analysis screening.* Toxicol Appl Pharmacol, 2016. **294**: p. 21-31.
153. Abella, V., et al., *Non-dioxin-like polychlorinated biphenyls (PCB 101, PCB 153 and PCB 180) induce chondrocyte cell death through multiple pathways.* Toxicol Lett, 2015. **234**(1): p. 13-9.
154. Costa, L.G., et al., *An in vitro approach to assess the toxicity of certain food contaminants: methylmercury and polychlorinated biphenyls.* Toxicology, 2007. **237**(1-3): p. 65-76.
155. An, J., et al., *The cytotoxic effects of synthetic 6-hydroxylated and 6-methoxylated polybrominated diphenyl ether 47 (BDE47).* Environ Toxicol, 2011. **26**(6): p. 591-9.
156. Canton, R.F., et al., *Inhibition and induction of aromatase (CYP19) activity by brominated flame retardants in H295R human adrenocortical carcinoma cells.* Toxicol Sci, 2005. **88**(2): p. 447-55.
157. Song, R., et al., *Effects of fifteen PBDE metabolites, DE71, DE79 and TBBPA on steroidogenesis in the H295R cell line.* Chemosphere, 2008. **71**(10): p. 1888-94.

158. Liu, Q., et al., *Role of Taurine in BDE 209-Induced Oxidative Stress in PC12 Cells.* Adv Exp Med Biol, 2017. **975**: p. 897-906.
159. Li, Y., et al., *Neuroprotection by Taurine on HBCD-Induced Apoptosis in PC12 Cells.* Adv Exp Med Biol, 2017. **975**: p. 95-106.
160. Slotkin, T.A., et al., *Developmental neurotoxicity of perfluorinated chemicals modeled in vitro.* Environ Health Perspect, 2008. **116**(6): p. 716-22.
161. Heusinkveld, H.J. and R.H.S. Westerink, *Comparison of different in vitro cell models for the assessment of pesticide-induced dopaminergic neurotoxicity.* Toxicol In Vitro, 2017. **45**(Pt 1): p. 81-88.
162. Slotkin, T.A., et al., *BDE99 (2,2',4,4',5-pentabromodiphenyl ether) suppresses differentiation into neurotransmitter phenotypes in PC12 cells.* Neurotoxicol Teratol, 2013. **37**: p. 13-7.
163. Corsini, E., et al., *In vitro characterization of the immunotoxic potential of several perfluorinated compounds (PFCs).* Toxicol Appl Pharmacol, 2012. **258**(2): p. 248-55.
164. Jurikova, M., et al., *Ki67, PCNA, and MCM proteins: Markers of proliferation in the diagnosis of breast cancer.* Acta Histochem, 2016. **118**(5): p. 544-52.
165. Bravo, R. and J.E. Celis, *A search for differential polypeptide synthesis throughout the cell cycle of HeLa cells.* J Cell Biol, 1980. **84**(3): p. 795-802.
166. Prelich, G. and B. Stillman, *Coordinated leading and lagging strand synthesis during SV40 DNA replication in vitro requires PCNA.* Cell, 1988. **53**(1): p. 117-26.
167. Kole, A.J., R.P. Annis, and M. Deshmukh, *Mature neurons: equipped for survival.* Cell Death Dis, 2013. **4**: p. e689.
168. Lim, S., et al., *Persistent organic pollutants, mitochondrial dysfunction, and metabolic syndrome.* Ann N Y Acad Sci, 2010. **1201**: p. 166-76.
169. Cocco, S., et al., *Polychlorinated Biphenyls Induce Mitochondrial Dysfunction in SH-SY5Y Neuroblastoma Cells.* PLoS One, 2015. **10**(6).
170. Pardini, R.S., *Polychlorinated biphenyls (PCB): effect on mitochondrial enzyme systems.* Bull Environ Contam Toxicol, 1971. **6**(6): p. 539-45.
171. Tang, L.L., et al., *Mitochondrial toxicity of perfluorooctane sulfonate in mouse embryonic stem cell-derived cardiomyocytes.* Toxicology, 2017. **382**: p. 108-116.
172. Napoli, E., et al., *Toxicity of the Flame-Retardant BDE-49 on Brain Mitochondria and Neuronal Progenitor Striatal Cells Enhanced by a PTEN-Deficient Background.* Toxicol Sci, 2013. **132**(1): p. 196-210.
173. Pereira, L.C., et al., *BDE-154 induces mitochondrial permeability transition and impairs mitochondrial bioenergetics.* J Toxicol Environ Health A, 2014. **77**(1-3): p. 24-36.
174. Picard, M. and B.S. McEwen, *Mitochondria impact brain function and cognition.* Proc Natl Acad Sci U S A, 2014. **111**(1): p. 7-8.
175. Hara, Y., et al., *Presynaptic mitochondrial morphology in monkey prefrontal cortex correlates with working memory and is improved with estrogen treatment.* Proc Natl Acad Sci U S A, 2014. **111**(1): p. 486-91.
176. Chang, D.T. and I.J. Reynolds, *Differences in mitochondrial movement and morphology in young and mature primary cortical neurons in culture.* Neuroscience, 2006. **141**(2): p. 727-36.
177. Wang, W., et al., *Mitochondrial DNA integrity is essential for mitochondrial maturation during differentiation of neural stem cells.* Stem Cells, 2010. **28**(12): p. 2195-204.
178. Wang, W., et al., *Mitochondrial DNA damage level determines neural stem cell differentiation fate.* J Neurosci, 2011. **31**(26): p. 9746-51.

179. Chaturvedi, R.K. and M. Flint Beal, *Mitochondrial diseases of the brain.* Free Radic Biol Med, 2013. **63**: p. 1-29.
180. Hamburger, V. and R. Levi-Montalcini, *Proliferation, differentiation and degeneration in the spinal ganglia of the chick embryo under normal and experimental conditions.* J Exp Zool, 1949. **111**(3): p. 457-501.
181. Cullen, D.K., et al., *Synapse-to-neuron ratio is inversely related to neuronal density in mature neuronal cultures.* Brain Res, 2010. **1359**: p. 44-55.
182. van den Pol, A.N., et al., *Early synaptogenesis in vitro: role of axon target distance.* J Comp Neurol, 1998. **399**(4): p. 541-60.
183. Courchesne, E., et al., *Neuron number and size in prefrontal cortex of children with autism.* Jama, 2011. **306**(18): p. 2001-10.
184. Lainhart, J.E. and N. Lange, *Increased neuron number and head size in autism.* Jama, 2011. **306**(18): p. 2031-2.
185. Lyche, J.L., et al., *Parental exposure to natural mixtures of persistent organic pollutants (POP) induced changes in transcription of apoptosis-related genes in offspring zebrafish embryos.* J Toxicol Environ Health A, 2016. **79**(13-15): p. 602-11.
186. Chen, H., et al., *A ROS-mediated mitochondrial pathway and Nrf2 pathway activation are involved in BDE-47 induced apoptosis in Neuro-2a cells.* Chemosphere, 2017. **184**: p. 679-686.
187. Zhang, C., et al., *Protective effect of N-acetylcysteine against BDE-209-induced neurotoxicity in primary cultured neonatal rat hippocampal neurons in vitro.* Int J Dev Neurosci, 2010. **28**(6): p. 521-8.
188. Sanchez-Alonso, J.A., et al., *Apoptosis-mediated neurotoxic potential of a planar (PCB 77) and a nonplanar (PCB 153) polychlorinated biphenyl congeners in neuronal cell cultures.* Toxicol Lett, 2003. **144**(3): p. 337-49.
189. Gerdes, J., et al., *Cell cycle analysis of a cell proliferation-associated human nuclear antigen defined by the monoclonal antibody Ki-67.* J Immunol, 1984. **133**(4): p. 1710-5.
190. Scholzen, T. and J. Gerdes, *The Ki-67 protein: from the known and the unknown.* J Cell Physiol, 2000. **182**(3): p. 311-22.
191. Viberg, H., *Neonatal ontogeny and neurotoxic effect of decabrominated diphenyl ether (PBDE 209) on levels of synaptophysin and tau.* Int J Dev Neurosci, 2009. **27**(5): p. 423-9.
192. Li, X., et al., *Neonatal exposure to BDE 209 impaired learning and memory, decreased expression of hippocampal core SNAREs and synaptophysin in adult rats.* Neurotoxicology, 2017. **59**: p. 40-48.
193. Elnar, A.A., et al., *Lactational exposure of mice to low levels of non-dioxin-like polychlorinated biphenyls increases susceptibility to neuronal stress at a mature age.* Neurotoxicology, 2016. **53**: p. 314-320.
194. Migaud, M., et al., *Enhanced long-term potentiation and impaired learning in mice with mutant postsynaptic density-95 protein.* Nature, 1998. **396**(6710): p. 433-9.
195. Savioz, A., G. Leuba, and P.G. Vallet, *A framework to understand the variations of PSD-95 expression in brain aging and in Alzheimer's disease.* Ageing Res Rev, 2014. **18**: p. 86-94.
196. Coley, A.A. and W.J. Gao, *PSD95: A synaptic protein implicated in schizophrenia or autism?* Prog Neuropsychopharmacol Biol Psychiatry, 2018. **82**: p. 187-194.
197. Patel, R., et al., *Alteration to Dopaminergic Synapses Following Exposure to Perfluorooctane Sulfonate (PFOS), in Vitro and in Vivo.* Med Sci (Basel), 2016. **4**(3).

198. Marchisella, F., E.T. Coffey, and P. Hollos, *Microtubule and microtubule associated protein anomalies in psychiatric disease.* Cytoskeleton (Hoboken), 2016. **73**(10): p. 596-611.
199. Li, T., et al., *A Hydroxylated Metabolite of Flame-Retardant PBDE-47 Decreases the Survival, Proliferation, and Neuronal Differentiation of Primary Cultured Adult Neural Stem Cells and Interferes with Signaling of ERK5 MAP Kinase and Neurotrophin 3.* Toxicol Sci, 2013. **134**(1): p. 111-24.
200. Viberg, H., W. Mundy, and P. Eriksson, *Neonatal exposure to decabrominated diphenyl ether (PBDE 209) results in changes in BDNF, CaMKII and GAP-43, biochemical substrates of neuronal survival, growth, and synaptogenesis.* Neurotoxicology, 2008. **29**(1): p. 152-9.
201. Nieto, R., M. Kukuljan, and H. Silva, *BDNF and Schizophrenia: From Neurodevelopment to Neuronal Plasticity, Learning, and Memory.* Front Psychiatry, 2013. **4**.
202. Angelucci, F., S. Brene, and A.A. Mathe, *BDNF in schizophrenia, depression and corresponding animal models.* Mol Psychiatry, 2005. **10**(4): p. 345-52.
203. Rizos, E.N., et al., *Association of serum brain-derived neurotrophic factor and duration of untreated psychosis in first-episode patients with schizophrenia.* Neuropsychobiology, 2010. **62**(2): p. 87-90.
204. Zuccato, C. and E. Cattaneo, *Brain-derived neurotrophic factor in neurodegenerative diseases.* Nat Rev Neurol, 2009. **5**(6): p. 311-22.
205. Sachana, M., S. Munn and A. Bal-Price, *Adverse Outcome Pathway on binding of agonists to ionotropic glutamate receptors in adult brain leading to excitotoxicity that mediates neuronal cell death, contributing to learning and memory impairment.* OECD Series on Adverse Outcome Pathways, 2016. **6**.
206. Alexandra Rolaki, F.P., Sharon Munn, and Anna Bal-Price. *Inhibition of Na+/I-symporter (NIS) leads to learning and memory impairment*. [AOP] 2018; Available from: https://aopwiki.org/aops/54.
207. Etnier, J.L., et al., *The Effects of Acute Exercise on Memory and Brain-Derived Neurotrophic Factor (BDNF)*. J Sport Exerc Psychol, 2016. **38**(4): p. 331-340.
208. Zhang, C., X. Liu, and D. Chen, *Role of brominated diphenly ether-209 in the differentiation of neural stem cells in vitro.* Int J Dev Neurosci, 2010. **28**(6): p. 497-502.
209. Courchesne, E. and K. Pierce, *Why the frontal cortex in autism might be talking only to itself: local over-connectivity but long-distance disconnection.* Curr Opin Neurobiol, 2005. **15**(2): p. 225-30.
210. Hattiangady, B. and A.K. Shetty, *Implications of decreased hippocampal neurogenesis in chronic temporal lobe epilepsy.* Epilepsia, 2008. **49**(0 5): p. 26-41.
211. Watkins, C.C., A. Sawa, and M.G. Pomper, *Glia and immune cell signaling in bipolar disorder: insights from neuropharmacology and molecular imaging to clinical application.* Transl Psychiatry, 2014. **4**(1): p. e350-.
212. Booth, H.D.E., W.D. Hirst, and R. Wade-Martins, *The Role of Astrocyte Dysfunction in Parkinson's Disease Pathogenesis.* Trends Neurosci, 2017. **40**(6): p. 358-70.
213. Windrem, M.S., et al., *Human iPSC Glial Mouse Chimeras Reveal Glial Contributions to Schizophrenia.* Cell Stem Cell, 2017. **21**(2): p. 195-208.e6.
214. Eguchi, Y., S. Shimizu, and Y. Tsujimoto, *Intracellular ATP levels determine cell death fate by apoptosis or necrosis.* Cancer Res, 1997. **57**(10): p. 1835-40.
215. Myhre, O., et al., *Early life exposure to air pollution particulate matter (PM) as risk factor for attention deficit/hyperactivity disorder (ADHD): Need for novel strategies for mechanisms and causalities.* Toxicol Appl Pharmacol, 2018.